UDC 621
CODEN: MINSC5
In print: ISSN 1857 – 5293
On line: ISSN 1857 – 9191

MECHANICAL ENGINEERING SCIENTIFIC JOURNAL

МАШИНСКО ИНЖЕНЕРСТВО НАУЧНО СПИСАНИЕ

Volume 42
Number 2

Skopje, 2024

Mech. Eng. Sci. J.	Vol. **42**	No. 2	pp. 71–136	Skopje 2024
Маш. инж. науч. спис.	Год.	Број	стр.	Скопје

MECHANICAL ENGINEERING – SCIENTIFIC JOURNAL
МАШИНСКО ИНЖЕНЕРСТВО – НАУЧНО СПИСАНИЕ

Published by
Faculty of Mechanical Engineering, Ss. Cyril and Methodius University in Skopje, North Macedonia
Издава
Машински факултет, Универзитет „Св. Кирил и Методиј” во Скопје, Северна Македонија

Published twice yearly – Излегува два пати годишно

UDC: "St. Kliment Ohridski" Library – Skopje	УДК: НУБ „Св.. Климент Охридски“ – Скопје
Copies: 300	Тираж: 300
Price: 520 denars	Цена: 520 денари

Address	Адреса
Faculty of Mechanical Engineering	**Машински факултет**
(Mechanical Engineering – Scientific Journal)	(Машинско инженерство – научно списание)
Editor in Chief	Одговорен уредник
P.O.Box 464	пошт. фах 464
MK-1001 Skopje, Republic of North Macedonia	МК-1001 Скопје, Република Северна Македонија

Mech. Eng. Sci. J. is indexed/abstracted in INIS (International Nuclear Information System)
www.mf.ukim.edu.mk

MECHANICAL ENGINEERING – SCIENTIFIC JOURNAL
FACULTY OF MECHANICAL ENGINEERING, SKOPJE, REPUBLIC OF NORTH MACEDONIA

МАШИНСКО ИНЖЕНЕРСТВО – НАУЧНО СПИСАНИЕ
МАШИНСКИ ФАКУЛТЕТ, СКОПЈЕ, РЕПУБЛИКА СЕВЕРНА МАКЕДОНИЈА

Mech. Eng. Sci. J.	Vol.	No.	pp.	Skopje
	42	2	71–136	2024
Маш. инж. науч. спис.	Год.	Број	стр.	Скопје

TABLE OF CONTENTS
(С О Д Р Ж И Н А)

WELDING ENGINEERING AND INSPECTION
(Заварување и контрола)

MECHANOTRONICS
(Механотроника)

ENERGY AND ENVIRONMENT
(Енергетика и животна средина)

Mechanical Engineering – Scientific Journal, Vol. **42,** No. 2, pp. 75–81 (2024)
Number of article: 681
In print: ISSN 1857–5293
Received: November 6, 2024
On line: ISSN 1857–9191
Accepted: November 15, 2024
UDC: 620.179.147:[621.643:620.194
https://doi.org/10.55302/MESJ24422075k

Original scientific paper

APPLICATION OF PULSED EDDY CURRENT TECHNIQUE FOR INSPECTION OF INSULATED PIPES

Aleksandra Krstevska[1], Filip Serafimovski[2], Marjan Gavriloski[1], Zoran Bogatinoski[1], Filip Zdraveski[1]

[1]*Faculty of Mechanical Engineering, "Ss. Cyril and Methodius" University in Skopje, P.O.Box 464, MK-1001 Skopje, Republic of North Macedonia*
[2]*Apave SEE South Eastern Europe, St. Fjodor Dostoevski 72, P.O. Box 67 – 1000 Skopje, Republic of North Macedonia*
aleksandra.krstevska@mf.edu.mk

A b s t r a c t: In this paper the use of Pulsed Eddy Current (PEC) technique is analyzed for inspecting insulated pipes, commonly used in industries such as power generation, petrochemical, and oil and gas. PEC technique uses pulsed electromagnetic fields to generate eddy currents in the conductive material, allowing detection in wall thickness and material integrity. In the experimental part an insulated pipe is investigated with the PEC technique for corrosion or wall thinning defect of the material, without the need to remove the insulation. The paper involves experimental testing on insulated pipe of structural steel with composite insulation and the results show the potential of PEC as a reliable tool for maintenance and inspection, especially for reducing operational costs and downtime associated with insulation removal.

Key words: insulated pipes; pulsed eddy current; non-destructive testing; corrosion

ПРИМЕНА НА ТЕХНИКАТА СО ВИОРНИ СТРУИ ЗА ИСПИТУВАЊЕ ИЗОЛИРАНИ ЦЕВКИ

А п с т р а к т: Во овој труд е анализирана примената на методот со пулсирачки виорни струи (PEC) за испитување изолирани цевки, често употребувани во енергетската, петрохемиската и нафтената индустрија. Техниката PEC користи пулсирачко електромагнетно поле кое генерира виорни струи во спроводлив материјал, овозможувајќи детектирање промена во дебелината на ѕидот и интегритетот на материјалот. Во експерименталниот дел изолирана цевка е предмет на истражување со помош на техниката PEC за детектирање на дефекти од корозија и промени на дебелината на ѕидот без да се отстранува изолацијата. Овој труд вклучува експериментално тестирање на изолирана цевка изработена од конструктивен челик со композитна изолација и резултатите го прикажуваат потенцијалот на PEC како сигурна алатка за одржување и инспекција, особено за редуцирање оперативни трошоци и прекини предизвикани со отстранување на изолацијата.

Клучни зборови: изолирани цевки; пулсирачки виорни струи; тестирање без разорување; корозија

1. INTRODUCTION

Non-destructive testing (NDT) plays a crucial role in ensuring the safety and integrity of industrial components, especially in the process and power industries. Between the different NDT techniques, Pulsed Eddy Current (PEC) technique is used for detecting corrosion and other defects in ferromagnetic materials with insulation. PEC technique uses the principles of electromagnetic induction to generate eddy currents within conductive materials, to evaluate the wall thickness of the material and to

identify defects without the need of expensive disassembly of the insulation of the inspected components [1, 2]. One of the key advantages of PEC technique is the ability to penetrate into the material, allowing detection of defects beneath the insulation without the need to remove it. This capability is essential for maintaining operational efficiency and minimizing downtime. Recent developments in PEC technology have improved its sensitivity and accuracy, making it a preferred solution for in-service inspections [1, 2]. This method has been proven to be effective in identifying corrosion and localized defects, providing accurate measurements of wall thickness and detect corrosion defects in ferromagnetic pipes [2, 3]. Furthermore, with the integration of advanced signal processing, PEC techniques improved the interpretation of data allowing more precise defect analysis [4].

Besides its advantages, the application of PEC testing experiences certain challenges. Factors like the electromagnetic properties of the materials and the influence of external conditions can impact on the accuracy of the measurements [1, 5]. This paper aims to provide a comprehensive overview of the application of pulsed eddy current testing for the inspection of insulated pipes and identify a localized defect in the wall thickness of the material. By recent research findings and advancements in PEC technology, this study aims to contribute to the reliability and effectiveness of NDT methods in industrial applications.

2. PRINCIPLES OF PULSED EDDY CURRENT INSPECTION

The pulsed eddy current (PEC) inspection is part of a non-destructive testing (NDT) technique and uses the principles of electromagnetic induction to detect defects in conductive materials. The method is especially effective for inspecting insulated pipes and other components where traditional inspection techniques may be limited or expensive to use.

The basic principle of PEC inspection is based on electromagnetic induction, where a time-varying magnetic field is generated by passing an alternating current through a coil. When this coil is placed near a conductive material, such as metal, it induces eddy currents within the material. These eddy currents flow in closed loops perpendicular to the magnetic field and are influenced by the electrical conductivity and magnetic permeability of the material [6, 7].

The conventional eddy current testing uses sinusoidal excitement, but PEC technique uses short-duration pulses of current. This short-duration pulses of current generates a broad spectrum of frequencies, allowing for deeper penetration into the material and improved sensitivity to defects located under surface layers or insulation (Figure 1) [8, 9].

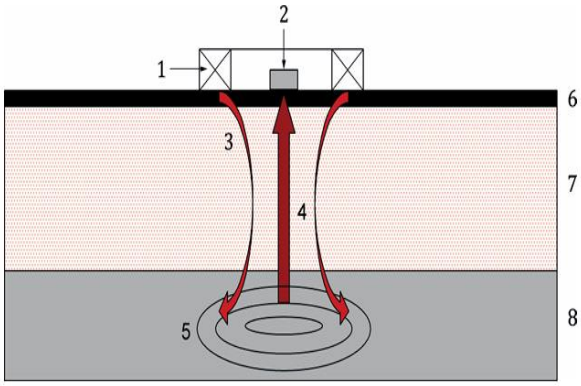

Fig. 1. Basic principle of pulsed eddy current testing technique [10]
1– sender coil, 2 – receiver devices, 3 – primary magnetic field, 4 – secondary magnetic field, 5 – eddy currents, 6 – cover/sheeting, 7 – insulation, 8 – tested component

The presence of defects, such as cracks or corrosion, interrupts the flow of eddy currents, leading to changes in the induced magnetic field. These changes can be detected by the sensor that measures the results of the electromagnetic field variations [11, 12]. The degree of eddy current flow disturbance is closely related with the size and nature of the defect [6, 12]. With the advancement in the field of signal processing, Fourier transformation and pattern recognition algorithms are used to analyze the data and to enhance defect characterization [13, 14]. The ability to accurately interpret these signals is crucial for determining the integrity and location of defects within the inspected material.

PEC inspection is particularly successful for evaluating insulated pipes, as it can penetrate insulation layers without requiring their removal (Figure 2).

This capability minimizes operational downtime and reduces the risks associated with traditional inspection methods, which may involve extensive disassembly of the insulation [8, 9]. The effecttiveness of PEC in detecting corrosion and other defects in insulated pipes has been demonstrated in various studies, highlighting its potential as a reliable NDT method in industrial applications [13, 15].

Fig. 2. Examples of PEC inspected insulated pipes

3. EXPERIMENTAL WORK

For the experimental work a pipe is inspected using PEC method (Figure 3). The pipe material and dimensions are given in Table 1. The PEC system generates a series of electromagnetic pulses and the PEC sensor detects variations in the magnetic field caused by anomalies such as corrosion, thinning of the material or cracks within the pipe. The data from the sensor is recorded and analyzed. Calibration using reference samples of known thickness is performed allowing the accuracy of the results. The experimental results provide critical information on the condition of the pipe, enabling decisions for maintenance or repair.

Fig. 3. Segment of pipeline that is subject of investigation

T a b l e 1

Technical data of tested material

Material (mm)	Structural steel
Diameter of the pipe	323.9
Length	1420
Nominal thickness of the wall	10.3
Thickness of the composite insulation	10

The step of the probe is calculated with the following equation:

$$FP = (0.65 \cdot LO) + FP_0 = (0.65 \cdot 10) + 35 = 41.5 \text{ mm},$$

where:

LO – thickness of the insulation,

FP_0 – probe surface (for the selected probe (PEC-025) = 35 mm).

Calibration was performed on a segment of the pipe which did not suffer any damage during its operation, on a segment with a nominal thickness of the pipe wall. The experimental work steps are given in Table 2. The initial scan is performed on the entire length of the insulated pipe using the first chosen PEC probe. The probe is moved along the pipe, maintaining a consistent speed and ensuring complete coverage of the pipe. After obtaining the data from the initial scan an analysis is performed to locate the potential areas with defects. The second scan is performed with the same probe only on the damaged segment in dynamic mode (higher resolution) to determine the defects dimensions. For accuracy and error analysis a third and fourth scan is performed with high resolution probe on the same damaged segment to compare data and assess the accuracy of defect characterization.

T a b l e 2

Experimental work steps

Scan	Measurement area	Probe	Resolution
First	Pipe	PEC-025	Reduced resolution
Second	Detected segment	PEC-025	Increased resolution
Third	Detected segment	PECA-HR	CWT ready option
Forth	Detected segment	PECA-HR	High resolution

4. RESULTS AND DISCUSSION

The inspection is performed in two different scans of the pipe. The first scan is performed on the entire surface of the pipe, in order to locate the damaged segment of the component. Scanning is performed in dynamic mode with reduced resolution (signal acquisition points) in order to quickly inspect and locate the defect. After the scan, the received signals are analyzed, and the following results are obtained, as shown in Figure 4. The minimum thickness measured with the first initial scan is 6.4 mm, while the maximum thickness is 11 mm.

Located reduced wall thickness during the initial scan is shown in Figure 4, marked in yellow. The second scan is performed in order to obtain precise data on the degree of damage. The second scan is performed with the same probe, in dynamic mode, but with increased resolution. The dimensions of the damaged segment covers an area of 800×200 mm.

Analyzed results obtained from the second scan of the damaged segment gives the following measurement: the minimum thickness of the material measured by pulses eddy currents is 6.3 mm, while the maximum thickness is 10 mm (Figure 5).

To continue with the analysis of the damaged pipe the next step in this research is to scan the damaged pipe segment with a high-resolution probe. The proposed approach is performed to compare the accuracy and error rate between the probes. The minimum material thickness obtained in the third scan with the CWT ready option is 5.8 mm (Figure 6), and the minimum material thickness obtained with the fourth scan with high-resolution option and the high-resolution probe is 5.5 mm (Figure 7). Summary of the obtained measurements are given in Table 3.

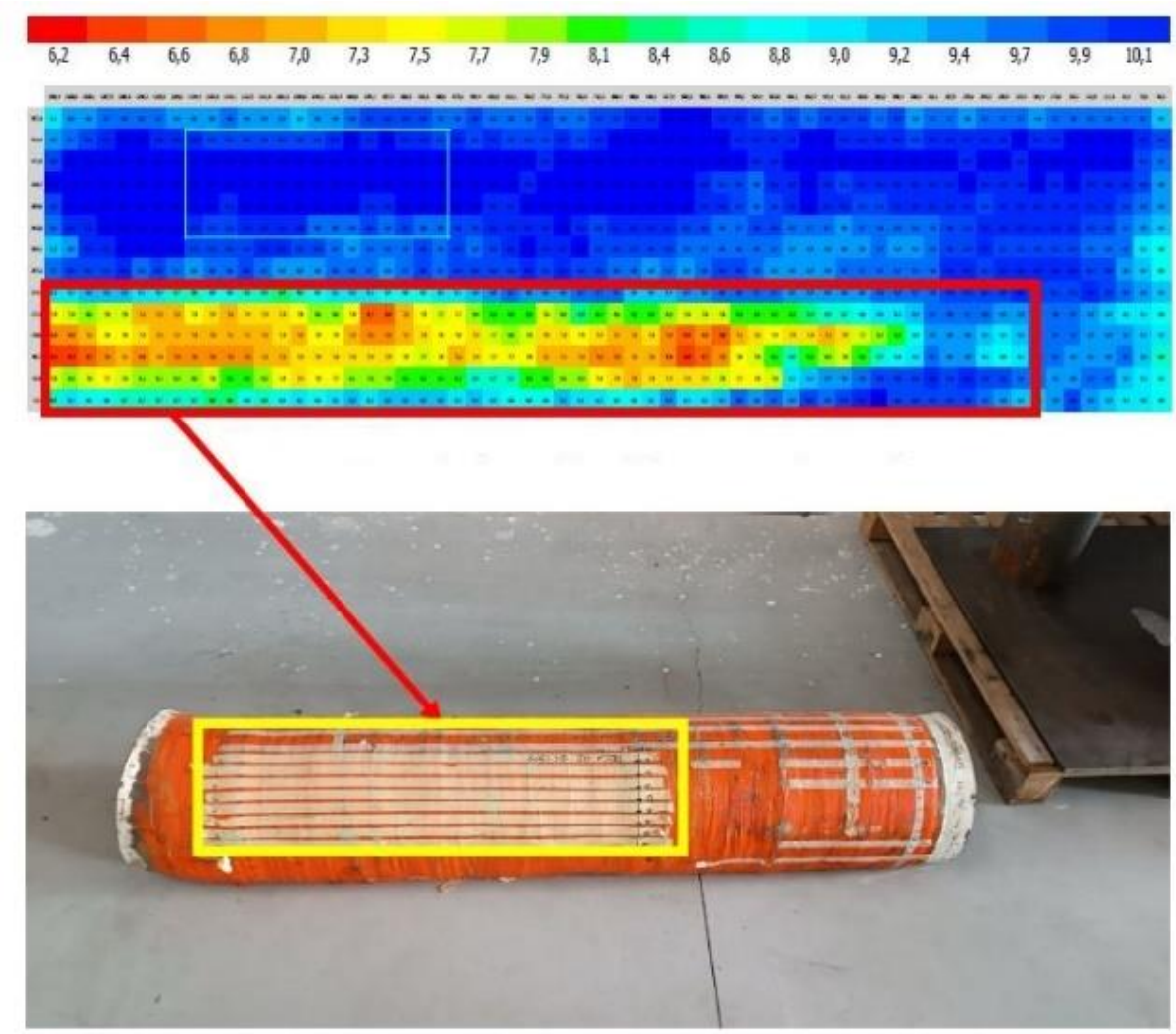

Fig. 4. Obtained results and location of the damaged pipe zone

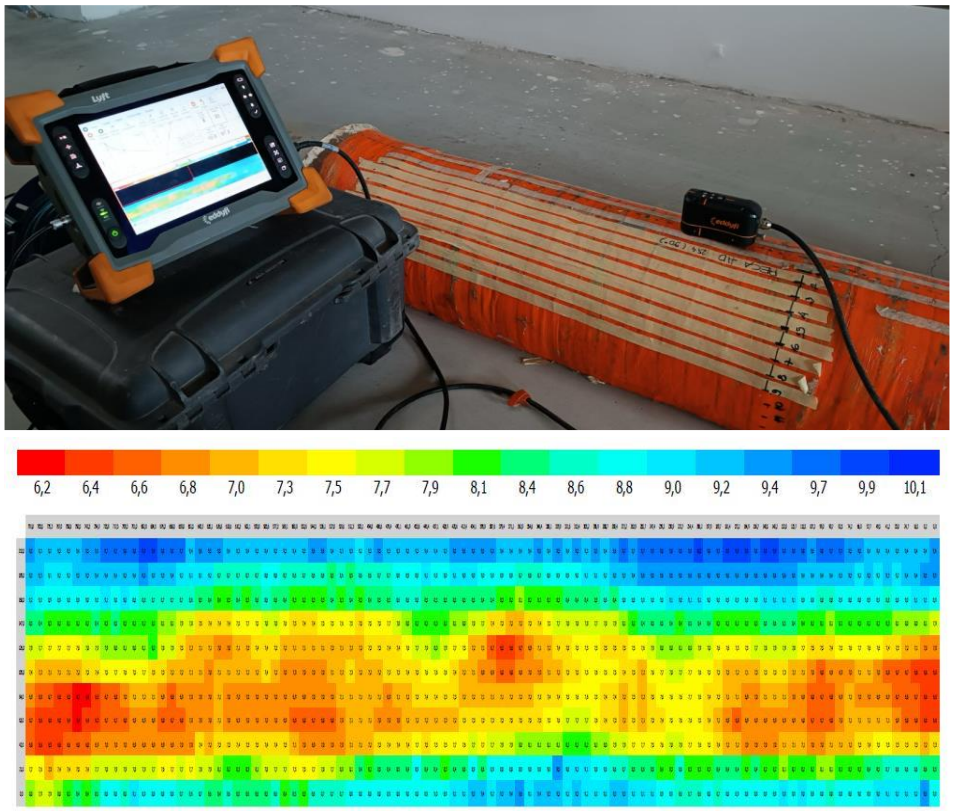

Fig. 5. Scan of the reduced thickness segment and results obtained

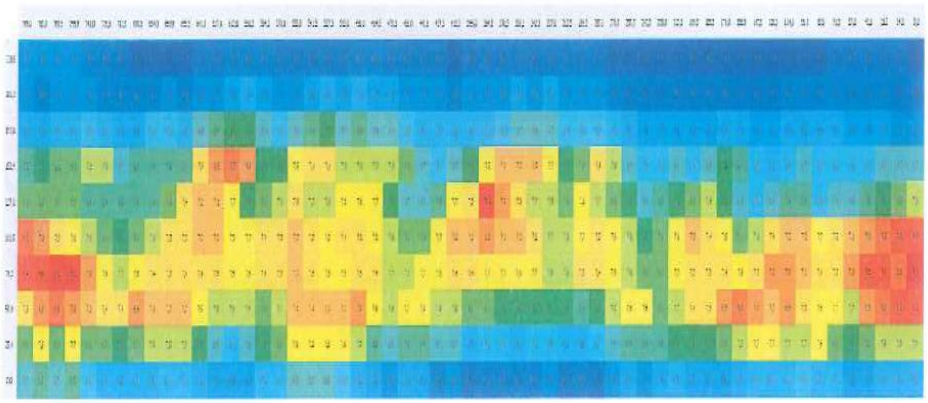

Fig. 6. Material thickness with CWT ready option

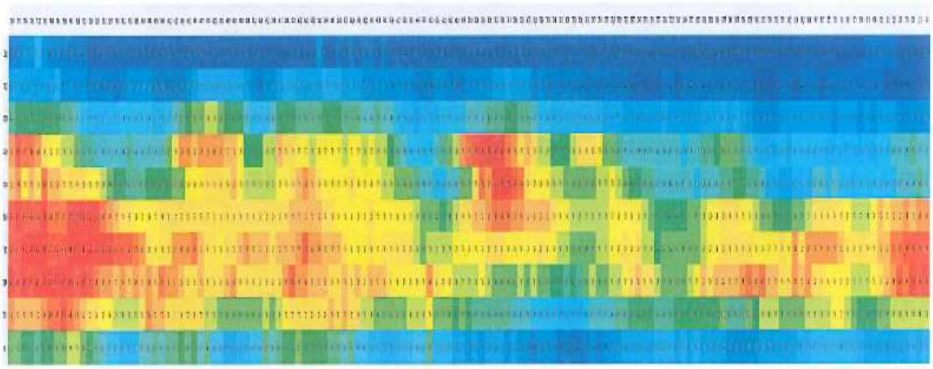

Fig. 7. Material thickness with high resolution option

Table 3

Measurement variations of detected defect with different probe and resolution

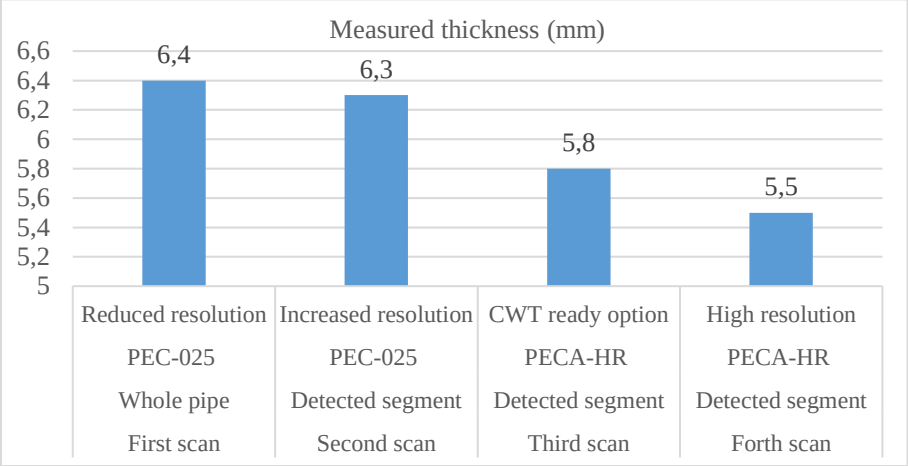

The difference in results between the PEC-025 single element probe and the PECA-HR high resolution probe is 0.8 mm. The time required to inspect the damaged segment is increased during scanning with the high-resolution probe. To confirm the values obtained by the inspection of pulsed eddy current, as well as the accuracy of the damaged location, an inspection of the inside of the pipe is carried out. As shown in Figure 8 the measured thickness of the pipe is 5.8 mm. After inspecting the inside of the pipe, it can be noted that the eddy current testing technique provides reliable information about the location of damage that can occur under the insulation of the pipelines. It can also be noted that they provide accurate material thickness data, with small deviations between the measured and actual minimum pipe wall thickness.

Fig. 8. Damaged location inside the pipe and measured minimum thickness in the damaged segment

5. CONCLUSIONS

The experimental investigation conducted in this paper was on a pipe with composite insulation and with the application of pulsed eddy current technique where its effectiveness was demonstrated in detecting defects such as corrosion and wall thinning without the need to remove the insulation. PEC technique can penetrate the composite insulation and accurately identify the variations in pipe wall thickness and material integrity. The technique proved to be useful for inspecting insulated pipes where conventional inspection methods would require costly and time-consuming insulation removal. According to the study the PEC technique can penetrate into insulation materials, including composites, while providing reliable defect detection. This technique presents a valuable solution for non-destructive testing in the industrial sector, offering a practical and efficient method for ensuring the safety of insulated piping systems.

REFERENCES

[1] Ulapane, N., Alempijevic, A., Vidal Calleja, T., Valls Mirom, J. (2017): Pulsed eddy current sensing for critical pipe condition assessment, *Sensors*, vol. **17** (10), p. 2208. DOI: 10.3390/s17102208

[2] Han, Y., Wang, Q., Liu, X. (2023): Research on pulsed eddy current technology for local corrosion defects, In: *Ninth International Conference on Mechanical Engineering, Materials, and Automation Technology (MMEAT 2023)*, H. Dong and H. Yu, Eds., SPIE, Oct., p. 30. DOI: 10.1117/12.3007044

[3] Yu, X., Zhu, Y., Cao, Y., Xiong, J. (2023): Time-domain numerical simulation and experimental study on pulsed eddy current inspection of tubing and casing, *Sensors*, vol. **23** (3), p. 1135. DOI: 10.3390/s23031135

[4] Al-Qubaa, A. R., Tian, G. Y., Wilson, J., Woo, W. L., Dlay, S. S. (2010): Feature extraction using normalized cross-correlation for pulsed eddy current thermographic images, *Meas Sci Technol*., vol. **21** (11), p. 115501. DOI: 10.1088/0957-0233/21/11/115501

[5] Yang, B., Li, X. (2013): Pulsed remote field technique used for nondestructive inspection of ferromagnetic tube. *NDT & E International*, vol. **53**, pp. 47–52. DOI: 10.1016/j.ndteint.2009.01.015

[6] Ahmad Latif, N. A., Zainal Abidin, I. M., Jamaludin, N. (2018): Simulation and experimental investigation of pulsed eddy current technique for defect evaluation, *Indonesian Journal of Electrical Engineering and Informatics (IJEEI)*, **6** (3). DOI: 10.11591/ijeei.v6i3.503

[7] Guo, W., Gao, B., Yun Tian, G., Si, D. (2020): Physic perspective fusion of electromagnetic acoustic transducer and pulsed eddy current testing in non-destructive testing system, *Philosophical Transactions of the Royal Society A: Mathematical, Physical and Engineering Sciences*, **378** (2182), p. 20190608. DOI: 10.1098/rsta.2019.0608

[8] Habibalahi, A., Safizadeh, M. S. (2014): Pulsed eddy current and ultrasonic data fusion applied to stress measurement, *Meas Sci Technol*., vol**. 25**, no. 5, p. 055601. DOI: 10.1088/0957-0233/25/5/055601

[9] Liu, S., Xin, W., Ding, K. (2010): Simulation of corrosion on detection for pulsed eddy current. In: *2010 Seventh International Conference on Fuzzy Systems and Knowledge Discovery*, IEEE, pp. 1839–1842. DOI: 10.1109/FSKD.2010.5569432

[10] International Organization for Standardization (2017): EN ISO 20669:2017, *Non-destructive testing* – Pulsed eddy current testing of ferromagnetic metallic components.

[11] Shu, L., Songling, H., Wei, Z. (2007): Development of differential probes in pulsed eddy current testing for noise suppression, *Sens Actuators A Phys*., vol. **135**, no. 2, pp. 675–679. DOI: 10.1016/j.sna.2006.10.013

[12] Lysenko, I., Kuts, Y., Protasov, A., Redka, M., Uchanin, V. (Sep., 2021): Enhanced feature extraction algorithms using oscillatory-mode pulsed eddy current techniques for aircraft structure inspection, *Transactions on Aerospace Research*, vol. **2021**, no. 3, pp. 1–16. DOI: 10.2478/tar-2021-0013

[13] Zhu, P., Tian, L., Cheng, Y. (2019): Improvement of defect feature extraction in eddy current pulsed thermography, *IEEE Access*, vol. **7**, pp. 48288–48294. DOI: 10.1109/ACCESS.2019.2908457

[14] Yusa, N., Ge, J., Fan, M. (2022): Whether 'Rich in frequency' means 'Rich in information' in pulsed eddy current testing to evaluate plate thickness: numerical investigation, *Mater Trans*., vol. **63** (4), p. MT-I2021001. DOI: 10.2320/matertrans.MT-I2021001

[15] Huang, S., Hong, M., Lin, G., Tang, B., Shen, S. (2023): The implementation and advantages of a discrete Fourier transform-based digital eddy current testing instrument. In: *ECSA-10*, Basel, Switzerland: MDPI, p. 84. DOI: 10.3390/ecsa-10-16214

Mechanical Engineering – Scientific Journal, Vol. **42,** No. 2, pp. 83–94 (2024)
Number of article: 682
In print: ISSN 1857–5293
Received: October 24, 2024
On line: ISSN 1857–9191
Accepted: November 27, 2024
UDC: 691:624.016]:[004.896.02:539.2.091
https://doi.org/10.55302/MESJ24422083ch

Original scientific paper

MODEL-BASED DESIGN STRATEGY FOR MECHANICALLY INTELLIGENT BUILDING BLOCKS

Qianyi Chen[1]*, Dingena Schot[1], Jovana Jovanova[1]

Faculty of ME, Delft University of Technology,
2628 CD Delft, The Netherlands
*Q.Chen-5@tudelft.nl

A b s t r a c t: Soft robots developed by smart materials and structures present advantages in adaptability and flexibility for tailored functions in complex environment. However, conventional design methodologies, which heavily depend on experimental procedures, present obstacles to rapid and efficient design iterations. Thus, employing model-based design emerges as an effective approach to support the designs of soft actuators. In this study, the building blocks was proposed employed by model-based design strategy to investigate the novel actuation approach in mechanically intelligent morphing structures. The simulation results demonstrate, utilizing model-based strategy is the efficient way to develop building blocks of different morphing structures. Furthermore, the combined effort of various smart materials enables varied adapabilities and flexibilities. In summary, by integrating different modeling approaches, material models, and contact models, it is feasible to efficiently design the inteligient structures based on the tailored building blocks to specific requirements, thereby providing guidance and support for engineering design.

Key words: soft actuator; smart material; model-based design; mechanically intelligent; building block

СТРАТЕГИЈА ЗА ДИЗАЈН ЗАСНОВАН НА МОДЕЛИ НА МЕХАНИЧКИ ИНТЕЛИГЕНТНИ ГРАДБЕНИ БЛОКОВИ

А п с т р а к т: Меките роботи направени од структури со паметни материјали имаат предност во приспособливоста и флексибилноста за извршување функции во сложено опкружување. Сепак, конвенционалните методологии за дизајн, кои во голема мера се темелат на експериментални пробувања, претставуваат пречка за брзи и ефикасни итерации на дизајнот. Дизајн базиран на модели се разви како ефективен пристап за поддршка на иновативен дизајн на меки актуатори. Во ова истражување се предложени градбени блокови со промени на кои нова методологија за дизајн базиран на модели може да придонесе за нова генерација механички интелигентни структури кои ја менуваат формата самостојно. Резултатите од симулацијата покажуваат дека користењето на стратегија заснована на модели е ефикасен начин за развој на градбени блокови со посебни променливи структури. Понатаму, комбинирањето на различни паметни материјали овозможува различни приспособувања и флексибилност. Накратко, со интегрирање на различни пристапи за моделирање, модели на материјали и модели за контакт, се овозможува ефикасно дизајнирање на интелигентни структури врз основа на градбени блокови приспособени на специфични барања.

Клучни зборови: мек актуатор; паметен материјал; дизајн базиран на модел; механички интелигентни структури; градбен блок

1. INTRODUCTION

Soft robotics exhibit a notable advantage in enhancing flexibility and adaptability, finding extensive utilization in diverse industrial applications [1, 2], from medical to agriculture and offshore. Soft actuators are essential components enabling soft robots to achieve various deformation behaviors, with morphing structures playing a central role in the design and functionality of these actuators. Soft actuators can be categorized into various traditional types, encompassing electrical, pneumatic, particle

jamming, and chemical reaction-based actuators. Dielectric elastomers (DE) represent a prominent class of materials primarily employed in electrical actuation, utilizing electrical systems as power sources to induce deformation. These materials find significant application in the construction of self-folding structures [3, 4]. Pneumatic actuators, widely favored for actuation in soft actuators, experience consistent deformation and elongation due to the exertion of air pressure through pneumatic systems [5]. Utilizing pneumatic principles, a technique known as particle jamming actuation has been devised to augment the rigidity of soft robots [6]. Through the removal of air within the enclosed space, a phenomenon of particle interlocking emerges, enabling grippers based on particle jamming to securely grasp a diverse range of objects, spanning from delicate to substantial ones [7]. The chemical reaction actuator, fueled by combustion, finds application primarily in jumping robots and bioinspired designs [8]. However, traditional actuation methods often require additional power systems, which limits their applicability. Smart materials, possessing distinct capabilities, offer novel avenues for advancing the design of adaptable and dynamic soft actuators. These materials can undergo structural or compositional changes in response to various external stimuli such as electricity, magnetic fields, light, heat, or chemical reactions [9, 10].

The evolution of soft actuators frequently necessitates cumbersome and ineffectual experimental investigations. Alternatively, computational simulations offer a more streamlined and potentially superior adjunct to this procedure. Modeling soft actuators poses significant challenges due to their pronounced nonlinear behavior and complex geometries. The finite element method (FEM), a widely utilized technique in nonlinear mechanics modeling, provides an efficient means to address these challenges without relying on explicit analytical frameworks [11]. FEM excels in accommodating substantial deformations and material nonlinearities during deformation processes. Consequently, FEM-based models offer a viable means to predict the performance of soft actuators and evaluate the viability of different designs under varying input conditions, thereby streamlining both cost and development timelines [12]. Besides, as for the actuator actuated by particle jamming, coupling method of finite element method and discrete element method (FEM-DEM) is also an effective method to investigate the interaction behaviors between the granular materials and flexible boundary [13]. In the coupling method, FEM serves as a precise tool for characterizing the deformations occurring within the chamber under external loads. Furthermore, the discrete element method (DEM) proves invaluable in modeling particle interactions within granular materials, particularly when dealing with a limited quantity of particles. Notably, DEM offers a computationally efficient alternative to traditional FEM approaches, making it particularly advantageous in scenarios where computational resources are constrained [14]. However, the prevailing focus of contemporary soft robot designs predominantly serves industries such as agriculture, logistics, and food processing. However, there exists a noticeable scarcity of designs tailored specifically for deployment in marine, offshore, and port engineering.

In this study, we developed a model-based design strategy using smart material structures to create mechanically intelligent building blocks for soft robotics. The key contributions are as follows: First, we demonstrated the effectiveness of the model-based approach for designing smart actuators. Second, we introduced the concept of building blocks to establish mechanically intelligent morphing structures for soft robotics. Third, we constructed numerical models, including FEM and coupled FEM-DEM models, to capture the nonlinear behavior of smart materials and the interactions between particles and soft bodies, verifying the feasibility of the proposed design strategy. Finally, this approach was successfully applied in various scenarios, such as underwater pipe manipulation, windmill blade installation, and seabed pipe maintenance.

2. DESIGN PROCESS

Model-based design offers a highly efficient and optimized approach in engineering, emphasizing the creation of an optimal design plan based on specific requirements. Unlike traditional methods that rely on physical prototypes, model-based design utilizes numerical models and simulation techniques for iterative improvements, resulting in resource savings and optimized structural designs. The basic design process is shown in Figure 1. In the initial phase, selecting the appropriate smart materials is critical, as they form the foundation for actuation. Once this is determined, the "building blocks" are created. These building blocks are fundamental units of mechanical intelligence, designed by integrating the chosen smart materials, geometric configurations, and external stimuli.

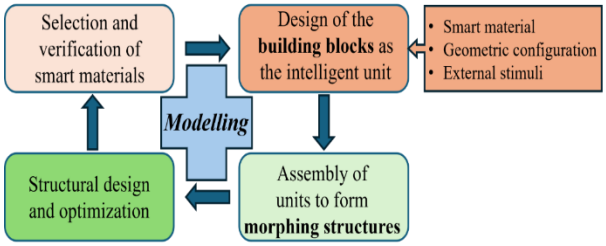

Fig. 1. The design process of the model-based design strategy

Using the modular concept of these building blocks, various configurations can then be assembled to achieve specific deformation behaviors, which are referred to as morphing structures. Furthermore, structural designs for specific applications are created by combining different building blocks. After optimization, different smart materials can be integrated to enhance the actuator's performance. Throughout all stages of this process, numerical modeling is the main approach in guiding the design.

3. METHODOLOGY

The model-based design approach is fundamental for developing the building blocks. The modelling flowchart, illustrated in Figure 2, begins with defining design requirements based on application scenarios, such as scale, environmental conditions, and boundary constraints. From these requirements, spatial and temporal domains are established.

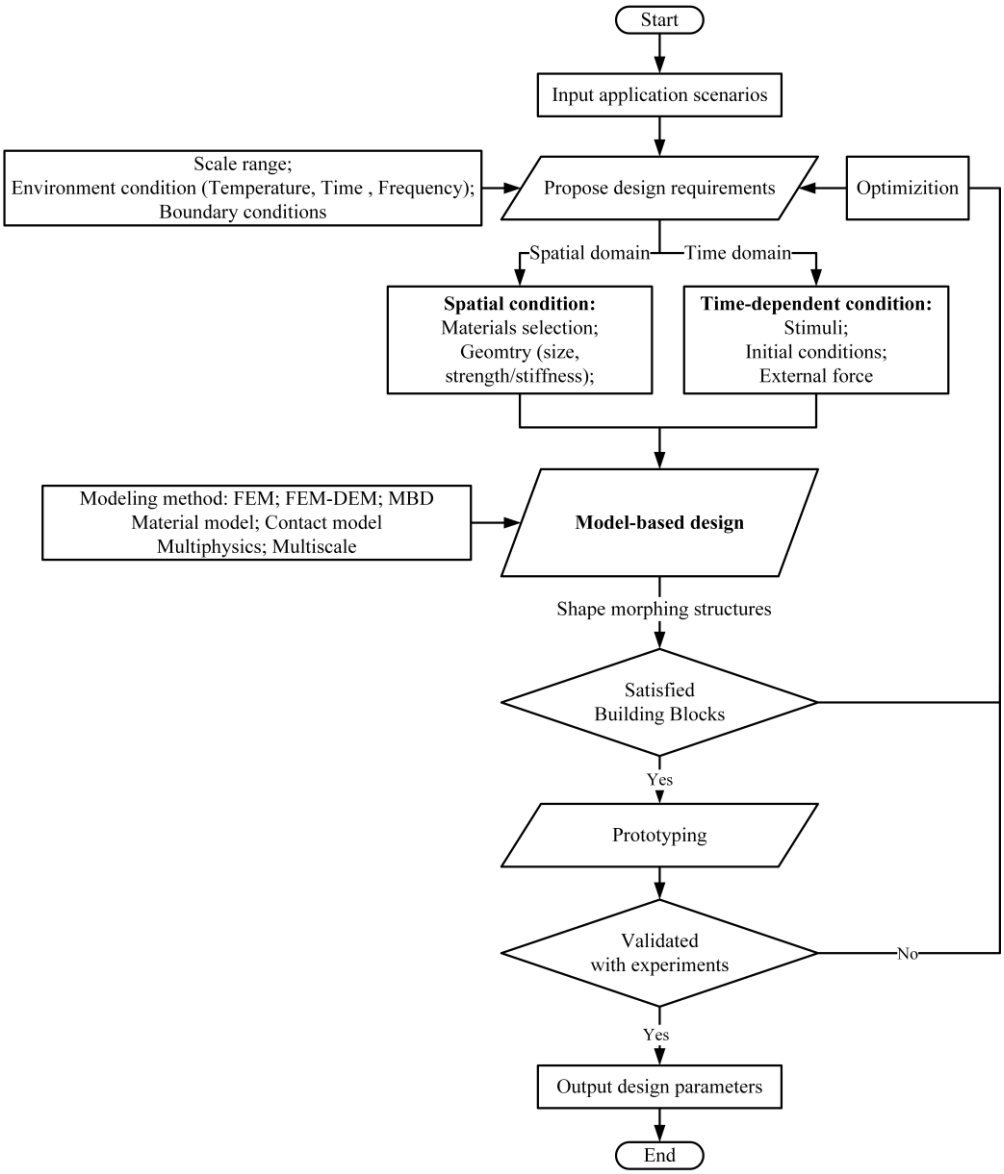

Fig. 2. The design process of the model based design

Spatial conditions include smart materials and structural geometries, while time-dependent factors involve environmental stimuli, initial conditions, and external loads. These inputs are incorporated into the model-based design framework. In the model-based design step, various numerical methods, such as FEM, DEM, multibody dynamics (MBD), and coupling techniques, are then employed for simulations across multiple scales. The simulation results inform the analysis of different design configurations, which are further refined through optimization. The final design is realized through fabrication and experimental validation. In general, numerical modeling, particularly for capturing the nonlinear properties of materials, is a critical aspect of this process, with commonly used methods also discussed in this section.

FEM model

FEM is commonly used in the structure and non-linear mechanics behavior analysis. In our study, we used FEM as the basis for smart materials, including temperature-sensitive hydrogel and shape memory polymers. Also, the hyperelastic properties of nonlinear materials are analyzed by FEM in the membrane configuration.

First, in our study, the thermos-responsive hydrogel is modeled by FEM. The temperature-sensitive hydrogel, polyhydrogel has garnered significant academic interest owing to its distinctive characteristics, including facile synthesis and robust stability. Considering hydrogel as a hyperelastic substance and applying the nonlinear field theory that integrates diffusion and deformation [15], the hydrogel can be expressed by free energy function,

$$W(I_1, I_3, \mu, T) = \frac{1}{2} N k_B T (I_1 - 3 - 2\log I_3) - \\ - \frac{k_B T}{\nu}\left[(I_3 - 1)\log\frac{I_3}{I_3 - 1} + \frac{\chi(T, I_3)}{I_3}\right] - \frac{\mu}{\nu}(I_3 - 1), \quad (1)$$

where $I_1 = F_{iK}F_{iK}$ and $I_3 = \det \mathbf{F}$ are the first and the third invariants of the deformation gradient tensor. Furthermore, μ is represents the chemical potential, T denotes the temperature, N signifies the number of chains per polymer volume, ν is the volume of a solvent molecule, and k_B stands for the Boltzmann constant. Then, it is conventional to establish a reference state wherein the polymer network achieves equilibrium with a solvent possessing a specific chemical potential denoted as μ_0. This reference state involves free swelling, where the swelling coefficient (λ) remains uniform in all spatial directions, denoted as $\lambda_x = \lambda_y = \lambda_z = \lambda_0$. Given the free swelling nature of the reference state, the swelling ratio (J) is determined as the cube of the swelling coefficient $J = {\lambda_0}^3$. Adhering to these stipulations, the equilibrium state can be delineated as follows,

$$\frac{\mu_0}{kT} = \frac{N\nu}{\lambda_0^3}(\lambda_0^2 - 1) + \log\left(1 - \frac{1}{\lambda_0^3}\right) + \frac{1}{\lambda_0^3} + \frac{\chi}{\lambda_0^6} \quad (2)$$

Moreover, the Flory-Huggins interaction parameter, χ, quantifies the enthalpy associated with the blending mechanism and is articulated with respect to T and I_3 for a temperature-sensitive hydrogel,

$$\chi(T, I_3) = A_0 + B_0 T + \frac{A_1 + B_1 T}{I_3} \quad (3)$$

The experiments can take the coefficients A_i and B_i as $A_0 = -12.947$, $B_0 = 0.0449\ \mathrm{K}^{-1}$, $A_1 = 7.92$, $B_1 = -0.0569\ \mathrm{K}^{-1}$ [16]. In addition, the expression of stresses immediately follows, and the first Piola-Kirchhoff stress is computed as,

$$\mathbf{P} = \frac{\partial W_0(I_1, I_3)}{\partial \mathbf{F}} = \frac{\partial W_0(I_1, I_3)}{\partial I_1}\frac{\partial I_1}{\partial \mathbf{F}} + \frac{\partial W_0(I_1, I_3)}{\partial I_3}\frac{\partial I_3}{\partial \mathbf{F}} \quad (4)$$

In the simulations, we standardize material stresses and Young's modulus by $k_B T/\nu$, where the estimated value is 4×10^7 Pa. Different synthesis conditions yield various initial swelling ratios, and without loss of generality, λ_0 is fixed to 1.5 is uniformly set to 1.5 for all three directions, representing an equilibrium chemical potential of $\mu_0 = -0.01$ for the hydrogel material [17].

In addition, hyperelastic model is also adopted for shape memory polymer (SMP). SMP demonstrates significant visco-elasticity throughout its shape memory, spanning temperatures both above and below the glass transition temperature. This viscos-elastic response exhibits a pronounced time–temperature dependency [18, 19]. In our study, we employed the superimposed generalized Maxwell model and Williams-Landel-Ferry (WLF) equation within FE solver to elucidate the mechanical behavior of SMP. The utilized constitutive equations for the multi-branch viscos-elasticity are as follows [20],

$$\sigma(t) = \varepsilon_0 E_n + \varepsilon_0 \sum_{i=1}^{n-1} E_i e^{\frac{-t}{\tau_i}}, \quad (5)$$

where $\sigma(t)$ represents stress at time t, ε_0 is the strain at the initial time, E_n denotes the instantaneous modulus, E_t and τ_i represent the elastic modulus and relaxation time of the Maxwell element i, respectively. The relation of relaxation modulus E in the

generalized Maxwell equation with time t is expressed as follows,

$$E(t) = E_n + \sum_{i=1}^{n-1} E_i e^{\frac{-t}{\tau_i}} \quad (6)$$

and satisfies the limit condition, $\lim_{t\to\infty} E(t) = E_n$.

Conducting relaxation experiments at various temperatures and applying the time–temperature equivalence principle is essential. This allows the conversion of the relaxation response curve of SMP across different temperatures into a comprehensive relaxation response curve at a specific temperature. According to the WLF equation [20], the connection between the relaxation time at the present temperature T and the relaxation time at the reference temperature of T_r can be written as,

$$\lg\alpha_T = \lg\frac{\tau}{\tau_r} = \frac{-C_1^S(T-T_r)}{C_2^S+(T-T_r)}, \quad (7)$$

where α_T represents shift factor, C_1^S and C_2^S are material constant.

Besides, silicone is frequently employed as the standard material in soft actuators to facilitate substantial deformations. The Neo-Hookean constitutive model is utilized in the finite element solver to articulate the stress-strain correlation and manifest hyperelasticity traits,

$$W_{\mathrm{NH}} = \mu_{\mathrm{NH}}(\overline{I_1} - 3), \quad (8)$$

where μ_{NH} represents a material constant, $\overline{I_1}$ denotes the first invariants of the deformation gradient tensor.

FEM-DEM model

The FEM typically analyzes deformations of components under external loads, while the DEM focuses on particle-level materials. To model a soft actuator driven by granular materials, it is essential to couple FEM and DEM for a comprehensive analysis.

The movements of both discrete element and finite element nodes adhere to Newton's Second Law. Consequently, the external force F_i acting on both discrete element and finite element node i is expressed as follows,

$$F_i = m_i\left(\frac{d^2\boldsymbol{u}_i}{dt^2}\right), \quad (9)$$

where m_i denotes the mass of element i, and $\boldsymbol{u}_i$ represents the displacement of element i. Furthermore, the centroidal moment of the discrete element i is expressed as follows [21],

$$M_i = I_i\left(\frac{d^2\boldsymbol{\theta}_i}{dt^2}\right). \quad (10)$$

where I_i is the inertia moment of element i and $\boldsymbol{\theta}_i$ is the rotation angle of element i. Both of the equation (8) and equation (9) are solved using explicit finite difference method.

Furthermore, the interaction force can be divided into normal force and the tangential force, the normal force F_n, and the tangential force F_s can be expressed as,

$$F_n = F_{n,e} + F_{n,v} \quad (11)$$

$$F_s = \begin{cases} F_{s,e} + F_{s,v} & |F_s| < \mu|F_n| \\ \mu F_n & |F_s| \geq \mu|F_n| \end{cases}, \quad (12)$$

where $F_{n,e}$ and $F_{n,v}$ are the normal spring force and the normal damping force. Moreover, $F_{s,e}$ and $F_{s,v}$ denote the tangential spring force and tangential damping force. Additionally, the μ is friction coefficient.

During the coupling process, FE elements, along with their grid information, are mirrored into the DEM solver as a wall condition [22]. This involves calculating interaction forces and loads between particles and the wall within each DEM time step. Subsequently, node forces are computed based on particle loads and interpolated onto each FEM element. These node forces are then transformed into distributed loads to facilitate interpolation onto each FE element, enabling the calculation of mesh element deformations and node displacements.

FEM-MBD model

The MBD approach is employed to comprehensively capture the motion information, enabling the simulation of scenarios involving significant deformations and the loading process. A coupling between the MBD and FEM models is established to facilitate the transfer of information between rigid and deformable components. This coupling strategy leverages the intrinsic properties of the MBD module to effectively constrain the actuator's motion. Additionally, the embedded characteristics of the MBD module allow for the formation of a rigid linkage between components, irrespective of the motion framework. In the coupling strategy, during each time step of the FEA-MBD algorithm, stress and strain are computed using the FE solver, while displacements are determined by the MBD model. Importantly, throughout this process, nodes involved in rigid connections receive stress information from the FE solver to aid in displacement calculations.

Additionally, the presence of various rigid connections restricts structural motion to a certain degree, allowing the MBD model to accurately represent the motion characteristics of the multibody system.

4. CASE STUDY

In this section, various building blocks have been proposed to demonstrate the feasibility of the model-based design strategy. The building block is the modular concept consists of structure geometry, smart materials and environmental stimuli. Shown in Figure 2, the structure geometries include the meta-structure or particles as the selection in our design, then the smart materials include smart hydrogels, shape memory polymers (SMPs), and shape memory alloys (SMAs). In addition, the enviroemental stimuli include temperature and chemical relating stimuli. To fit specific scearios, different structure geometris, smart materials, and stimuli will be combined into any new building blocks to achieve tailored functions, then based on the building blocks, the mechanically intelligent morphing structures can be developed.

Smart materials and smart mechanism building blocks

The first is the proposition of a particle-based actuator, formulated through model-based design, aims to fulfill the demands for significant deformation and substantial bending stiffness. The analysis of this proposed actuator is conducted utilizing the FEM-DEM approach. The design concept is shown in Figure 3, different sized particles are filled into different chambers, separated by a middle layer. The chambers are enveloped by an elastic membrane. During the actuation phase, the membrane undergoes contraction, facilitated by a specified shrinking coefficient, resulting in the deformation of the whole element. This deformation causes the actuator to exhibit a bending motion towards the left, propelled by the discrepancy in volume between the two chambers. Furthermore, subsequent to the contraction process, the actuator's stiffness experiences augmentation due to the phenomenon known as particle jamming. The phenomenon of particle jamming denotes a transition in the packing state of particles. Initially, particles are loosely encapsulated, representing a state of natural packing that permits particle mobility within the membrane. However, as the packing state transitions to a tighter configuration, the spatial arrangement of particles undergoes alteration. Consequently, the inter-particle contact forces and interactions between particles and the membrane intensify, impeding particle mobility. This transition results in the aggregation of particles into a solid-like state, leading to the formation of a jammed configuration.

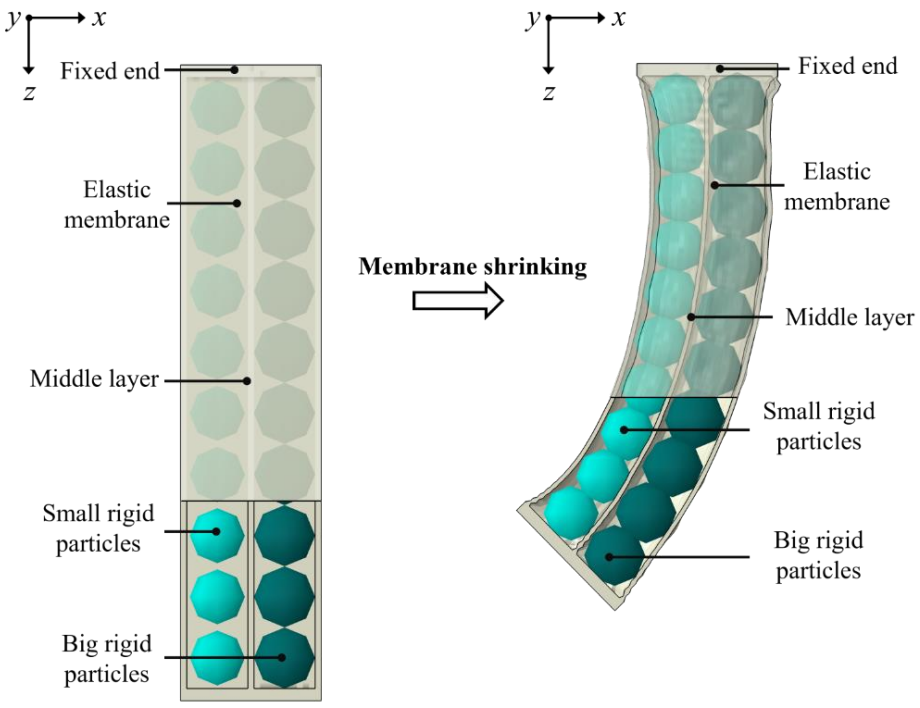

Fig. 3. The actuation process of the particle-based actuator

Secondly, to meet the demands of active actuation, the adoption of responsive materials capable of autonomous response to external stimuli holds promise for integration into soft grippers. Operating as an active smart material, hydrogels demonstrate changes in shape in response to particular external stimuli. Among these, thermally responsive hydrogels offer enhanced adaptability and compatibility [23]. Actuators employing thermally responsive hydrogels undergo alterations in hydrogel volume in response to fluctuations in ambient temperature, consequently demonstrating notable directed deformations within defined temperature ranges. Thus, this section elucidates the characterization of hydrogels and other nonlinear materials through the hyperelastic model by employing FEM. The smart structure depicted in Figure 4 employs a thermally responsive hydrogel as its foundation. This hydrogel particle is connected to a conventional soft particle, typically composed of silicone or rubber, known for its stable chemical characteristics. Initially, both the hydrogel particle and the normal soft particle exhibit identical dimensions. Subsequently, the hydrogel particle undergoes swelling upon exposure to a water environment with temperature change. As the results, this smart element will exhibit a configuration featuring particles of two distinct sizes, which can be used as the basis for different configurations.

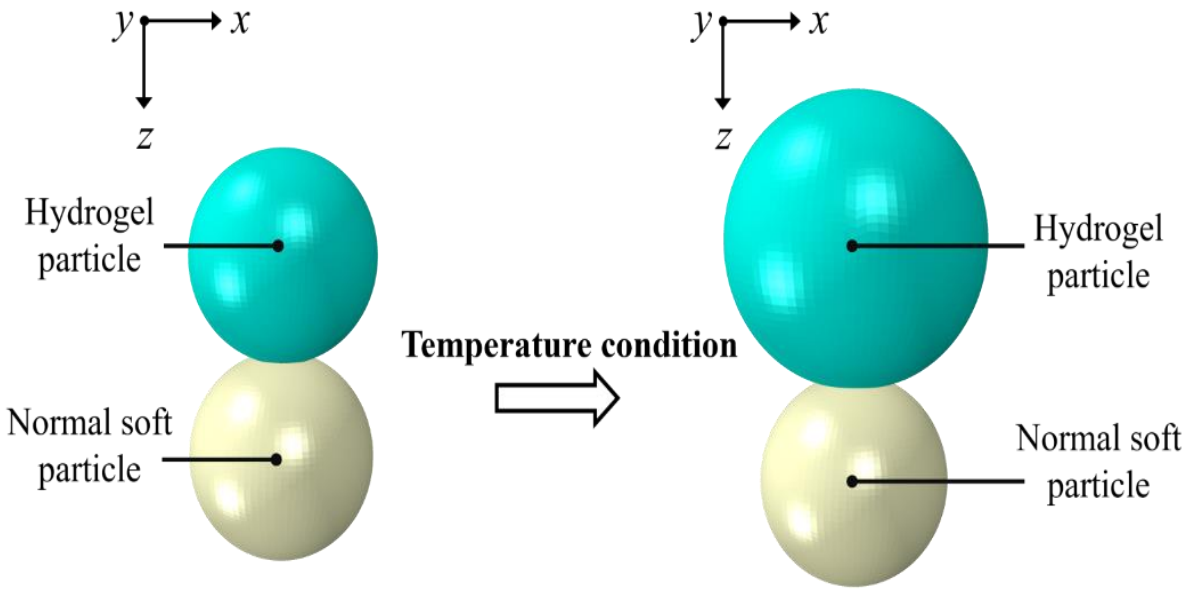

Fig. 4. Smart structure element based on hydrogel particle

The smart structures based on the smart element are developed by the modeling and the configurations are shown in Figure 5. Figure 5a illustrates a smart structure capable of both expansion and contraction. This smart structure comprises elementary smart elements arranged in an alternating fashion. In the initial state, all the particles are in the same size. Subsequently, the hydrogel particles undergo swelling induced by changes in temperature, leading to elongation of the structure. Hydrogel particles assume a primary role in actuation, with normal soft particles serving a supplementary function in maintaining structural stability. Temperature manipulation is employed to achieve the expansion and contraction of the hydrogel particles, thus governing the elongation and contraction of the structure. Figure 5b shows a smart structure that can achieve grasping behaviours. This smart structure consists of modular smart elements organized to construct a dual-layered framework with 4 branches. In the initial phase, all branches exhibit a straight configuration characterized by uniform-sized hydrogel and normal elastic particles. Subsequently, the hydrogel particles undergo a swelling phenomenon. Due to constraints imposed by the normal elastic particles, each branch gradually undergoes bending towards the central axis during the swelling of the hydrogel particles, thereby manifesting a grasping behavior.

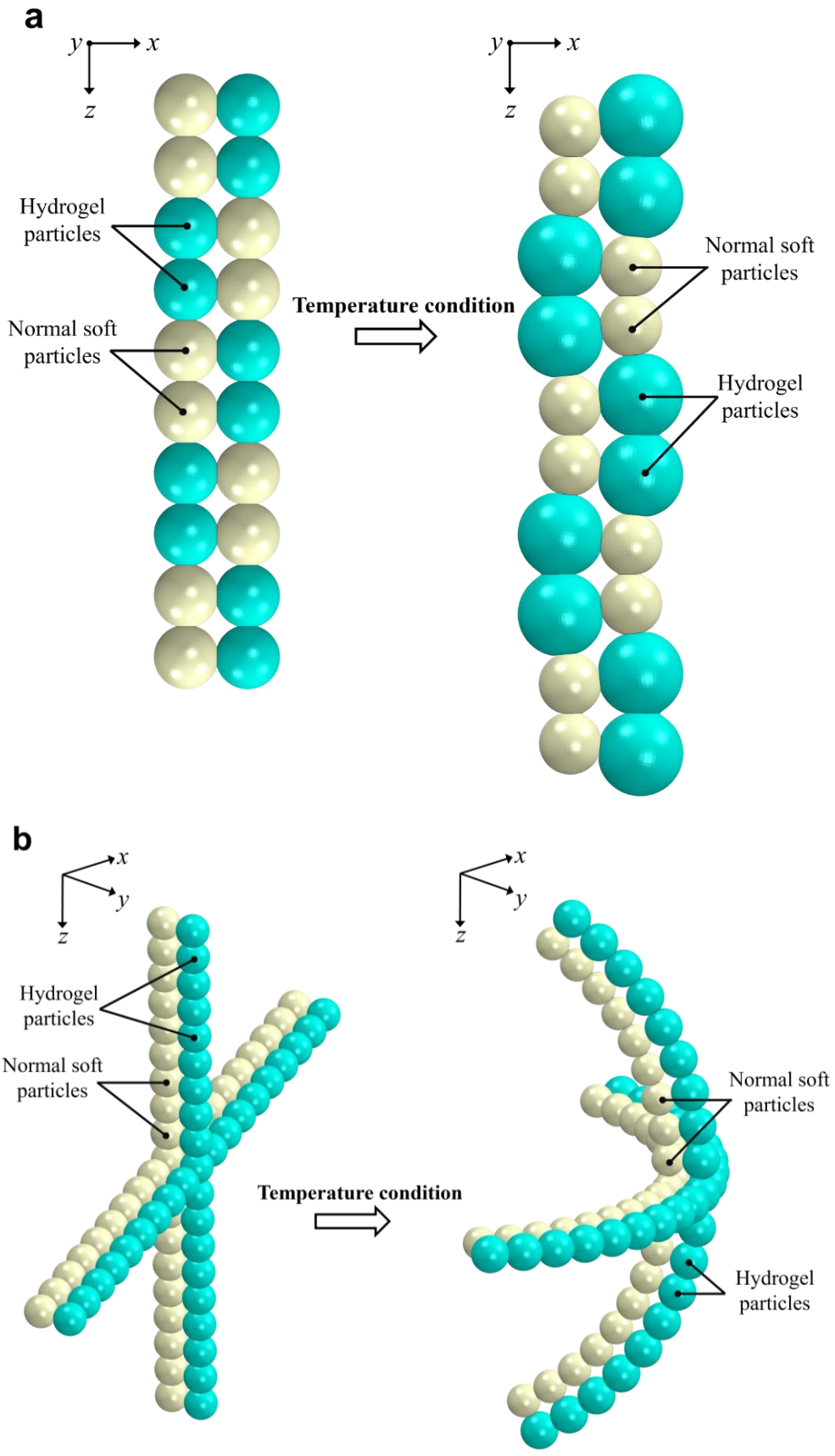

Fig. 5. Different smart structures based on the smart elements:
(a) Configuration of elongation structure.
(b) Configuration of grasping structure

Multiple smart materials based building blocks

In the situation of underwater pipe manipulation and seabed pipe maintenance installation, attaining active deformation along with high stiffness and adaptability is imperative. Consequently, the integration of various smart materials becomes essential for effective implementation. SMPs are materials distinguished by their ability to retain a predetermined, permanent shape, undergo manipulation to adopt a temporary configuration under specific conditions of temperature and stress, and subsequently revert to their original, stress-free state upon exposure to thermal, electrical, or environmental stimuli. Given their unique capacity to maintain two distinct shapes under varying conditions, SMPs hold significant promise for utilization in smart actuator systems. The illustration presented in Figure 6 depicts the integration of a building block incorporating SMP as its base along with hydrogel protrusions. The SMP base primarily functions as the actuation mechanism facilitating substantial deformation. Conversely, the hydrogel protrusions serve as the supportive framework aimed at enhancing the adaptability of the smart actuator. In the initial state, the SMP base exhibits a curved form, while the hydrogel protrusions maintain a state of minimal swelling. Upon the application of an external force or stimuli, the SMP base undergoes a temporary morphological change. Subsequently, when the temperature surpasses the critical threshold of the SMP, the material reverts to its original shape. Following the shape recovery process, lowering the temperature again serves to both fix the SMP shape and induce further swelling of the hydrogel protrusions. Through this cycle process, the SMP base achieves bending behavior, facilitated by the swelling and contraction of the hydrogel protrusions to modulate the structure's thickness and enhance its adaptability.

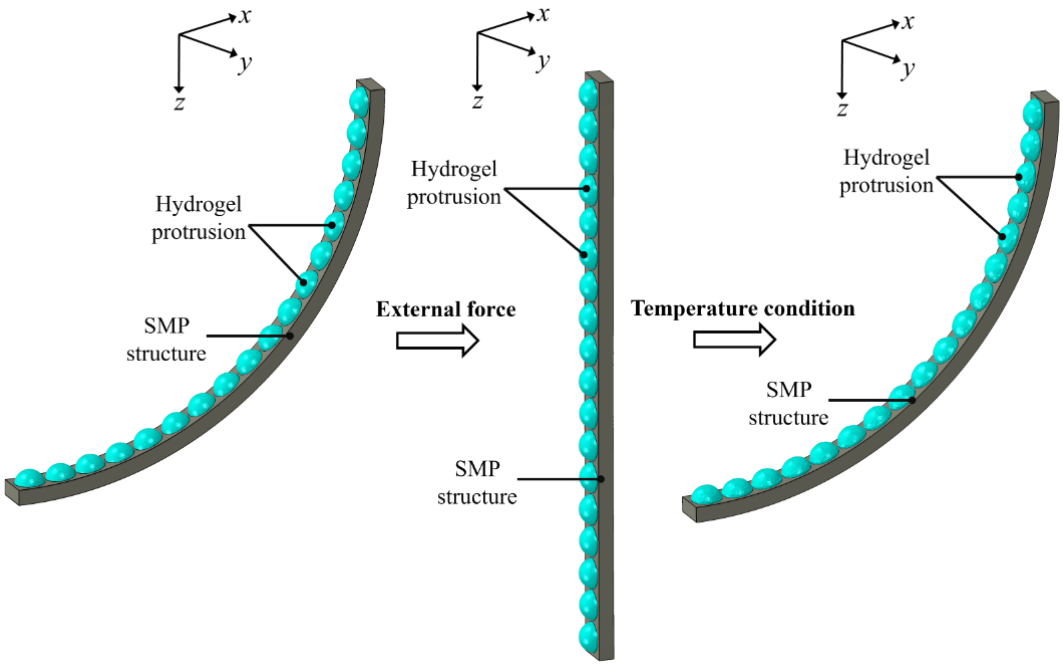

Fig. 6. The building block based on SMP and hydrogel

As shown in Figure 7, the proposed building block exhibits potential for development in specific applications. This potential finds utility within underwater environments for tasks of pipeline maintenance. The operational sequence involves initial deformation of the composite structure through external force, maintaining it in a temporary configuration. Following immersion in water, the entire structure gradually approaches the local section of the pipeline. Subsequently, the pressure valve initiates opening to release high-pressure hot gas. As a result of the elevated temperature of the hot air, adjacent water experiences thermal conduction, leading to its heating. With the increased temperature, the SMP base undergoes bending, reverting to its original configuration, thus enveloping the pipeline in need of maintenance to ensure safety. Upon the gradual decrease in nearby water temperature, the hydrogel

protrusion undergoes swelling, subsequently making contact with both the pipe valve and its outer wall. The inherent softness of the hydrogel structure serves to shield the pipe from potential damage due to collisions. Furthermore, the hydrogel functions to fill the space between the pipe and actuator, thereby promoting pipe stability.

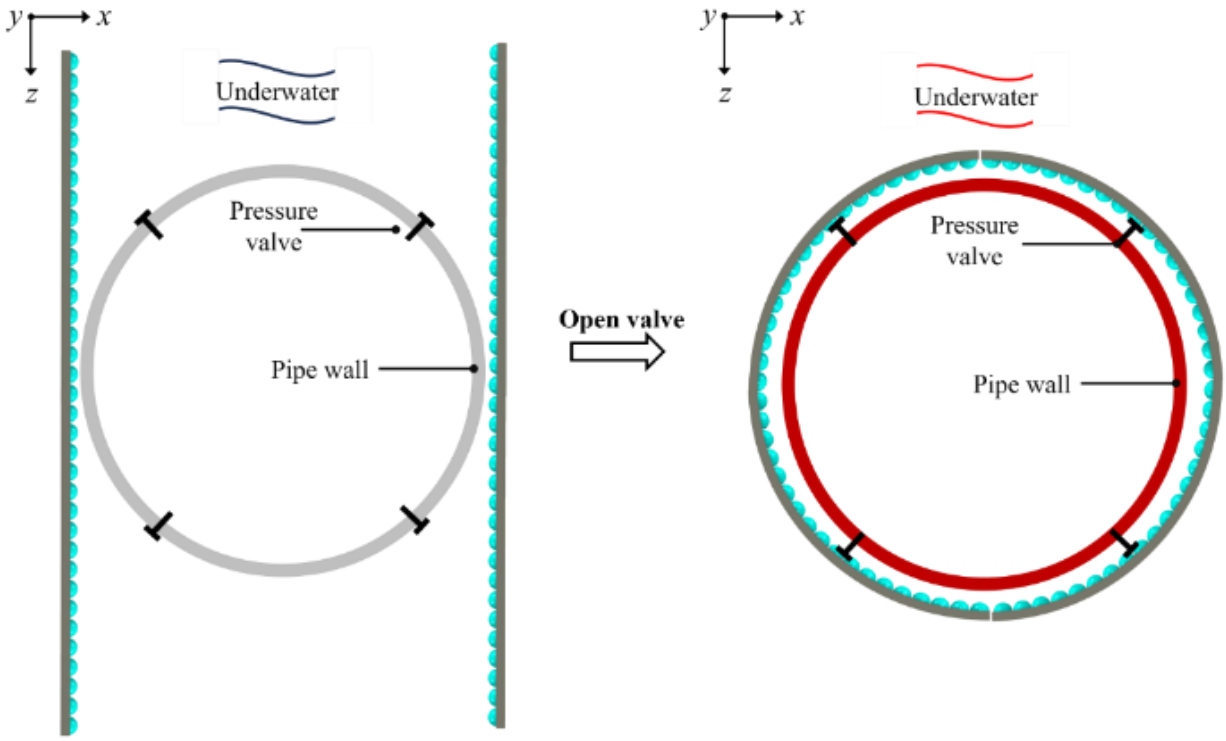

Fig. 7. Potential application of the multiple smart materials based building blocks

Based on the cases study, the advantages, application, and stimuli of the smart hydrogels and SMPs can be concluded (Table 1). Hydrogels and SMPs are tailored for distinct applications due to their unique properties. Hydrogels, with their ability to undergo large deformations and respond to stimuli like pH or temperature, are ideal for actuation in soft robotics and artificial muscles. Their flexibility and water absorption make them perfect for dynamic environments. Conversely, SMPs are prized for their stiffness variation and shape recovery, excelling in applications like underwater components in unpredictable environment. Besdeis, the lightweight and programmable properties of SMPs also ensure structural integrity and precision where stability is critical.

T a b l e 1

Conclusion of hydrogels and SMPs

Smart material	Advantages	Stimuli	Applications
Hydrogel	Large deformation capability High water absorption	pH Temperature Light Magnetic field Electric field	Soft actuators Sensors
SMP	Tunable stiffness variation High recoverable strain Programmable shapes	Heat Light Magnetic field	Smart textiles Self-healing Underwater component

In conclusion, the comprehensive design framework is shown in Figure 8. The process begins with the selection of smart materials capable of changing shape, volume, and stiffness in response to environmental stimuli. Replacing conventional soft materials with these smart materials enables energy harvesting from natural sources and reduces dependence on external power, facilitating self-actuation in complex or unpredictable environments. In addition, smart materials like shape memory materials also enable stiffness changes, enhancing adaptability and stability in real-world applications. By combing multiple smart materials, the self-actuation unit, which refers to "building blocks", can be developed to achieve specific deformations, such as surface folding, shell volume changes, or joint bending. Then, the morphing structures are assembled into more complex structures, which can be modularly configured to perform different behav-iours. Finally, the mechanical intelligence relating to the soft robotics can be developed by the structural design based on the morphing structure for various tasks, such as locomotion or manipulation.

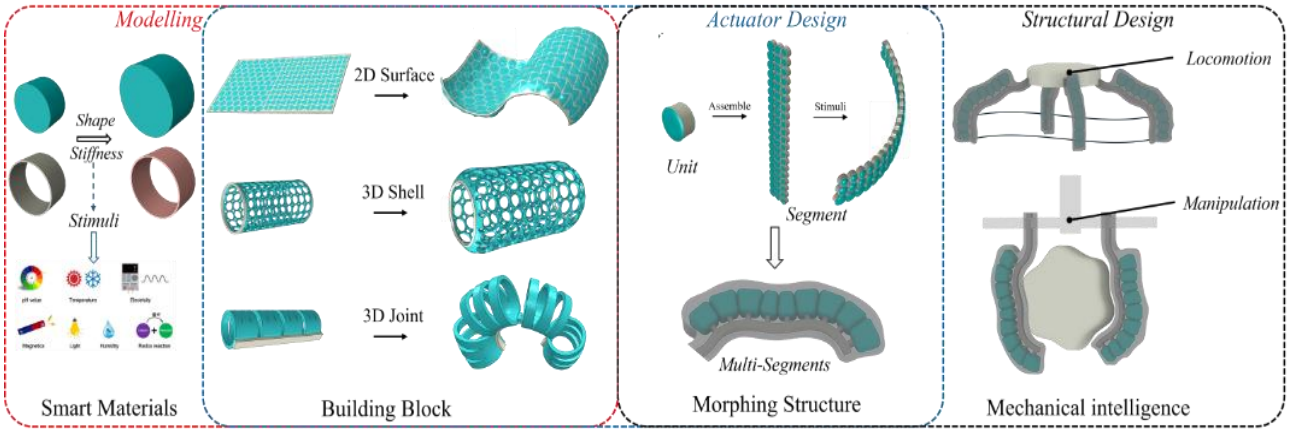

Fig. 8. The model-based design process of the smart building blocks

5. CONCLUSION

The soft robot in this study demonstrates advanced capabilities with high-level adaptabilities and flexibilities, enabling the creation of complex structures. The soft actuator, a key component of the soft robotic system, is crucial in driving the robot's overall functionality. This research explored the potential of model-based design approaches for developing building blocks of modular components that can be combined to form mechanically intelligent structures with specialized functions.

Numerical methods, such as the finite element method (FEM) and the combined finite element and discrete element method (FEM-DEM), offer significant potential for advancing smart actuator systems. FEM, in particular, is highly effective for characterizing the hyperelastic behavior of shape memory polymers (SMPs) and smart hydrogels. Additionally, the FEM-DEM approach has proven useful in analyzing particle-based mechanisms that undergo large deformations.

By employing variable smart actuation methods, it is possible to tailor the functions of these components to specific applications. Particle-based building blocks, for example, demonstrate substantial deformation capabilities and can increase stiffness. Temperature-sensitive hydrogels exhibit active deformation properties, making the building blocks suitable for applications such as elongation and grasping. A hybrid design combining SMP and smart hydrogel can further enhance these actuators by offering both active deformation and stiffness control, enabling functions such as grasping, installation, and maintenance while improving the adaptability of the modular building blocks.

In the future, an improved methodology grounded in model-based design principles will be developed. This approach will integrate theoretical models with experimental validation, ultimately enabling the systematic design and manufacturing of engineering-ready building blocks for soft robotic systems.

Acknowledgment

This work is supported by the National Natural Science Foundation of China Grant No. 52071240, the Higher Education Discipline Innovation Project Grant No. BP0820028, and China Scholarship Council Grant No. 202006950011. The financial contributions are gratefully acknowledged.

REFERENCE

[1] Albu-Schaffer. A., Eiberger, O., Grebenstein, M., Haddadin, S., Ott, C., Wimbock, T., Wolf, S., Hirzinger, G. (2008): Soft robotics, *IEEE Robotics & Automation Magazine*, vol. **15**, no. 3, pp. 20–30.

[2] Chen, A., Yin, R., Cao. L., Yuan, C., Ding, H., Zhang, W. (2017): Soft robotics: Definition and research issues. *24th International Conference on Mechatronics and Machine Vision in Practice (M2VIP)*, Auckland, New Zealand, pp. 366–370. DOI: 10.1109/M2VIP.2017.8267170

[3] Koh, S. J. A., Keplinger, C., Li, T., Bauer, S., Suo, Z. (2010): Dielectric elastomer generators: How much energy can be converted?, *IEEE/ASME Transactions on mechatronics*, vol. **16**, no. 1, pp. 33–41. DOI: 10.1109/TMECH.2010.2089635

[4] Chen, F., Wang, M. Y. (2016): Simulation of networked dielectric elastomer balloon actuators, *IEEE Robotics and Automation Letters*, vol. 1, no. 1, pp. 221–226.

[5] Bishop-Moser. J., Kota, S. (2015): Design and modeling of generalized fiber-reinforced pneumatic soft actuators, *IEEE Transactions on Robotics*, vol. **31**, no. 3, pp. 536–345.

[6] Li, Y., Chen, Y., Yang, Y., Wei, Y. (2017): Passive particle jamming and its stiffening of soft robotic grippers, *IEEE Transactions on Robotics*, vol. **33**, no. 2, pp. 446–455.

[7] Wei H., Shan, Y., Zhao, Y., Qi, L., Zhao, X. (2022): A soft robot with variable stiffness multidirectional grasping based on a folded plate mechanism and particle jamming, *IEEE Transactions on Robotics*, vol. **38**, no. 6, pp. 3821–3831.

[8] Shepherd, R. F., Stokes, A. A., Freake, J., Barber, J., Snyder, P. W., Mazzeo, A. D., Cademartiri, L., Morin, S. A., Whitesides, G. M. (2013): Using explosions to power a soft robot, *Angewandte Chemie International Edition*, vol. **52**, no. 10, pp. 2892–2896.

[9] Bahl, S., Nagar, H., Singh, I., Sehgal, S. (2020): Smart materials types, properties and applications: A review, *Materials Today: Proceedings*, vol. **28**, pp. 1302–1306.

[10] Sobczyk, M., Wiesenhütter, S., Noennig J. R., Wallmersperger, T. (2022): Smart materials in architecture for actuator and sensor applications: A review, *Journal of Intelligent Material Systems and Structures*, vol. **33**, no. 3, pp. 379–399.

[11] Polygerinos, P., Wang, Z., Overvelde. J. T., Galloway, K. C., Wood, R. J., Bertoldi, K., Walsh, C. J. (2015): Modeling of soft fiber-reinforced bending actuators, *IEEE Transactions on Robotics*, vol. **31**, no. 3, pp. 778–789

[12] Gharavi, L., Zareinejad, M., Ohadi, A. (2022): Dynamic Finite-Element analysis of a soft bending actuator, *Mechatronics*, vol. **81**, pp. 102690. https://doi.org/10.1016/j.mechatronics.2021.102690

[13] Xu, F., Ma, K., Jiang, Q., Guo-Ping, J. (2023): Kinematic modelling and experimental testing of a particle-jamming soft robot based on a DEM-FEM coupling method, *Bioinspiration & Biomimetics*, Vol. **18**. No. 4. DOI 10.1088/1748-3190/acdc73

[14] Chen, Q., Schott, D., Jovanova, J. (2024): Conceptual design of a novel particle-based soft grasping gripper, *Journal of Mechanisms and Robotics*, vol. **16**, no. 5, DOI:10.1115/1.4062647

[15] Hong, W., Liu, Z., Suo, Z. (2009): Inhomogeneous swelling of a gel in equilibrium with a solvent and mechanical load, *International Journal of Solids and Structures*, **46** (17), pp. 3282–3289. https://doi.org/10.1016/j.ijsolstr.2009.04.022

[16] Cai S., Suo, Z. (2011): Mechanics and chemical thermodynamics of phase transition in temperature-sensitive hydrogels, *Journal of the Mechanics and Physics of Solids*, vol. **59**, no. 11, pp. 2259–2278. https://doi.org/10.1016/j.jmps.2011.08.008

[17] Guo, W., Li, M., Zhou, J. (2013): Modeling programmable deformation of self-folding all-polymer structures with temperature-sensitive hydrogels, *Smart Materials and Structures*, vol. **22**, no. 11, pp. 115028. DOI 10.1088/0964-1726/22/11/115028

[18] Haseebuddin, S., Raju, K., Yaseen, M. (1997): Applicability of the WLF equation to polyurethane polyols and film properties of their resins, *Progress in Organic Coatings*, vol. **30**, no. 1–2, pp. 25–30. https://doi.org/10.1016/S0300-9440(96)00650-9

[19] Rudolph, N. M., Agudelo, A. C., Granada, J. C., Park, H. E., Osswald, T. A. (2016): WLF model for the pressure dependence of zero shear viscosity of polycarbonate," *Rheologica Acta*, vol. 55, pp. 673–681.

[20] Ward, I. M., Sweeney, J. (2012): *Mechanical Properties of Solid Polymers*: John Wiley & Sons.

[21] Cundall, P. A., Strack, O. D. (1979): A discrete numerical model for granular assemblies, *Géotechnique*, vol. **29**, no. 1, pp. 47–65. https://doi.org/10.1680/geot.1979.29.1.47

[22] Dratt, M., Katterfeld, A. (2017): Coupling of FEM and DEM simulations to consider dynamic deformations under particle load, *Granular Matter*, vol. **19**, no. 3, pp. 49. https://doi.org/10.1007/s10035-017-0728-3

[23] Haq, M. A., Su, Y., Wang, D. (2017): Mechanical properties of PNIPAM based hydrogels: A review, *Materials Science and Engineering: C*, vol. **70**, pp. 842–855. https://doi.org/10.1016/j.msec.2016.09.081

Mechanical Engineering – Scientific Journal, Vol. **42,** No. 2, pp. 95–100 (2024)
Number of article: 683
In print: ISSN 1857–5293
Received: September 24, 2024
On line: ISSN 1857–9191
Accepted: November 25, 2024
UDC: 665.092-977:[628.33:629.3.027.3
658.511.2
https://doi.org/10.55302/MESJ24422095a

Original scientific paper

EVALUATION TIRE PYROLYSIS PRODUCTS

Slavčo Aleksovski[1], Igor Aleksovski[2], Karmina Miteva[1]

[1]*Faculty of Technology and Metallurgy, "Ss Cyril and Methodius" University in Skopje, Republic of North Macedonia*
[2]*Alkaloid, A.D., Blvd. Aleksandar Makedonski 12, Skopje, Republic of North Macedonia*
slavcho@tmf.ukim.edu.mk

A b s t r a c t: Generating large amounts of solid hazardous waste, such as scrap motor tires, has raised the question of seeking an appropriate method for their recycling. The pyrolysis of waste tires presents a viable solution not only for addressing environmental challenges, but also for converting discarded tires from landfills into valuable products. This thermochemical process offers an opportunity to produce cost-effective fuel. In this study, waste truck tires were converted into value-added products using the pyrolysis method. The pyrolysis process was carried out in a semi-batch reactor in an oxygen-free environment. A semi-batch reactor was automatically controlled, and three thermostatic separators were used for the pyrolysis of waste rubber. The pyrolysis of waste truck tires yields three main products: solid residue, which constitutes 36.50 %; a liquid fraction known as carbon black, accounting for 51.28 %; and a 12.22 % gas fraction, syngas. The basic characteristics of the obtained liquid and solid products were examined.

Key words: pyrolysis; waste tire; semi-batch reactor; products evaluation

ПРОЦЕНА НА ПРОДУКТИ ДОБИЕНИ СО ПИРОЛИЗА НА ГУМА

А п с т р а к т: Создавањето големи количества цврст опасен отпад како што се отпадни автомобилски гуми, го наметнува прашањето за барање соодветен метод за нивно рециклирање. Пиролизата на отпадните гуми претставува остварливо решение не само за справување со еколошките предизвици туку и за конверзија на отпадните гуми од депониите во вредни производи. Овој термохемиски процес дава можност за производство на економично гориво. Во оваа студија, со примена на методот на пиролиза, отпадните гуми од камиони беа конвертирани во производи со додадена вредност. Процесот на пиролиза беше спроведен во полушаржен реактор во средина без присуство на кислород. Полушаржниот реактор е автоматски контролиран, а за пиролизата на отпадна гума беа користени три термостатирани сепаратори. Со пиролизата на отпадни гуми од камиони се добија три главни производи: цврст остаток, кој сочинува 36,50 %; течна фракција позната како црн јаглен, со 51,28 %; и 12,22 % гасна фракција, сингас. Испитувани се основните карактеристики на добиените течни и цврсти производи.

Клучни зборови: пиролиза; отпадна гума; полушаржен реактор; процена на продукти

1. INTRODUCTION

The automobile industry, a fundamental sector in highly developed nations, generates an increasing volume of waste rubber annually. Tire disposal is growing in importance as an environmental issue that still has to be properly resolved. This waste typically finds its way into urban landfills, posing a significant environmental issue due to its non-biodegradable nature. Consequently, utilizing this waste material as a feedstock for fuel production has become an increasingly pressing challenge for numerous researchers. Alternative energy sources arise with the passage of time because fossil energy sources like coal and crude oil are getting exhausted. Waste tires are not biodegradable, and their reuse or recycling requires mechanical or thermochemical treatment [1].

The thermochemical pyrolysis process is a promising technology for the management of organic solid waste. Pyrolysis has been regarded as the

most common and eco-friendly option among waste thermal conversion technologies. This is due to reduced environmental pollution and increased economic advantages [2–5]. The European Tyre & Rubber Manufacturers Association (ETRMA) reports that the annual tire sales in the European Union reach 289 million units, representing merely 20% of the global market, which totals around 1.5 billion tires sold each year worldwide [6, 7]. The pyrolysis method demonstrates its effectiveness by transforming these materials into valuable end products under regulated process conditions. This approach allows for the optimization of specific fractions of interest, particularly the liquid fraction, commonly known as pyrolysis oil, which has a minimal environmental pollution impact [8]. During the pyrolysis process, waste tires are converted into valuable fuel products such as pyrolysis oil, carbon black and syngas. Pyrolysis oil has been derived from polymer materials, used tires, waste textiles, and various biomass compounds. The characteristics of tire pyrolysis oil fuel, such as calorific value (41–44 MJ/kg), density (0.90–98 kg/l), and viscosity (2.5–5.5 mm^2/s), are comparable to those of diesel derived from crude oil [9–13]. Waste rubber, owing to its unique chemical composition, includes 60–65% natural rubber and styrene-butadiene rubber, 25–35% carbon as a filler, 5–7% oil, 1–2% zinc oxide, 1–2% sulfur, along with fatty acids, phenolic resins, stabilizers, antioxidants, petroleum waxes, canvas, and steel wires. It serves as a valuable raw material that can be processed into fuel for use in the automotive sector through refining [14].

The pyrolysis process of waste tires presents a viable solution to address the energy crisis. However, challenges persist regarding the quality of the resulting liquid fraction. These challenges encompass a considerable presence of sulfur, elevated water content, and aromatic compounds, all of which are associated with environmental pollution and health issues [15–17]. The pyrolysis of waste tires serves as an alternative energy source in this world. Diesel fuel can be effectively replaced by waste tire pyrolysis oil. Significant volumes of SOx, NOx, and CO are emitted during tire incineration, making them challenging to handle.

The liquid fuel produced contains significant proportion of aromatic compounds. It exhibits greater viscosity and a higher sulfur content compared to fossil-derived diesel. Consequently, it necessitates further processing either purification or fractional distillation to yield fuels with specific quantities of paraffins, olefins, naphthenes, and aromatic compounds. This additional treatment ensures that the fuel can be utilized safely and complies with the established standards for this category of fuel. Solid residue and gas are produced as by-products, and at times as primary products, each possessing distinct economic value and suitable applications [10, 11, 18].

The pyrolysis of waste rubber is a thermochemical procedure conducted in an oxygen-free environment, frequently utilizing nitrogen, at elevated temperatures ranging from 250 to 550°C, either under vacuum or atmospheric pressure, with or without a catalyst. This process yields three primary products: approximately 50% liquid fuel, around 40% solid residue, and about 10% gas. The yields of products obtained from the pyrolysis process vary based on the type of waste, which has distinct chemical compositions, as well as the type of reactor and specific conditions applied during the process.

The objective of this study was to assess the pyrolysis products derived from the thermochemical conversion of waste tires. The process parameters were optimized to achieve the highest yield of liquid fuel.

2. MATERIALS AND METHODS

The raw material, consisting of shreds from truck tires with an average particle size of 5 mm, underwent pyrolysis in a semi-batch reactor with a volume of 0.4 dm^3. Between 120 and 170 grams of finely chopped rubber are added to a semi-batch reactor. To ensure an inert atmosphere, nitrogen, as an inert gas, is flown into the reactor for 15 minutes. The pyrolysis process was carried out according to a temperature regime (temperature and heating rate) that was programmed by a PID controller (Unitronics V570). The reactor was heated from ambient room temperature to 505°C at a heating rate of 10 °C/min. The optimal conditions for the pyrolysis process of truck tires in a semi-batch reactor to achieve the highest possible yield of pyrolysis oil are depicted in Table 1. The resulting liquid products were separated using three thermostatically controlled, serially connected separators. The first separator is at a temperature of 90 °C, and the second and third are at 0°C. The collected pyrolysis oil is analyzed and characterized according to standard test methods for examining this type of fuel. The pyrolysis oil is a dark-brown liquid with a strong odor, Figure 1.

T a b l e 1

Optimal conditions of the pyrolysis process

Parameter	Measured values
Pyrolysis temperature, °C	505
Heating rate, °C/min	10
Pyrolysis oil, wt.%	51.28
Carbon black wt.%	36.50
Syngass, wt.%	12.22
Start of pyrolysis, °C	325
End of pyrolysis, °C	505

Fig. 1. Pyrolysis oil

3. RESULTS AND DISCUSSION

The chemical analysis was conducted on the properties of the resulting pyrolysis products, which include the amounts of pyrolysis oil (51.28 %) and carbon black (36.50 %). The generated syngas (12.22 %) was calculated based on the mass balance. The density, viscosity, and sulfur content of the pyrolysis oil were measured at 0.9071 g/cm³, 1.865 mm²/s, and 0.42 %, respectively (Table 2). The fixed carbon and ash content of the carbon black were determined to be 41.06 % and 25.63 %, respectively (Table 3 and Figure 2).

T a b l e 2

Chemical analysis of unrefined pyrolysis oil

c	Measured values	Test method
Appearance (visual)	Opaque liquid	
Color (visual)	Black	
Density at 15 °C, kg/m^3	0.9071	ASTM D4052
Kinematic viscosity at 40 °C, mm^2/s	1.865	EN ISO 3104
Ignition point, °C	<40	ASTM D 93
pH	9	
Refractive index	1.6893	ASTM D 1218
Distillation at 101.3 kPa*		
Initial boiling point/IBP, °C	45.2	ASTM D 86
Flow temperature, °C	< minus 41	ASTM D 5950
Contain water and sediments, v/v. %	2	ASTM D 2709
Sulfur contents, wt.%	0.42	ASTM D 4294

T a b l e 3

Chemical analysis of carbon black

Parameter	Measured values	Test method
Water content, wt.%	0.35	ISO 589:2008
Volatile substances, wt.%	33.21	ISO 562:2010
Ash content, %	25.63	ISO 1171:2010
Granulometric composition, <500 μm	67.15	ISO 1953:1994
Bulk density, kg/m^3	456.87	ASTM D 2854
Fixed coal, wt.%	41.06	Estimated

Fig. 2. Carbon black

Depending on reactor type and catalyst type, process conditions, raw materials and their composition, product yields can vary significantly. During pyrolysis, about 33–39 % of the solid residue is obtained, 34–45 % of the liquid products, and the rest consists of gases [19–22]. The results of the studies indicate that a semi-batch pyrolysis reactor is a good choice for generating pyrolysis oil from solid tire waste. In this study, the pyrolysis process takes place in a temperature interval of 180°C (from 325°C to 505°C) at a heating rate 10°C/min. The properties of the total pyrolysis oil, including density and viscosity, are found to be nearly equivalent to those of automotive diesel fuels and truck pyrolysis oil [23]. The obtained pyrolysis oil was fractionated into light (36.32%) and heavy (30.18%) diesel fuel. The densities of the obtained fractions for light and heavy diesel fuel are 0.8780 g/cm^3 and 0.9381 g/cm^3, respectively. The density of the mixture and the amounts of the two fractions of diesel (0.9071 g/cm^3) show that the pyrolysis oil can be classified as a heavy diesel fraction in which there is a presence of light components. A low initial boiling point (IBP) of 45.2°C indicates the presence of light components in the pyrolysis oil. The generation of sulfur compounds in the pyrolysis liquid products is attributed to the thermal degradation of the vulcanizing agents incorporated into the rubber [10, 24]. The relatively low sulfur content of pyrolysis oil of 0.42% allows it to be safely used as a heating oil (according to the ASTM standard, the maximum is 0.5%). Therefore, it is within the permissible limits for its safe use. However, fractional distillation and desulfurization are necessary to enable their use as alternative fuels for engines. Certain researchers have determined that liquid oil obtained by pyrolysis of waste automobile tires, when mixed with diesel fuel at concentrations up to 75%, can be effectively used in diesel engines without the need for any modifications to the engine [25, 26]. Research shows that the application of pyrolysis oil mixed with diesel fuel at concentrations of 20%, 40%, 60%, and 75% in a direct injection diesel engine has shown comparable performance and lower emissions to the operation of the same engine when running on pure diesel fuel. They suggest that tire pyrolysis oil could serve as a viable alternative fuel for diesel engines in the future [26–28].

Numerous studies on the pyrolysis of waste tires are focused on obtaining pyrolysis oil and less on obtaining and characterizing solid residue. There are very few studies related to the gas product, pyrolysis gas [29]. The pyrolysis process results in the formation of a huge amount of solid carbonaceous material referred to as solid residue, pyrolysis char, or carbonized residue (commonly known as carbon black). The properties of this solid residue are determined by the specific conditions of the pyrolysis process, as well as the composition of the rubber being processed. It has been established, that part of the organic gaseous products generated during pyrolysis can be adsorbed on the surface of the solid residue. This affects a change in the structural characteristics of the carbon black. To improve these characteristics, increase the diameter of pores, increase the specific surface of the carbon black, demineralization and carbon black activation are required. After that, it can be used in the production of tires, adsorbents, or catalyst carriers [30, 31]. The amount of carbon black obtained during the pyrolysis of truck tires and its characteristics are within the limits of expectations and literature data [6, 15].

4. CONCLUSIONS

The pyrolysis of waste tires serves as a method to generate a substantial quantity of high-quality pyrolysis oil and carbon black. Analysis of the fuel characteristics of tire pyrolysis oil shows similarities with diesel fuel or light fuel oil and can safely be used as a heating oil. Also, because of its relatively low sulfur contents and improving quality, it can be blended with diesel fuel for use in diesel engines. This is of particular importance due to the wide application of diesel engines in the transport sector. The yield of carbon black obtained from the pyrolysis of tires is substantial and exhibits a significant ash content. To enhance the quality of the carbon black, aiming to convert it into higher-grade carbon black, demineralization and activation processes are necessary.

REFERENCES

[1] Karagoz, M., Ağbulut, U., Sarıdemir, S. (2020): Waste to energy: production of waste tire pyrolysis oil and comprehensive analysis of its usability in diesel engines. *Fuel*, **275**, 117844. https://doi.org/10.1016/j.fuel.2020.117844

[2] Czajczyńska, D., Czajka, K., Krzyżyńska, R., Jouhara, H. (2020): Waste tyre pyrolysis − impact of the process and its products on the environment. *Therm. Sci. Eng. Prog*., **20**, 100690. http://dx.doi.org/10.1016/j.tsep.2020.100690

[3] Jahirul, M. I., Hossain, F. M., Rasul, M. G., Chowdhury, A. A. (2021): A review on the thermochemical recycling

of waste tyres to oil for automobile engine application. *Energies*, **14**, 3837. https://doi.org/10.3390/en14133837

[4] Li, W., Wang, Q., Jin, J., Li, S. (2014): A life cycle assessment case study of ground rubber production from scrap tires. *Int. J. Life Cycle Assess*, **19**, 1833−1842. https://www.researchgate.net/publication/278173578 DOI 10.1007/s11367-014-0793-3

[5] Antoniou, N., Zabaniotou, A. (2013): Features of an efficient and environmentally attractive used tyres pyrolysis with energy and material recovery. *Renewable Sustainable Energy Rev.*, **20**, 539−558. https://doi.org/10.1016/j.rser.2012.12.005

[6] Pyshyev, S., Lypko, Y., Demchuk, Y., Kukhar O., Korchak B., Pochapska, I., Zhytnetskyi, I. (2024): Characteristics and applications of waste tyre pyrolysis products: A review. *Chem. Chem. Technol*., Vol. **18**, No. 2, pp. 244–257. https://doi.org/10.23939/chcht18.02.244

[7] Formela, K. (2021): Sustainable development of waste tires recycling technologies – recent advances, challenges and future trends. *Adv. Ind. Eng. Polym. Res*., **4** (3), 209–222. https://doi.org/10.1016/j.aiepr.2021.06.004

[8] Osayi, J. I., Iyuke, S., and Ogbeide, S. E. (2014): Biocrude production through pyrolysis of used tyres: A review, *J. Catal.* Volume **2014** (1), 386371. http://dx.doi.org/10.1155/2014/386371

[9] Diez, C., Martinez, O., Calvo, L. F., Cara, J., Moran, A. (2004): Pyrolysis of tyres. Influence of the final temperature of the process on emissions and the calorific value of the products recovered. *Waste Manag* **24**, pp. 463–9. https://doi.org/10.1016/j.wasman.2003.11.006

[10] Laresgoiti, M. F., Caballero, B. M., Marco, I. D., Torres, A., Cabrero, M. A., Chomon, M. J. (2004): Characterization of the liquid products obtained in tyre pyrolysis. *J Anal Appl Pyrolysis*, **71**, 917–34. https://doi.org/10.1016/j.jaap.2003.12.003

[11] Ucar, S., Karagoz, S., Ozkan, A. R., Yanik. J. (2005): Evaluation of two different scrap tires as hydrocarbon source by pyrolysis. *Fuel,* **84**, pp. 1884–92. https://doi.org/10.1016/j.fuel.2005.04.002

[12] Rodriguez, I. M., Laresgoiti, M. F., Cabrero, M. A., Torres, A., Chomon, M. J., Caballero, B. M. (2001): Pyrolysis of scrap tyres. *Fuel Process Technol*. **72**, pp. 9–22. https://doi.org/10.1016/S0378-3820(01)00174-6

[13] Gonzalez, J. F., Encinar, J, M., Canito, J. L., Rodriguez, J. J. (2001): Pyrolysis of automobile tyre waste. Influence of operating variables and kinetics study. *J Anal Appl Pyrolysis* **58–59**, 667–83. https://doi.org/10.1016/S0165-2370(00)00201-1

[14] Pilusa, T. J., Shukla, M., Muzenda, E. (2013): Pyrolitic tyre derived fuel: A review, *International Conference on Chemical, Mining and Metallurgical Engineering*, Nov. 27 –28, pp. 265–268.

[15] Williams, P. T. (2013). Pyrolysis of waste tyres: A review, *Waste Manage* **33** (8), 1714–1728. http://dx.doi.org/10.1016/j.wasman.2013.05.003

[16] Quek, A. and Balasubramanian, R. (2013): Liquefaction of waste tyres by pyrolysis for oil and chemicals: A review, *J. Anal. Appl. Pyrolysis* **101**, 1–16. https://doi.org/10.1016/j.jaap.2013.02.016

[17] Jahirul, M. I., Rasul, M. G., Chowdhury, A. A., and Ashwath, N. (2012): Biofuels production through biomass pyrolysis – A technological review, *Energies* **5** (12), 4952–5001. https://doi:10.3390/en5124952

[18] Stratiev, D., Shishkova, I., Pavlova, A., Stanulov, K., Mitkova. M., Skumov, M., Tzaneva, T. (2013): Characterization of spent tyre catalytic pyrolysis liquid products: gasoline and remaining fraction boiling above 200ºC, *Petroleum & Coal* **55** (4) 283–290; ISSN 1337-7027

[19] Pyshyev, S., Lypko, Y., Chervinskyy, T., Fedevych, O., Kułażyński, M., Pstrowska, K. (2023): Application of tyre derived pyrolysis oil as a fuel component. *S. Afr. J. Chem. Eng.* **43**, 342–347. https://doi.org/10.1016/j.sajce.2022.12.003

[20] Xu, J., Yu, J., Xu, J., Sun, C., He, W., Huang, J., Li, G. (2020): High-value utilization of waste tires: A review with focus on modified carbon black from pyrolysis. *Sci. Total Environ.* **742**, 40235. https://doi.org/10.1016/j.scitotenv.2020.140235

[21] Singh, R. K., Ruj, B., Jana, A., Mondal, S., Jana, B., Sadhukhan, A. K., Gupta, P. (2018): Pyrolysis of three different categories of automotive tyre wastes: product yield analysis and characterization. *J. Anal. Appl. Pyrolysis*, **135**, 379–389. https://doi.org/10.1016/j.jaap.2018.08.011

[22] Kardnkeyan, S., Sathiskumar, C., Moorthy, R. S. (2012): Effect of process parameters on tire pyrolysis: A review. *J. Sci. Ind. Res*. **71**, 309–315. http://nopr.niscpr.res.in/handle/123456789/13986

[23] M. Rofiqul Islam, M. U. Hossain Joardder, M. A. Kader, M. R. Islam Sarker, Hiroyuki HANIU, Valorization of solid tire wastes available in Bangladesh by thermal treatment, *Proceedings of the Waste Safe 2011 – 2nd International Conference on Solid Waste Management in the Developing Countries, 13–15 February 2011*, Khulna, Bangladesh. https://eprints.qut.edu.au/53484/

[24] Jantaraksa, N., Prasassarakich, P., Reubroycharoen, P., Hinchiranan, N. (2015): Cleaner alternative liquid fuels derived from the hydrodesulfurization of waste tire pyrolysis oil. *Energ. Convers. Manage*. **95**, 424–434. https://doi.org/10.1016/j.enconman.2015.02.003

[25] Kennedy, Z. R., Rathinaraj, D. (2007): Exhaust emissions and performance of diesel engine fuelled with tire based oil blends. *J Inst Eng*. **88**, pp. 13–8.

[26] Doğan, O.; Celik, M. B.; Ozdalyan, B. (2012): The effect of tire derived fuel/diesel fuel blends utilization on diesel engine performance and emissions. *Fuel* **95**, 340–346. https://doi.org/10.1016/j.fuel.2011.12.033

[27] Murugan, S., Ramaswamy, M. C., Nagarajan, G. (2008): Performance, emission and combustion studies of a di diesel engine using distilled tires pyrolysis oil-diesel blends. *Fuel Process. Technol*. **89**, 152–159. https://doi.org/10.1016/j.fuproc.2007.08.005

[28] Murugan, S., Ramaswamy, M. C., Nagarajan, G. (2008): The use of tires pyrolysis oil in diesel engines. *Waste Manage*. **28**, 2743–2749. https://doi.org/10.1016/j.wasman.2008.03.007

[29] Berrueco, C., Esperanza, E., Mastral, F. J., Ceamanos, J., Garcia-Bacaicoa, P. (2005): Pyrolysis of waste tires in an atmospheric static-bed batch reactor: Analysis of the gases

obtained. *J. Anal. Appl. Pyrol*., **74**, 245–253. https://doi.org/10.1016/j.jaap.2004.10.007

[30] Miguel, G. S.; Fowler, G. D.; Sollars, C. J. (1998): Pyrolysis of tire rubber: porosity and adsorption characteristics of the pyrolytic chars. *Ind. Eng. Chem. Res*. **37**, 2430–2435. https://doi.org/10.1021/ie970728x

[31] Helleur, R., Popovic, N., Ikura, M., Stanciulescu, M., Liu, D. (2001): Characterization and potential applications of pyrolytic char from ablative pyrolysis of used tires. *J. Anal. Appl. Pyrol.* **58**, 813–824. https://doi.org/10.1016/S0165-2370(00)00207-2

Mechanical Engineering – Scientific Journal, Vol. **42,** No. 2, pp. 101–106 (2024)
Number of article: 684
In print: ISSN 1857–5293
Received: September 24, 2024
On line: ISSN 1857–9191
Accepted: November 24, 2024
UDC: UDC: 665.092-977:678.5]:[665.63:542.48
https://doi.org/10.55302/MESJ24422101m

Original scientific paper

EVALUATION OF DISTILLATION CURVE OF PYROLYTIC LIQUID FUEL

Karmina Miteva[1], Slavčo Aleksovski[1], Gordana Bogoeva-Gaceva[1,2]

[1]*Ss. Cyril and Methodius University, Faculty of Technology and Metallurgy, Rudjer Bošković 16, Skopje, North Macedonia*
[2]*Research Center for Environment and Materials, Macedonian Academy of Sciences and Arts, Krste Misirkov 2, 1000 Skopje, North Macedonia*
karmina@tmf.ukim.edu.mk

A b s t r a c t: The natural catalyst, opalized silicate-tuff, was demonstrated to be an excellent catalyst for the breakdown of plastic waste and produced a high-yield liquid fraction. Polyethylene (PE) and polypropylene (PP) waste mixture has been catalytically degraded in a batch reactor operating in dynamic conditions, and the obtained liquid fuel is in the petrol and kerosene range. The yield of condensed product formation was higher than 85%. The ASTM distillation according to the requirements of the ASTM D86 Standard Test Method was performed. Under ambient pressure, the test method of determining the boiling range of a petroleum product by performing a simple batch distillation has been used. Some physical and qualitative characteristics of the condensed product were determined. The obtained condensed product, 65% is in the diesel range between 180°C and 320°C. The most common compounds in condensate are paraffin (78%) and aromatic (22%). The quantity of naphthenic is minor.

Key words: pyrolysis; ASTM distillation; natural catalyst; ASTM D86 Standard Test Method

ЕВАЛУАЦИЈА НА КРИВАТА НА ДЕСТИЛАЦИЈА НА ПИРОЛИТИЧКО ТЕЧНО ГОРИВО

А п с т р а к т: Природниот катализатор, опализиран силика-туф, се покажа како одличен катализатор за разградување на пластичен отпад и добивање висок принос на течно гориво. Отпадната смеса од полиетилен (PE) и полипропилен (PP) е каталитички разградена во шаржен реактор што работи во динамични услови, а добиеното течно гориво е во видот на бензин и керозин. Приносот на добиениот кондензиран производ е поголем од 85%. Извршена е ASTM дестилација според барањата на стандардниот тест-метод ASTM D86. Под амбиентален притисок, тест методот е користен за одредување на интервалот на вриење на нафтениот производ со спроведување едноставна шаржна дестилација. Утврдени се некои физички и квалитативни карактеристики на кондензираниот производ. Добиениот кондензиран производ е 65% во рангот на дизел помеѓу 180°C и 320°C. Најчести соединенија во кондензатот се парафини (78%) и аромати (22%). Количеството на нафтени е минорно.

Клучни зборови: пиролиза; ASTM дестилација; природен катализатор; стандарден тест-метод ASTM D86

1. INTRODUCTION

Petroleum is used excessively in modern civilizations as both a fuel and a raw resource for numerous businesses. Four percent is used to create plastic, four percent is used as feedstock for the petrochemical sector, five percent is utilized for other purposes, and about forty-five percent is used internationally to generate electricity [1]. Finding alternative energy sources to petroleum is therefore necessary. Recycling of waste plastics is a very important

issue in order to relieve environmental pollution. Worldwide, the conversion of plastic waste to fuel by application of different pyrolysis methods has been intensively researched [2]. Particularly post-consumer plastics are a very attractive opportunity for utilization as a valuable and reusable source of hydrocarbons if they're broken down into lower molecular weight products [3]. Apart from energy concerns, the most promising substitute for plastics pyrolysis or recycling seems to be the development of more efficient techniques for transforming these inexpensive waste polymers in a way that is environmentally friendly [4].

During the cracking process of long polymer molecules, the degradation of polymer chains can be enhanced by applying various catalysts. The used catalysts have a high conversion effect over the plastic wastes at lower temperatures and decrease the activation energy [5]. The impact of zeolitic catalysts has been highlighted in polymer degradation catalytic processes that provide valuable hydrocarbons [6–9]. The effectiveness of non-zeolitic catalysts in the breakdown of polymers is far less understood. There have been reports on the catalytic conversion of plastic wastes using various non-zeolite catalysts. They consist of the following: alumina, silica, and basic catalysts like $BaCO_3$ [10], bimetallic catalysts, Al-Zn composites [11], FCC catalysts [12, 13], and mesoporous catalysts like Al-MCM-41 [14]. Hydrocarbons are produced during catalytic degradation, which occurs at temperatures that are comparatively low and within the motor fuel range [15, 16]. Liquid fuel is probably the most valuable in such a degrading process. Natural opalized silicate–tuff proved to be an excellent catalyst for plastic waste degradation and producing a high yield liquid fraction with gasoline and kerosene [17].

The liquid fuel obtained from catalytic pyrolysis could be used as a transport fuel because of the high amount of aromatic and some naphthenic compounds that could be a good motor fuel since. Aromatic and naphthenic compounds improve the quality of gasoline by increasing the octane number [18]. Olefinic compounds are industrially more attractive than even the pure saturated compounds [19], as they are intermediaries of many valuable and expensive chemicals.

Distillation is a primary process widely used in the oil and petrochemical industries, providing important qualitative and quantitative information on complex fuel mixtures [20]. The ASTM D86 distillation process is presented with a curve that plots the liquid mixture's boiling temperature against the total volume of distillate at a specific pressure [21]. This standard of the American Society for Testing and Materials (ASTM) covers distillation characterization techniques, describing a basic distillation procedure [22].

In this work, the efficiency of these natural catalysts for the production of liquid fuel from waste plastic was analyzed. The obtained condensed fraction obtained from catalytic degradation of polyethylene (PE) and polypropylene (PP) is much larger than the gaseous fraction. The physical properties of obtained liquid fuel were determinate. The pyrolytic fuel was analyzed according the ASTM D86 standard. The main constituents of pyrolytic oil, paraffin's, naphthenic, and aromatics, were determined using the n-d-M method.

2. EXPERIMENTAL

2.1. *Materials*

The waste polymer mixture used in this work was consisted of 76.2% high-density and 23.8% polypropylene. The natural alumina-silicate catalyst tuff was screening through the sieve, and the fraction of 0.03 mm was employed in the experiments. The catalyst activation was performed at 800°C for 3 h.

2.2 *Experimental setup*

A stainless steel 400 ml batch reactor was used for the production of liquid fuel in the presence of tuff catalysts. The PID (Unitronics V570) controller controlled the temperature and maintained a constant heating rate of 10°C/min.

The full procedure for the production of liquid fuel was presented in our previous work [23].

The obtained pyrolytic oil was evaluated using ASTM distillation, according to the requirements of the ASTM D86 Standard Test Method, in the apparatus depicted in Figure 1. A basic test method of determining the boiling range of a petroleum product by performing a simple batch distillation has been used. The yield of condensate product and temperature are systematically measured. Additionally, are noted the residual volume. The ASTM D86 test method determines quantitatively the boiling range characteristics of products as light and middle distillates. Also, standard assays are used for fuel quality control, and results rely on several fuel characteristics, such as specific gravity and distillation curve. These attributes are closely linked to the composition of the fuel, and predicting them requires understanding the features of its constituent parts.

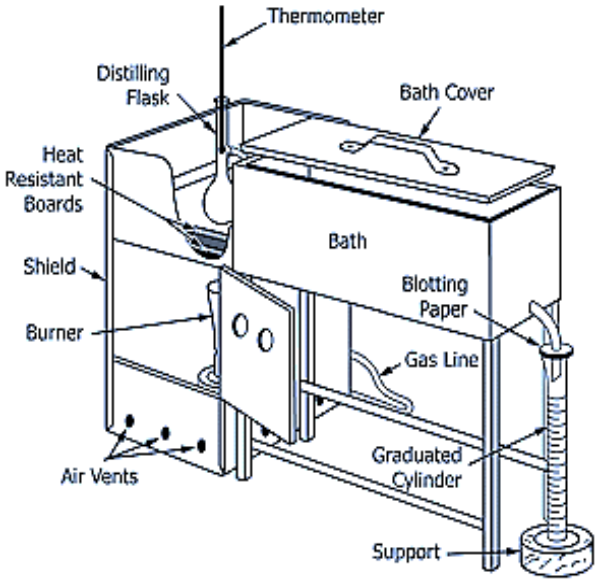

Fig. 1. ASTM distillation apparatus according ASTM D86 test method [20]

3. RESULTS AND DISCUSSION

The experimental measurements are made on each 5 vol% of distillates. In calculations of characteristics of pyrolysis fractions, the essential boiling points of 10, 30, 50, 70, and 90 vol%, were used. The distillation (volatility) characteristics of hydrocarbons have an important effect on their safety and performance. Understanding the volatility of complex fluids, and particularly the behavior of fuels in a refinery or engine, depends on their characteristics. Plotting a liquid mixture's boiling temperature against its distilled volume percentage is the ASTM distillation curve method (Figure 2). The distillation curve relies on the type and quantity of compounds present in the mixture. The volumes of the lighter phase of the pyrolytic fuel with a boiling point below 175ºC is the fraction that corresponds to the gasoline range (220ºC), and are only 35% of the total collected sum of all fractions. Consequently, a greater amount, 65% of condensate, is obtained in the diesel range between 175°C and 320°C. Distillation ended at 316ºC and 90% volume.

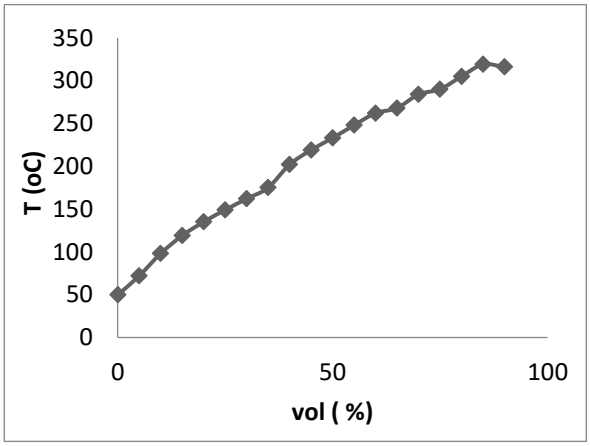

Fig. 2. ASTM distillation curve

The distillation characteristics of fuel are critically important. The presence of high boiling point components in these and other fuels can significantly affect the degree of formation of solid combustion deposits.

The determination of the chemical properties of pyrolytic fuel is usually complex and expensive due to the large number of different compounds. Physical properties such as density, kinematic viscosity and refractive indexes were determined by measurable laboratory tests, according to specific standards. The fundamental variables for calculating correlations that meet the standard test method are the density and distillation curve. The density and kinematic viscosity were determined according to ASTM D4052 and ASTM D445 and D446, consequently. Refractive index follows ASTM D1218 and aniline point ASTM D611 (Table 1).

T a b l e 1

Measured physical properties of obtained liquid fuel

Physical properties	Labels	Units	Measured values
Density	d	g/cm^3	0.7801(15^{o}C) 0.7764 (20^{o}C)
Refractive index	RI	–	1.4410 (25^{o}C)
Kinematic viscosity	V	cSt	0.9765 (40^{o}C)
Aniline point	AP	^{o}C	66.3

The values shown below are computed using the distillation data according the ASTM D86:

API – American Petroleum Institute gravity

SG – Specific gravity

VABP – Volumetric of average boiling point temperature (^{o}C)

S^{ASTM} – The slope of ASTM curve (^{o}C/vol%)

MeABP – Mean average boiling point (^{o}C)

MABP – Molar average boiling point (^{o}C)

CABP – Cubic average boiling point (^{o}C)

vsus (SUS) – Kinematic viscosity to Saybolt Universal seconds

MW – Molecular weight (g/mol)

Kw – Watson characterization factor

These properties rely on the volumetric and volatility characteristics of the mixture, which, in principle, can be obtained by the use of a thermodynamic model and the chemical composition of the mixture.

It is possible to predict the parameters for pyrolytic oil characterization based on the results shown in Table 2, including molecular weight (MW), volumetric average boiling point (VABP), mean average boiling point (MeABP), and the value of Kw. Therefore, lower values of VABP and MeABP, 213 and 218, as well as MW 138, suggest lighter fuel, whereas higher values are expected for heavier fuels. Therefore, a MW ranges from 70 to 200 for lighter fractions and between 200 and 600 for heavier fractions. This is even more confirmed with the value of the Kw factor, which comprises a classification method according to the variety of paraffinic, naphthenic, intermediate, or aromatic in the pyrolytic oil. Typical ranges of Kw are between 10 and 13. The obtained value for the Kw factor of 11.9 ~ 12 implies a hydrocarbon compound predominantly paraffin in nature. Hydrocarbons with higher naphthenic or aromatic content are indicated by lower values of this factor. Values of 10.0 or less are seen in highly aromatic hydrocarbons. The boiling range gives information on the composition (Table 3), the properties, and the behavior of the fuel during storage and use.

T a b l e 2

Calculated values using n-d-M correlation

SG	0.78
VABP	218.6
CABP	208.6
S^{ASTM}	3.1
MeABP	213.6
MABP	172.6
Kw	11.9075
vsus	1.02
MW	138.18

T a b l e 3

Calculated % of groups of compounds using n-d-M

C_A	18.660
C_N	3.14
C_P	78.20

C_A – Aromatic ring structure (%)
C_N – Naphthenic ring structure (%)
C_P – Paraffin chains (%)

The volatility properties of gasoline are closely related to its performance within the engine; particularly, the adequate balance between light and heavy hydrocarbons is a determinant for engine cold start, engine heating, and fuel economy at cruising speed. If excess light hydrocarbons are present in gasoline, problems such as vapors lock and engine freezing may occur [24].

4. CONCLUSION

In this work, the ASTM D86 Standard Test Method was used for characterization obtained pyrolytic fuel over employed catalys – opalized silica tuff. This test method covers the atmospheric distillation of petroleum products and liquid fuels using a laboratory batch distillation unit to determine quantitatively the boiling range characteristics of such products as light and middle distillates. A characterization of the obtained pyrolytic fuel was made using the data obtained from ASTM distillation curve. The results obtained from the distillation curves indicate that pyrolytic fuel is a complex mixture of compounds.

The obtained pyrolytic oil was quantitative and qualitatively characterized. The fraction that corresponds to the gasoline range (175ºC) is only 35%, and a greater amount, 65% of condensate is obtained in the diesel range between 175°C and 316°C. The most common compounds in oil are paraffin's 78% and aromatics 22%. The quantity of naphthenic is minor, only 3%.

The molecular weight of fuel is 138, and the two estimated boiling points (VABP and MeABP) values of 213 and 218 suggest lighter fuel. As well as obtained value Kw of 12 implies a fuel with paraffinic nature.

REFERENCES

[1] Costa, P. A.; Pinto, F. J.; Ramos, A. M.; Gulyurtlu, I. K.; Cabrita, I. A.; Bernardo, M. S. (2007): kinetic evaluation of the pyrolysis of polyethylene waste, *Energy & Fuels*, vol. **21**, pp. 2489–2498.

[2] Moinuddin, S.; Mohammad, M. R. (2013): Food Container Waste Plastic Conversion into Fuel, *International Journal of Engineering and Applied Science*, vol. **3**, No. 1, pp.13–18.

[3] Strobel, B.O.; Dohms, D. (1993): *Proceedings of International Conference on Coal Science,* vol. **2**, pp. 536–545.

[4] Gimouhopoulos, K.; Doulia, D.; Vlyssides, A.; Georgiou, D. (1998): Organic solvent effects on waste plastics–lignite coliquefaction, *Resources, Conservation and Recycling*, vol. 23, pp. 47–56.

[5] Lina, Y.-H.; Yanga, M.-H.; Yehb, T.F.; Gerb, M.D. (2004): Catalytic degradation of high density polyethylene over mesoporous and microporous catalysts in a fluidised-bed reactor, *Polymer Degradation and Stability*, vol. **86**, pp. 121–128.

[6] Audisio, G.; Bertini, F.; Beltrame, P.L.; Carniti, P. (1992): Catalytic degradation of polyolefins, *Makromolecular Chemie. Macromol. Symposia*, vol. **57** (1), pp. 191–209.

[7] Guohua, L.; Tomohiko, S.; Satomi, Y.; Kunio, K. (2000): Catalytic degradation of high density polyethylene and polypropylene into liquid fuel in a powder-particle fluidized bed, *Polymer Degradation and Stability*, vol. **70**, No. 1, pp. 97–106.

[8] Garforth, A. S.; Harris, A. A.; Rawlence, D. J.; Uemichi, Y. (2002): Polymer waste recycling over used catalysts, *Catalysis Today*, vol. **75,** pp. 247–257.

[9] Lee, K. H., Noh, N. S., Shin, D. H., Seo, Y. H. (2002): Comparison of plastic types for catalytic degradation of waste plastics into product with spent FCC catalyst, *Polymer Degradation and Stability*, vol. **78**, No.3, pp. 539–545.

[10] Jan, M. R.; Shah, J.; Gulab, H. (2010): Catalytic degradation of waste high-density polyethylene into fuel products using $BaCO_3$ as a catalyst, *Fuel Processing Technology*, vol. **91**, pp.1428–1437.

[11] Tang, C.; Wang, Y. Z.; Zhou Q., Zheng, L. (2003): Catalytic effect of Al-Zn composite catalyst on the degradation of PVC-containing polymer mixtures into pyrolysis oil, *Polymer Degradation and Stability*, vol. **81**, pp. 89–94.

[12] Miskolczi, N., Bartha, L., Deak, G. (2006): Thermal degradation of polyethylene and polystyrene from the packaging industry over different catalysts into fuel-like feed stocks, *Polymer Degradation and Stability*, vol. **91**, pp. 517–526.

[13] Huang, W.C.; Huang, M. S.; Huang, C.F.; Chen, C. C., Ou, K. L. (2010): Thermochemical conversion of polymer wastes into hydrocarbon fuels over various fluidizing cracking catalysts, *Fuel*, vol. **89,** pp. 2305–2316.

[14] Saha, B., Chowdhury, A. K.; Ghoshal, A. K. (2008): Catalyzed decomposition of propylene and hybrid generic algorithm for kinetics analysis *Applied Catalysis B: Environmental*, vol. **83**, pp. 265–276.

[15] Tiwari, D. C., Ahmad E.; Singh, K. K. (2009): Catalytic degradation of waste plastic into fuel range hydrocarbons, *International Journal of Chemical Research*, vol. **1**, No. 2, pp. 31–36.

[16] Sivakumar, P.; Anbarasu, K. (2012): Catalytic pyrolysis of dairy industrial waste LDPE film into fuel. *International Journal of Chemistry Research*, vol. **3**, No.1, pp. 52–55.

[17] Mosio-Mosiewski, J.; Warzal, M., Morawski, I., Dobrzanski, T. (2007): High-pressure catalytic and thermal cracking of polyethylene, *Fuel Processing Technology*, vol. **88**, No. 4, pp. 359–364.

[18] Aguado, J.; Serrano, D. P.; Escola, J. M.; Peral, A. (2009): Catalytic cracking of polyethylene over zeolite mordenite with enhanced textural properties, *Journal of Analytical and Applied Pyrolysis*, vol. **85**, pp. 352–358.

[19] Buekens, A. G.; Huang, H. (1998): Catalytic plastics cracking for recovery of gasoline-range hydrocarbons from municipal plastic wastes, *Resources Conservation and Recycling*, vol. **23**, pp.163–181.

[20] Santos, R.N.G.; Lima, E. R.A.; Paredes, M.L.L. (2021): ASTM D86 distillation curve: Experimental analysis and premises for literature modeling, *Fuel*, vol. **284**, pp. 118958.

[21] USA: American Society for Testing and Materials International; ASTM, Standard D86-11b. *Standard Test Method for Distillation of Petroleum Products at Atmospheric Pressure*. West Conshohocken, PA, 19428–2959,

[22] Harries, M. E.; McDonald, A. G.; Bruno, T. J. (2017): Measuring the distillation curves of non-homogeneous fluids: Method and case study of two pyrolysis oils, *Fuel*, vol. **204**, pp. 23–27.

[23] Miteva, K.; Aleksovski, S.; Bogoeva-Gaceva, G. (2019) Characterisation of fuel produced from polyolefin waste over Al_2O_3–SiO_2 mixture as catalyst. *Journal of Environmental Protection and Ecology*, vol. **20**, pp. 246–253.

[24] Lanzer Tvon Meien, O. F.; Yamamoto, C. I. (2005): A predictive thermodynamic model for the Brazilian gasoline, *Fuel*, vol**. 84**, No. 9, pp. 1099–1104.

Mechanical Engineering – Scientific Journal, Vol. **42,** No. 2, pp. 107–115 (2024)
Number of article: 685 In print: ISSN 1857–5293
Received: November 8, 2024 On line: ISSN 1857–9191
Accepted: November 30, 2024 UDC: 621.548.4-253.6:[658.512.2:004.356.2-023.5
https://doi.org/10.55302/MESJ24422107t

Original scientific paper

EXPERIMENTAL AND NUMERICAL INVESTIGATION OF THE POSSIBILITY FOR INCREASING WIND TURBINE EFFICIENCY BY NEW ROTOR HUB DESIGN

Petar Tanevski, Viktor Iliev, Marija Lazarevikj, Zoran Markov

Faculty of Mechanical Engineering, "Ss. Cyril and Methodius" University in Skopje,
P.O.Box 464, MK-1001 Skopje, Republic of North Macedonia
petar.tnv@gmail.com

A b s t r a c t: The aerodynamic performance of a wind turbine heavily depends on the blade airfoil designs, therefore the initial strategy for enhancing efficiency involves using multiple airfoils with varied geometries in blade construction. Building on this, a more innovative approach introduces new geometries for turbine hubs, allowing designers to retain the primary blade shape and dimensions during the design process. This process leverages theoretical aerodynamic principles, mathematical models and data from turbine operation under wind flow conditions. The numerical model, originally developed with various airfoils, is validated by comparison with experimental results, confirming its reliability. The unsteady airflow model reveals changes in wind turbine efficiency and aerodynamic coefficients at varying angles of attack of the blades. The next phase includes experimental testing of a wind turbine scaled physical model with a newly designed hub with a hemispherical shape. The 3D-printed model allows for testing at different angles of attack, enabling comparability between numerical and experimental outcomes. Adjusting the position of the hemispherical hub in relation to the blade root provides insights into its effect on wind capture. This method highlights the differences between a conventional turbine hub and an unconventional hemispherical hub, utilizing the same blade configuration. The first approach is implemented in software for airfoil design and analysis, while the second method is employed in software for designing structural elements of the whole turbine.

Key words: wind turbine; blade design; airfoils; hub design

ЕКСПЕРИМЕНТАЛНО И НУМЕРИЧКО ИСТРАЖУВАЊЕ НА МОЖНОСТА ЗА ЗГОЛЕМУВАЊЕ НА ЕФИКАСНОСТА НА ВЕТЕРНА ТУРБИНА ПРЕКУ НОВ ДИЗАЈН НА НОСОТ НА РОТОРОТ

А п с т р а к т: Аеродинамичките перформанси на ветерна турбина во голема мера зависат од дизајнот на аеропрофилот на лопатките. Оттаму почетната стратегија за подобрување на ефикасноста вклучува користење повеќе аеропрофили со различни геометрии при нивната конструкција. Последователно, поиновативниот пристап воведува нови геометрии за носот (центарот) на работното коло, дозволувајќи им на дизајнерите да ја задржат примарната форма и димензии на лопатките при процесот на дизајнирање. Во овој процес се користат теоретски аеродинамички принципи, математички модели и податоци за работата на турбините во услови на струење на ветер. Нумеричкиот модел, првично развиен со различни аеропрофили, е валидиран преку споредба со експериментални резултати, потврдувајќи ја неговата веродостојност. Моделот на нестационарно струење на воздух ги открива промените во ефикасноста и аеродинамичките коефициенти при различни нападни агли на лопатките на ветерната турбина. Следната фаза вклучува експериментално испитување на скалиран физички модел на ветерната турбина со нов дизајн на носот во облик на хемисфера. Моделот отпечатен со 3Д техника овозможува тестирање при различни нападни агли, овозможувајќи споредливост помеѓу нумеричките и експерименталните резултати. Приспособувањето на положбата на хемисферичниот центар во однос на коренот на лопатката дава увид во влијанието врз зафаќањето на ветерот. Овој метод ги истакнува разликите помеѓу конвенционален центар и неконвенционален хемисферичен центар, користејќи ја истата конфигурација на лопатката. Првиот пристап е имплементиран во софтвер за дизајнирање и анализа на аеропрофили, додека вториот метод е применет во софтвер за проектирање на конструктивните елементи на целата турбина.

Клучни зборови: ветерна турбина; дизајн на лопатка; аеропрофили; дизајн на центар на ротор

1. INTRODUCTION

The global strategy to gradually move from fossil fuels to renewable energy sources has become increasingly urgent in recent years. This initiative is driven by the pressing need to confront climate change by reducing greenhouse gas emissions and securing a sustainable energy future. Given the inherent variability in electricity demand on a daily basis, a new challenge arises to integrate various renewable energy resources, thereby ensuring a reliable and stable electricity network capable of meeting fluctuating demand patterns. The idea for combining renewable energy resources has embraced the act for taking new innovative steps in the attempt of increasing their power generation efficiency and reliability. In addition to hydropower, which is widely recognized as the largest and most cost-effective renewable energy source globally, with a notable capacity for balancing the ratio of energy demand and energy production, wind energy has appeared as a standout resource with a great potential regarding power generation flexibility. It is acclaimed for its scalability, environmental benefits, and continuous technological advancements [1].

Understanding the impact of wind flow on the turbine's rotor construction is of great importance due to the nature of the turbulent flow, which appears regardless of the rotor aerodynamics, and significantly reduces the wind turbine power generation efficiency. The fundamental of this understanding are the blades, composed of various airfoils in order to form an entity which will optimize and enhance the aerodynamics of the rotor, concerning lift and drag force. A common strategy to enhance wind turbine power generation efficiency focuses on improvements of the blade design for efficiently capturing and transferring the potential wind energy to the shaft, and ultimately the electrical generator. Blade efficiency, in terms of the ability to capture the wind flow, peaks at their upper portions and declines towards the turbine hub due to the turbulence from the hub's interaction with wind flow and the shape of the blades at that region. Increasing the surface area of the blades allows for greater wind energy capture, leading to increased energy production and improved efficiency. However, this approach is constrained by the costs associated with blade production and transportation [2, 3].

Other techniques for improving the performance of a horizontal axis wind turbine (HAWT) are constantly being carried out. The number of blades is one of the factors that impact how well wind turbines perform [4]. Wang and Chen [5] used CFD to numerically examine the impact of blade numbers 2, 4, 6, and 8, on a small-scale ducted wind turbine's performance at an inflow speed of 12 m/s. The k-e turbulence model was used for the numerical calculations. It was observed that adding more blades results in a higher starting torque and a slower cut-in speed. However, more blades result in more obstruction and slower blade entrance velocity, which reduces the power coefficient of the rotor. On the other hand, Shintake [6] notes that the performance of a HAWT increased with an increase of the blade number from 1 to 3 and decreased with an increase of the blade number from 3 to 5. The effect of blade number on the aerodynamic performance of a small-scale HAWT was investigated experimentally and numerically by Eltayesh [7]. The study was conducted by installing an experimental setup of wind turbine rotors with three-, five-, and six-bladed wind turbines at a constant pitch angle, different velocities and tip speed ratios. The study also used ANSYS Fluent for conducting numerical calculation using the SST k-w turbulence to monitor the effect of blade number on the power and thrust coefficient. The results showed that compared to the five-bladed and six-bladed wind turbines, the performance of a three-bladed wind turbine increased by 2% and 4%, respectively, while keeping a good agreement between the calculated and measured values.

The X-Rotor concept [10], a wind turbine rotor design developed to face the challenges of offshore spaces, combines horizontal-axis and vertical-axis wind turbine technologies to optimize efficiency and reduce costs. The innovative rotor comprises a primary rotor in a double-V configuration and secondary rotors attached to the primary blades' tips. These secondary rotors (HAWT), consequently to their reduced size, can reach significantly higher rotor speed, therefore provide enough power take-off, eliminating the need for gearbox or bespoke generators, and reducing maintenance costs.

Joining the trend of producing new innovative designs for enhancing wind turbine efficiency, Hui Hu and colleagues at Iowa State University [11] introduced the Dual-Rotor Wind Turbine (DRWT) concept. Their research focused on mitigating root losses near the hub and reducing aerodynamic inefficiencies caused by wake interactions in wind farms. The DRWT system bring into service a secondary, smaller, co-axial rotor designed to capture energy in regions typically underutilized by conventional HAWT. Through experimental and numerical studies, the team demonstrated that the secondary

rotor not only improved energy capture but also enhanced wake mixing, leading to greater overall efficiency.

Simillar to the DRWT, Sandip A Kale and S.N. Sapali analyzed various innovative multi rotor wind turbine designs. By utilizing multiple smaller rotors [12], these systems can increase the swept area without the need for excessively large rotors. Multi-rotor configurations, such as co-planer, co-axial, and counter-rotating designs, amount to the potential for higher energy capture while addressing challenges like structural weight and complexity. These systems have been evaluated for their technological advantages, feasibility, and cost-effectiveness, demonstrating benefits in both power output and structural efficiency compared to traditional single-rotor system

In the pursuit of achieving optimal techno-economic solutions for enhancing the efficiency of conventional HAWTs, this study addresses the less-explored role of turbine hubs in maximizing wind energy utilization. The focus is on the implementation of an unconventional novel hemispherical hub design, aiming to optimize airflow interaction at the root of the blades - a region associated with energy losses - while maintaining the number of blades, and blade configuration, including shape, and length.

This paper presents a comparative analysis of the wind energy harnessing ability between a conventional HAWT, and a HAWT with a hemispherical hub. The comparison is conducted by obtaining key performance metrics, including the power coefficient (Cp), revolutions per minute (RPM), and cut-in wind speed, as functions of wind velocity. The results were acquired by performing experimental measurements under varying wind flow for both designs, validated by a numerical model.

2. THEORETICAL BACKGROUND

As airflow interacts with a wind turbine, it induces a boundary layer near the turbine's surface due to fluid disturbances forcing blades to move. This boundary layer, influenced by fluid viscosity, plays a pivotal role in understanding the dynamics of velocity at the fluid-solid interface. Variations in fluid pressure, governed by the Bernoulli principle, contribute to the development of lift and drag forces [10].

To optimize turbine efficiency, specific airfoil shapes are strategically chosen to generate a turbulent boundary layer, thereby delaying separation [10]. Figure 1 illustrates the intricate airflow patterns around turbine blades. The lift coefficient and drag coefficient, detailed in subsequent formulas, quantitatively assess the boundary layer's impact on lift and drag forces, respectively.

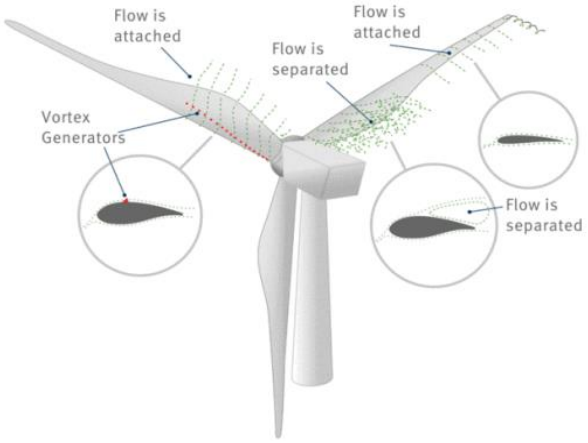

Fig. 1. Airflow behavior around turbine blades

The conveyance of mechanical forces between a solid body and a fluid occurs across the body's entire surface through fluid pressure. In wind turbines, the combined effect of natural wind and rotor-induced flow generates an aerodynamic force on the rotating blades [10].

Figure 2 illustrates the resultant force represented as F, decomposed into perpendicular (lift) L and parallel (drag) D components relative to the wind velocity W. Lift counteracts gravity and both forces are influenced by the angle of attack, which is the angle between the blade chord line and the wind direction.

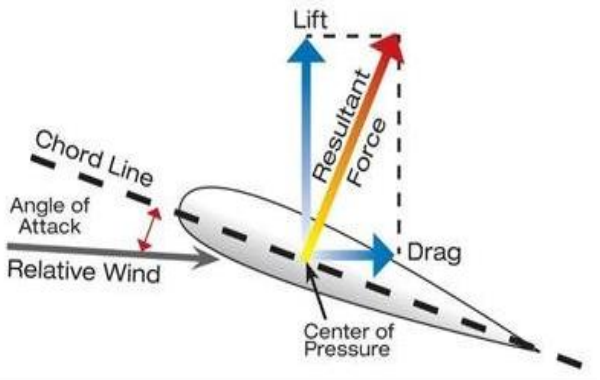

Fig. 2. Forces acting over an airfoil

The forces are given by the following expressions:

$$L = \frac{1}{2} C_L \rho A W^2 \quad (1)$$

$$D = \frac{1}{2} C_D \rho A W^2 \quad (2)$$

where ρ is the density of air, C_L and C_D are the lift and drag coefficients, respectively, A is the aifoil planform area.

3. NUMERICAL MODEL

Airflow over a wind turbine is modeled and simulated using the XFOIL software tool, part of the Qblade software suite. The wind turbine rotor blades are composed of multiple asymmetrical NACA4412 airfoils. Initial boundary conditions used for the modeling setup were Reynolds number of $1 \cdot 10^6$ indicating a turbulent flow, N_{crit} of 9 indicating the critical value of detachment of the air current from the airfoil, angle of attack in the range from –15 to +20° and constant air density of 1,225 kg/m^3.

Figure 3 and Figure 4 illustrate the simulated optimal angle of attack which is determined for optimal airflow over the blades and boundary layer. The value of that angle is 6°.

The wind turbine rotor with 44 cm in diameter, is designed consisting of three blades, each blade comprised of ten segments. The first two segments of every blade are designed from circular airfoils for the purpose of easy installation in the turbine hub, while the remaining eight segments are designed using the NACA4412 airfoil, as shown in Figure 5.

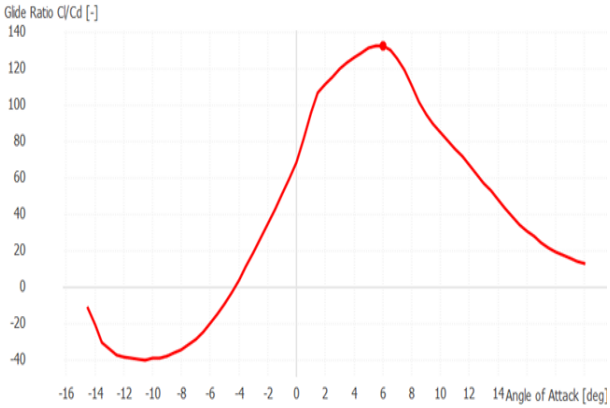

Fig. 3. Glide-ratio to angle of attack ratio (Optimal angle of attack)

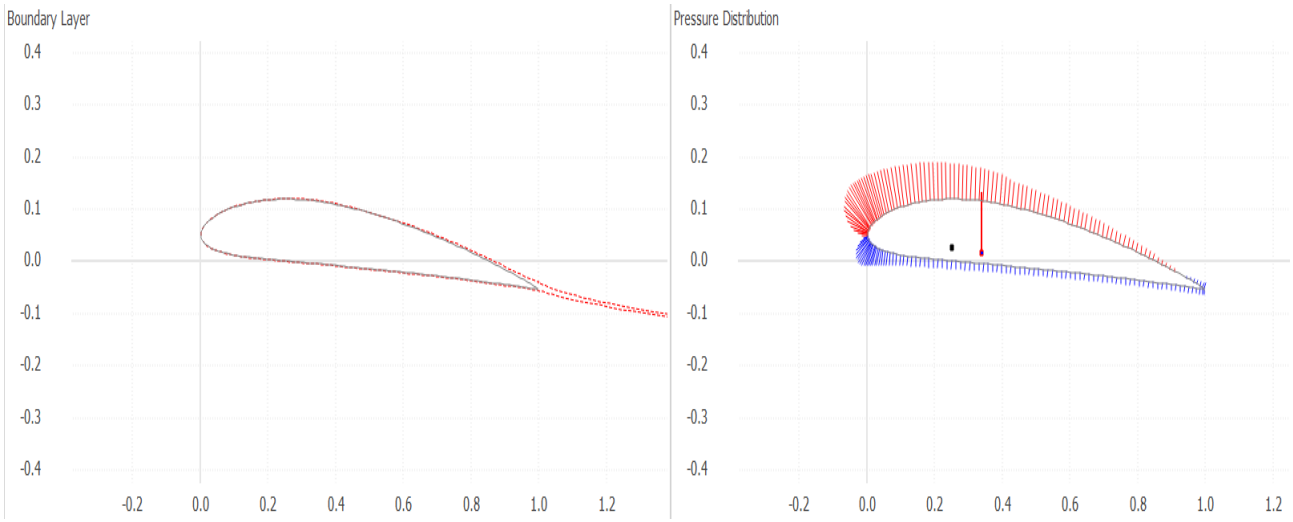

Fig. 4. Boundary layer and pressure distribution at optimal angle of attack

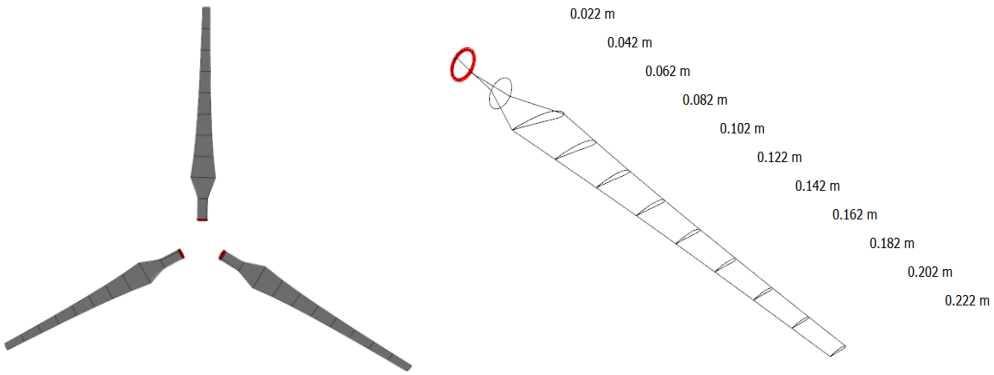

Fig. 5. Wind turbine blade design

The standard chord line optimization, twist optimization and Tip Speed Ratio (TSR) λ are used for the optimization of the blade geometries. The TSR is determined iteratively using the following equation:

$$C_p = C_1(C_2 - C_3\beta^2 - C_4)e^{C_5}, \qquad (3)$$

where: C_1 = 0.5, $C_2 = \frac{R}{\lambda}$, C_3 = 0.022, C_4 = 5.6, $C_5 = -\frac{0.17R}{\lambda}$, and β = 1°. Optimal C_p is achieved at TSR of 5.2.

The standard Betz model is applied to optimize the chord line for maximum efficiency. This model is an indicator of the best efficiency that can be achieved for a wind turbine under ideal conditions – utilizing the wind power excluding the occurrence of power losses. The Stall method is used for optimizing the blades twisting for a predetermined optimal TSR value, enabling automatic regulation of turbine operation.

Rotor operation is simulated using the Blade Element Momentum (BEM) model – a 2D model which performs discretization of the blades and calculates loads based on local fluid flow, incorporating mass and momentum conservation. Correction methods such as Prandtl Type factor and 3D correction factor are utilized for accurate simulation, accounting for rotor three-dimensionality.

4. EXPERIMENTAL SETUP

Experimental measurements of the number of rotations of the turbine rotor are performed at the laboratory of fuid mechanics and hydraulics at the Faculty of Mechanical Engineering in Skopje. Three blades are designed in SolidWorks using coordinates from the wind turbine rotor's numerical model in Qblade, ensuring identical geometry between the experimental and numerical models.

A standard hub and a modified hemispherical hub are created for the conventional and unconventional rotor assemblies, respectively, as shown on Figure 6.

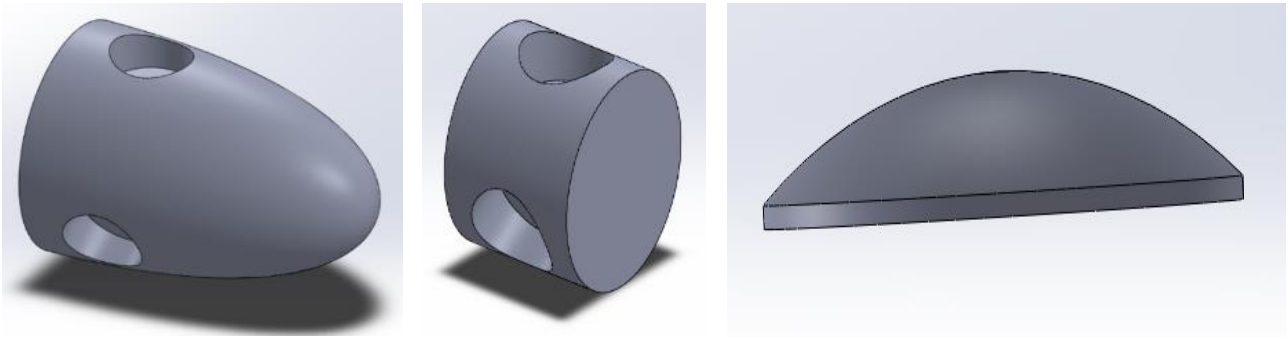

Fig. 6. Design of two turbine hubs

The rotor geometries are produced using a 3D printer and assembled into a single unit, mounted on a 36 cm metal stand. Balancing of the metal pole is achieved using two metal ropes to reduce vibrations from airflow during testing. The wind turbine is positioned at the air tunnel exit, measuring 275×275 mm in area. The fluid stream inlet speed, generated by a fan at the tunnel entrance, is controlled using a frequency regulator. A net is installed in the air tunnel to disrupt vortex effects caused by the fan's positioning.

Measurements are conducted at seven different speeds for both rotor configurations. In addition, two additional tests were performed on the modified hub rotor, adjusting the distance of the hemisphere from the blade center. Airspeed is measured using a digital anemometer, and the number of rotations of the rotor with a digital tachometer. The experimental system consisting of a balanced wind turbine, wind tunnel, and accompanying measuring devices is shown in Figure 7.

The experiment is used in order to validate the numerical model for the wind turbine operation in the wind tunnel, and to use it in an attempt to increase the utilization of the air flow, increase the number of revolutions of the rotor and eventually increase its efficiency, by implementing the new turbine hub.

Fig. 7. Experimental system

5. NUMERICAL MODEL VALIDATION

Validation of the numerical model was done by comparing the experimentally measured values and numerically obtained results for the number of revolutions per minute of the turbine rotor as an essential factor in power generation. This was facilitated by the rotor adaptable design, allowing for blade rotation and precise angle adjustments. Figures 8 and 9 show the comparison between the experimental and numerical data for angle of attack 3° and 6°, respectively. It can be seen that the results are in good agreement. The differences that exist can be assigned to the measurement errors, errors of the numerical model and the influence of surrounding airflow conditions.

After the numerical model is being validated, it can be used for simulations of operation for other wind turbines with different airfoils, blade design and rotor configuration, furthermore they can serve as a basis for further adjustments to the experimental model and subsequent validation through the numerical analysis.

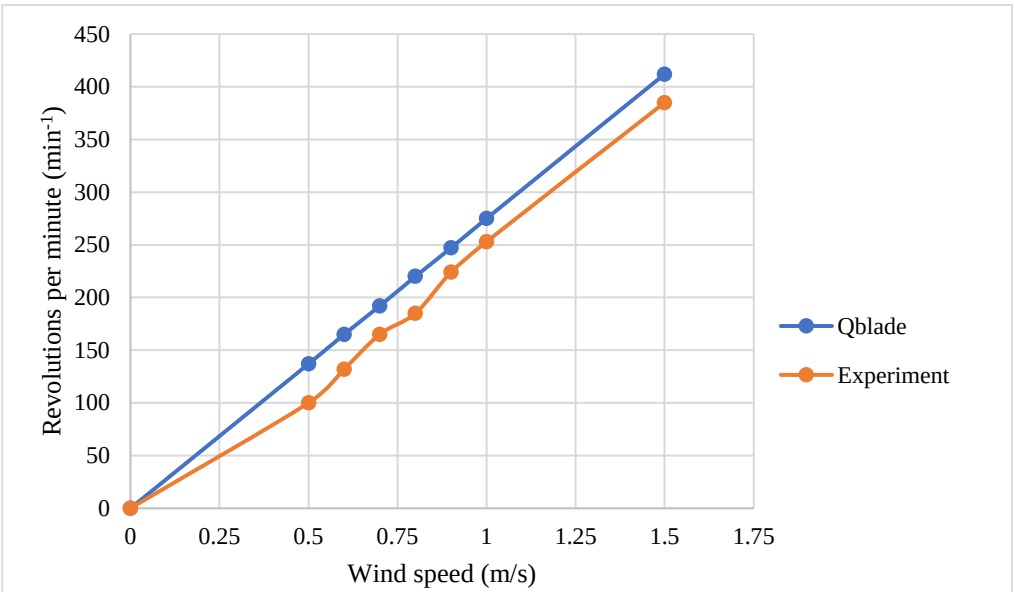

Fig. 8. Collective pitch 3°

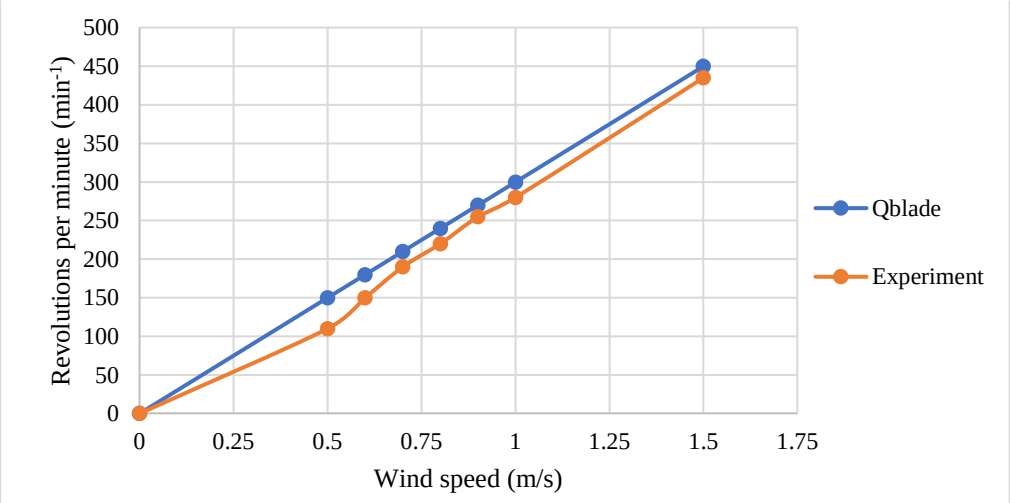

Fig. 9. Collective pitch 6º

6. RESULTS AND DISCUSSION

The wind turbine performance was observed with a modified configuration using the hemispherical hub. The number of rotations was measured under identical installation conditions as the standard turbine, which had been validated through both numerical and experimental models. With the optimal 6º angle of attack determined from simulations and verified experimentally, measurements were taken of the rotor rotations at speed of 0.5, 0.6, 0.7, 0.8, 0.9, 1, and 1.5 m/s.

Furthermore, these measurements are expanded to include another variable – the distance of the hemispherical hub from the center of blade placement. This alteration affects the timing and duration of contact with the fluid current, consequently impacting the blade efficiency in capturing the fluid flow. The distances for this measurement were 5, 10, and 15 mm, respectively. Figure 10 shows the influence of the distance of the hub from the blade placement center on the number of revolutions.

In the case of the wind turbine with the hemispherical hub distanced 15 mm from the center of the blades, which is determined by the intersection of the blade's axis, a significant increase in revolutions per minute is observed. A portion of the wind flow is directed to the upper parts of the blades, resulting in enhanced utilization of wind power, therefore in increased rotational speed. The same portion of wind flow in the case of wind turbine with standard hub design is flowing by the hub and the lower parts of the blades, resulting in wake effect and increased losses, hence the lower value of the rotational speed.

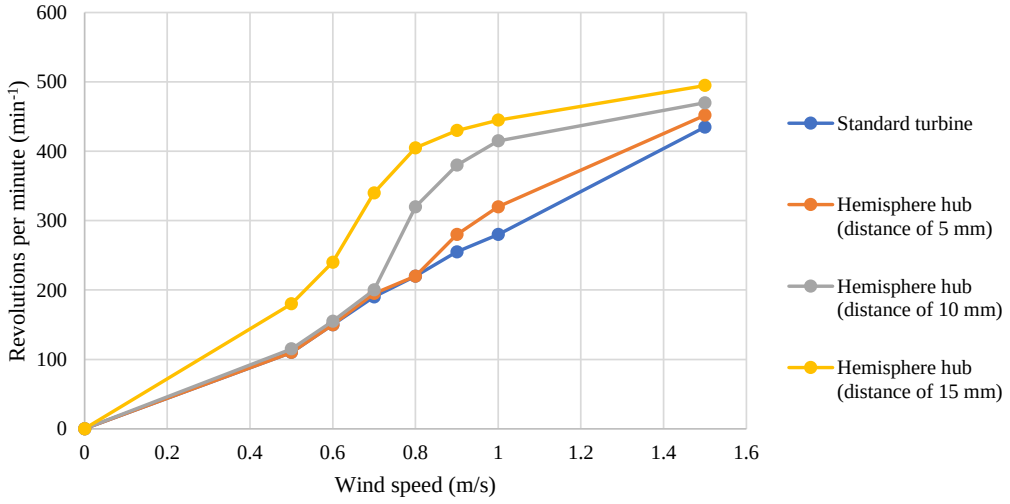

Fig. 10. RPM at wind speed from 0 to 1.5 m/s for different rotor configurations

While comparing the obtained experimental results, it must be noted that the discrepancy between the rotational speed of the standard wind turbine rotor and the one with the hemispherical hub distanced 5 mm from the center of the blades is relatively small. This indicates the limited benefit of implementing the hemispherical hub, which visibly depends on the distance between the center of the blades and the hemispherical hub itself

For these particular models, a simulation for determining the variation of the power coefficient as a function of the wind speed was conducted (Figure 11). Comparing Figures 10 and 11, we can clearly note that the examined turbine models are experiencing their full potential between wind speed of 1.3 and 1.35 m/s. This indicates an increase in vorticies and losses for higher wind speeds and higher rotational speed of the rotor, due to the stall effect.

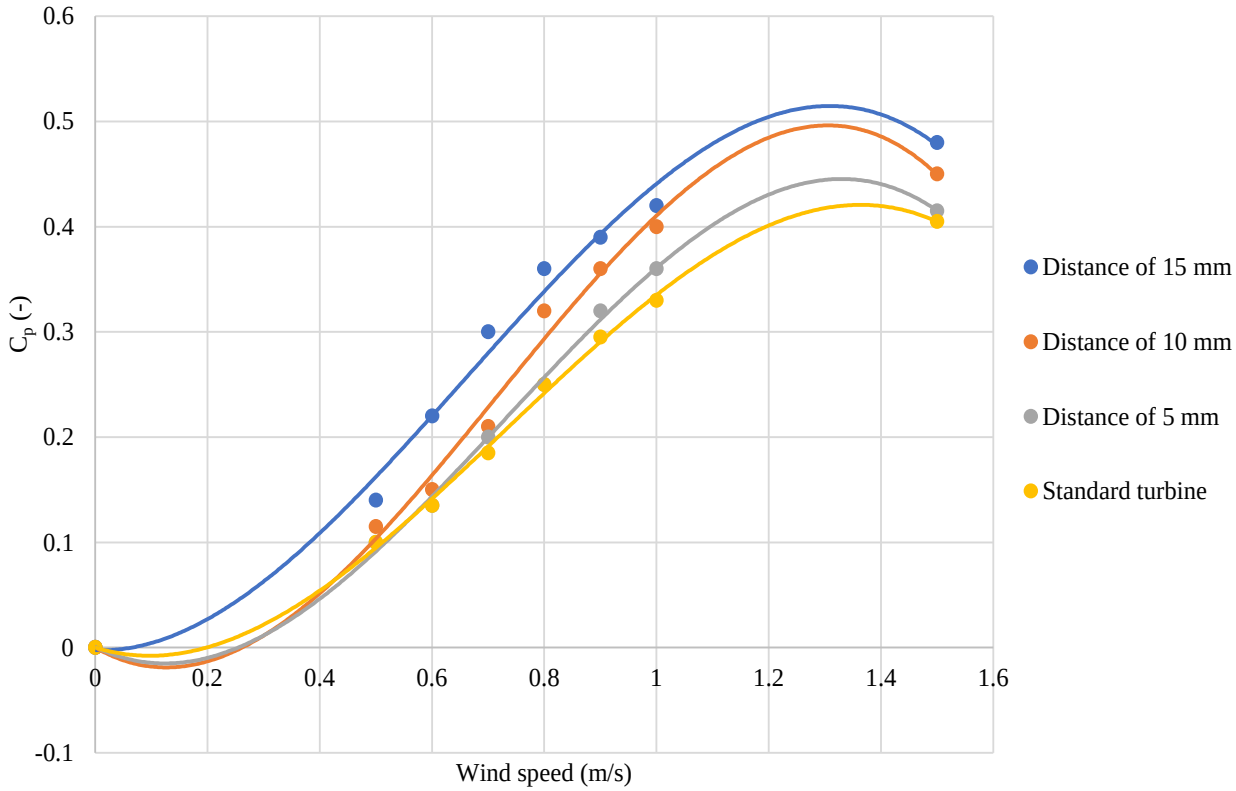

Fig. 11. C_p variation as a function of different wind speed

For the wind turbine rotor with a hemispherical hub distanced 15 mm from the blade center, at the optimal wind speed of 1.3 m/s, the value of the C_p is approximately 21.5% higher than the power coefficient of the standard wind turbine rotor configuration. For the rotor configuration with the hemispherical hub distanced 10 mm from the rotor center, at the optimal wind speed, the C_p percentage difference is reduced, yet still amounts to a significant approximate of 19 %.

Additionally, it is notable that the right positioning of the hemisphere results in a better cut-in speed. Distancing the hemisphere 15 mm from the original hub center for this particular design, allows for better wind flow mitigation to the tip of the blades, enabling the rotor to start rotating and generating power earlier, and at lower wind velocities than the rest of the rotor configurations.

The experimentally obtained values of rotor revolutions cannot be directly compared to those of full-scale wind turbines due to its significantly smaller size. Scaling this experiment also means taking into consideration the rotor aerodynamic influence in a wind farm.

Regarding the aerodynamic similarity, the Reynolds number for a full-scale turbine would be significantly higher than the experimtal setup. The difference could impact boundary layer behaviour and the aerodynamic forces acting on the blades.

Although the loads on the wind turbine structure caused by the various rotor configurations were

not subject in this paper, we must note that the hemispherical hub design may introduce different static and dynamic loads at full scale. Larger structures of this kind might require adjustments to ensure material strength and stability, particularly under high wind speeds or turbulent conditions.

The implementation of new geometries for this kind of structure will involve cost and practical feasibility, relating to manufacturing, installation, and maintenance.

The introduction of the hemispherical hub has shown a positive impact on increasing the rotor revolutions and power coefficient under identical operating conditions. This is attributed to its geometry, which directs the wind current towards the upper part of the blades, preventing losses from flow disruption between the blades.

The hemispherical hub could be a great efficiency solution for the multi-rotor wind turbines which use multiple smaller rotors instead of a single larger one, to increase the swept area, without the structural challenges of larger blades. Smaller rotors mean smaller hemispherical geometries, reducing the manufacturing cost and structural challenges, while enhancing every rotor efficiency.

Upwind rotors avoid tower shadowing but require complex yaw mechanisms to align with the wind. In contrast, downwind rotors simplify the design by aligning passively, but face efficiency losses due to tower interference. In both cases, the focus is on the blades, which in the optimization phase will eventually reach their full potential. Implementing the hemispherical hub could only strengthen the wind turbine's ability to harness wind power.

Morphing blades, inspired by natural structures, are dynamically adjustable blades to changing wind conditions in order to improve aerodynamic performance. Implementing these blades to the multi-rotor wind turbine design, and utilizing the hemispherical hub design, could provide a novel hybrid approach to enhancing turbine efficiency.

Of course, this type of additional geometry, after examination of the multiple considerations regarding the scaling process, can be used not only for designing new wind turbines, but also for enhancing the efficiency of existing ones.

7. CONCLUSION

In this paper an experimental analysis on the number of rotations of two wind turbine rotor assemblies was conducted. Additionally, a numerical analysis on a standardly designed wind turbine rotor was performed for various angles of attack and different flow velocities, using NACA4412 airfoil-based blades. For the optimization of the rotor, the standard chord line optimization, twist optimization and TSR were used. This analysis was conducted using the Qblade software in order to produce a numerical model that can be experimentally validated. For this particular model, the optimal angle of attack was achieved at 6°, which gives the best glide ratio for the model, hence the instructions regarding the blade placement.

Changing the standard configuration of the wind turbine hub assembly by adding an unconventional geometry on the experimental setup, while maintaining the same geometry of the blades, for different angles of attack, different air flow speed, identical to the numerical model, an increase in the number of revolutions per minute of the rotor is achieved. The result notes an increased utilization of the potential wind energy, therefore an increase of the turbine efficiency.

These numerical and experimental models can be used for further analysis regarding the placement of the hemisphere, improving its aerodynamic geometry and its influence on the statics and loads on the whole construction of the turbine. Finally, these models can be used for further analysis regarding the influence of this geometry on the air flow at a wind farm.

REFERENCES

[1] Vargas, S. A., Esteves, G., Macaira P., Bastos B., Oliveira F., Souza R. (2019): Wind power generation: A review and a research agenda, *Journal of Cleaner Production* **218**, pp. 850–870. https://doi.org/10.1016/j.jclepro.2019.02.015

[2] Burton, L. T., Jenkins, N., Bossanyi, E., Sharpe D., Graham, M. (2021): *Wind Energy Handbook*, WILEY, 3rd Edition. ISBN: 978-1-119-45109-9

[3] Hau, E., Renouard, H. (2006): *Wind Turbines: Fundamentals, Technologies, Application, Economics*, Springer, 2nd Edition. https://link.springer.com/book/10.1007/3-540-29284-5

[4] Kassa, B. Y., Baheta, A. T., Beyenne, A. (2024): Current trends and innovations in enhancing the aerodynamic performance of small-scale, Horizontal Axis Wind Turbines: A review, ASME *Open Journal of Engineering* **3**, https://doi.org/10.1115/1.4064141

[5] Wang, S. H., Chen S. (2008): Blade number effect for a ducted wind turbine, *Journal of Mechanical Science and Technology*, **22**, pp. 1984–1992. https://doi.org/10.1007/s12206-008-0743-8

[6] Shintake, T. (2016): Harnessing the power of breaking waves, *Proceedings of the 3rd Asian Wave & Tidal Energy Conference (AWTEC2016)*, pp. 623–-630.

[7] Eltayesh, A., Castellani F., Burlando M., Hanna, B. M., Huzayyin, A. S., El-Batsh, H. M., Becchetti, M. (2021): Experimental and numerical investigation of the effect of blade number on the aerodynamic performance of a small-scale horizontal axis wind turbine, *Alexandria Engineering Journal* **60** (4), pp. 3931–3944. https://doi.org/10.1016/j.aej.2021.02.048

[8] Lee, M. H., Shiah, Y. C., Bai, C. J. (2016): Experiments and numerical simulations of the rotor-blade performance for a small-scale horizontal axis wind turbine, *Journal of Wind Engineering and Industrial Aerodynamics* **149**, pp. 17–29. https://doi.org/10.1016/j.jweia.2015.12.002

[9] Thangavelu S. K., Chow S. F., Sia C. C. V., Chong K. H. (2021): Aeroelastic performance analysis of horizontal axis wind turbine (HAWT) swept blades, *Materials Today*: *Proceedings 2021,* **47** (15), pp. 4965–4972. https://doi.org/10.1016/j.matpr.2021.04.315

[10] Stoevesandt, B., Schepers, G., Fuglsang P., Sun, Y. (2022): *Handbook of Wind Energy Aerodynamics, 2022*.

Mechanical Engineering – Scientific Journal, Vol. **42,** No. 2, pp. 117–125 (2024)
Number of article: 686
In print: ISSN 1857–5293
Received: July 11, 2024
On line: ISSN 1857–9191
Accepted: November 14, 2024
UDC: 620.92-048.37:340.13(497.7)
https://doi.org/10.55302/MESJ24422117m

Orginal scientific paper

REVIEW OF THE REQUIRED LEGISLATIVE CHANGES TO FACILITATE N. MACEDONIA'S TRANSITION TO RENEWABLES

Nikola Manev[1], Eleonora Jovanović[2], Dame Dimitrovski[2]

[1]*Military Academy "General Mihailo Apostolski", Skopje, Goce Delčev University, Štip*
Vasko Karangeleski bb, Skopje, Republic of North Macedonia
[2]*Faculty of Mechanical Engineering, "Ss. Cyril and Methodius" University in Skopje,*
P.O.Box 464, MK-1001 Skopje, Republic of North Macedonia
manev.nikola@yahoo.com

A b s t r a c t: North Macedonia's recent steps towards clean energy have mirrored the country's ambitions to join the European Union and have included a significant revamp of its 2030 energy development strategy putting a lot of emphasis on the liberalization of the energy sector and an increase in the share of renewables in energy production. However, facilitating this energy transition that seeks to embody the postulates of the European Green Deal, as predicted in the newly adopted, 2040 energy strategy would encompass the combined efforts by existing and newly created entities (both government and private) that form the energy sector in the country. This in turn requires the unification of their efforts through the creation of a legislative framework that will include major regulation changes to ensure that the focused actions of the energy sector entities are controlled, and do not overload the grid, or endanger its stability. Analyzing the successful outcomes provided by regulation advancement in the last 5 years, while relying on the lessons learned principle, will provide the backdrop against which these new regulation changes can be proposed.

Key words: legislation; renewable energy sources; grid stability; energy liberalization; energy transition

ОСВРТ НА ПРОМЕНИТЕ ПОТРЕБНИ ВО ПРАВНАТА РЕГУЛАТИВА НА С. МАКЕДОНИЈА ЗА ОЛЕСНУВАЊЕ НА ТРАНЗИЦИЈАТА КОН ОБНОВЛИВИ ИЗВОРИ НА ЕНЕРГИЈА

А п с т р а к т: Чекорите на С. Македонија кон почиста енергија совршено ги отсликуваат амбициите на земјата да стане дел од Европската Унија и подразбираат обновување на целите од Стратегијата за развој на енергетскиот сектор до 2030 година, ставајќи акцент на либерализацијата на енергетскиот сектор и значителното зголемување на уделот на обновливите извори на енергија во производството на електрична енергија. Меѓутоа, остварувањето на енергетската транзиција која цели да ги отелотвори постулатите на Европскиот зелен договор, вметнати во новата Стратегија за развој на енергетскиот сектор до 2040 година, ги опфаќа здружените напори на сите постојни и новосоздадени правни ентитети (од владиниот, но и од приватниот сектор) кои го сочинуваат енергетскиот сектор во државата. Ова повлекува потреба од унифицирање на нивните напори преку создавање правна рамка со значителни регулативни промени кои ќе служат како контролен механизам за обединетите активности на енергетските ентитети, со чија помош би се избегнало оптоварување на мрежата за пренос на електричната енергија и би се осигурила нејзината стабилност. Потпирајќи се на принципот за научени лекции, анализирањето на позитивните практики од изминатите 5 години, кои произлегле од промените во правната регулатива, е добра основа врз која би се предложиле новите регулативни промени.

Клучни зборови: легислатива; обновливи извори на енергија; стабилност на електро-енергетската мрежа; енергетска либерализација; енергетска транзиција

1. INTRODUCTION

The geopolitical turmoil of the last few years has made Europe's excessive energy dependence painfully obvious. However, a geopolitically influential, stable and secure European Union (EU) can do nothing less than ensure its energy security in a manner compatible with its climate objectives. For-

tunately, in the medium and long-term, the goals of the European Green Deal (EGD) coincide with the goals related to the EU's energy security, as European policymakers find the EU's climate agenda a vital part of the response to Russian aggression. In fact, it seems that the war in Ukraine has acted as a catalyst for the EU. It has accelerated its transition to using more renewable energy [1]. Renewable energy sources (RES) are clean and potentially endless, and they produce no emissions during operation. Subsequently, the rise in renewable energy use for electricity generation is key in helping the EU reach its European Green Deal (EGD) goals. This shift, along with increased use of biofuels and green hydrogen, has helped reduce fossil fuel reliance.

Almost in the same timeframe (2020–2023) the Republic of North Macedonia, a candidate country for accession and membership in the EU for the better part of the last two decades, that gets around 280 sunny days per year, was said to have "pioneered the energy transition towards renewables in the Western Balkans" [2]. Recently, the country has seen an exponential growth of its photovoltaic (PV) electricity generation capacities, with figures stating a 140% rise in installed capacity for the 2022–2023 period alone [3]. This might be the only positive aspect in an otherwise challenging energy landscape. The country's 2030 energy development strategy stresses the need for greater energy security. This requires diversifying energy resources by type, source, and supplier. To achieve this, the country must maximize the use of domestic resources [4]. However, the strategy faces several challenges. These include outdated technologies and insufficient investments in maintenance, modernization, and expansion. There are also high electricity losses, both technical and commercial. The current energy mix is unfavourably structured from an environmental and economic standpoint, and the country remains heavily dependent on energy imports. Finally, there is incomplete harmonization of legislation with European standards.

As a direct consequence, the spike in electric energy production due to the newly installed PV capacities has resulted in a heightened risk of grid overload without no immediate solution to the intermittent nature of renewables since the current energy needs rarely correlate with the disposability of the generated energy [5]. However, this challenge has already been addressed in the more recent – 2040 energy development strategy, but it seems a legislative framework that would coordinate and unify the efforts of all energy sector entities is still lacking [6]. In summary, this paper aims to examine the steps North Macedonia is taking to draft and adopt the necessary policy changes. These changes are intended to support a smooth transition to renewable energy, reduce energy dependency, and enhance energy security. The goal is to achieve this transition at a pace that does not jeopardize the country's electricity distribution grid or existing generation capacities.

2. REGULATION WITH REGARDS TO THE USE OF RES

Regulation development basis

The energy development strategy of the Republic of North Macedonia is created by a working group composed of academics, researchers, and experts from diverse fields. This group operates under the Research Centre for Energy and Sustainable Development (RCESD), a body of the Macedonian Academy of Arts and Sciences, which conducts both fundamental and applied research in the energy sector. Due to the interdisciplinary nature of the research involved, the strategy addresses a broad range of issues, including the energy, economic, organizational, institutional, legislative, and educational dimensions of energy sector development. It focuses on key areas such as energy production, distribution, and utilization. The primary objective of the strategy is to outline the most favourable long-term path for the sector's development, while identifying potential challenges and proposing solutions to mitigate them.

Once formulated and adopted by the government, the Strategy serves as a critical framework for the country's sustainable development and its integration into broader European processes. To date, the RCESD has drafted two Strategies: one covering the period 2010–2030 and another for 2020–2040 (Figure 1).

While the Strategies provide valuable foresight, they should be regarded as dynamic documents, with varying degrees of precision in their projections. As such, the Strategy must be regularly updated to reflect new developments in both the national and global energy landscape. Nonetheless, the Strategy offers a robust foundation for the proactive engagement of all stakeholders in the Macedonian energy sector. It ensures that relevant authorities and entities collaborate towards a common goal, guided by a shared vision.

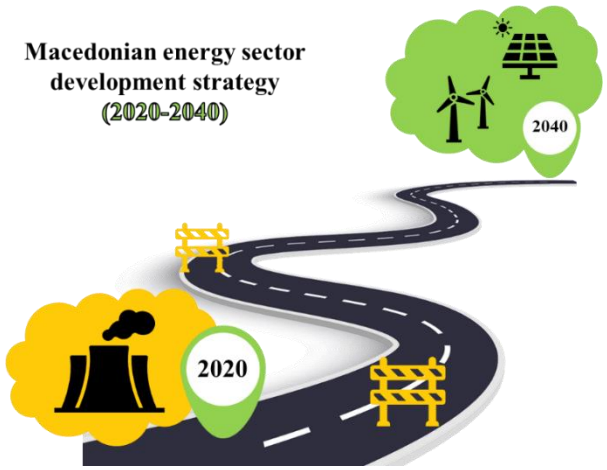

Fig. 1. Energy sector development strategy 2020–2040

Institutional framework

The institutional framework of North Macedonia's energy sector begins with the government, which is responsible for proposing policy measures and overseeing their implementation. At the other end, municipal councils at the local level are tasked with proposing and enacting measures aligned with the goals of the energy development strategy. Between these two levels, numerous entities exist, with overlapping and often interchangeable roles in the energy sector.

At the government level, the ministry responsible for the energy sector up to 2024 was the Ministry of Economy. It had a dedicated Energy Department whose main tasks were the strategic planning and development of the legislation in the energy sector, implementation of the energy policy including the policies for energy efficiency and renewable energy sources, and the use of new technologies. The government, through this department, also encouraged the development of the private sector in the area of energy and supported the scientific and technological development, particularly in the utilization of renewable energy sources. At the same level, however, part of the responsibilities related to energy used to belong to the Ministry of Environment and Physical Planning and the Ministry of Transport and Communications.

To assist the government in implementing energy policy, the Energy Agency (EA) was established in 2006. The EA was responsible for preparing strategies, development plans, and programs related to energy efficiency and renewable energy utilization. It also coordinated regional projects, prepared proposals for energy-related laws and technical regulations, and supported the implementation of investment projects.

Following the general elections in North Macedonia, however, in the second half of 2024, amid a major government restructuring, a new Ministry of Energy, Mining and Mineral Resources was established. The new ministry complements the existing governmental structure by consolidating and streamlining energy-related responsibilities under one dedicated authority. This move aims to enhance coordination, policy development, and implementation within the energy sector. The Ministry of Energy is expected to play a central role in managing the country's energy transition, ensuring the alignment of national energy policies with European Union standards, and overseeing key areas such as renewable energy, energy efficiency, and infrastructure development. By focusing specifically on energy issues, it allows for more focused leadership and better alignment of strategies, while also improving the oversight and integration of energy-related projects across various sectors of government.

The Energy Regulatory Commission (ERC), an independent body, plays a crucial role in regulating energy activities. Operating under the Law on Energy, the ERC is tasked with overseeing specific energy sector issues and making decisions within its defined legal framework.

Finally, at the municipal level, the mayor and municipal councils propose actions on implementing specific segments of the energy policy, based on public interest and local significance. They determine the need and sources of funding for new and the reconstruction and upgrade of existing facilities, propose measures and activities for increasing energy efficiency and support the production of energy from RES. These proposals had to be approved by the Ministry of Economy (now the new Ministry of Energy), upon which they are enacted in the form of a municipal energy development program for a period of five years.

Standing regulation

North Macedonia has historically signed and ratified the Agreement of the Energy Charter, the Energy Community (EnC) Treaty, the United Nations Framework Convention on Climate Change and the Kyoto Protocol. According to the Energy Community Treaty, a major part of the country's successful energy transition is the full compliance and harmonization with the EU's energy community core legislation on energy, environment, RES, energy efficiency and oil reserves.

Consequently, North Macedonia's strategic commitments in the energy sector have been incorporated in the Law on Energy, first drafted in 2008 and adopted in 2011, albeit heavily revised in 2018. The revised Law on Energy in 2018 transposed the EU's Third Energy Package in the electricity sector, as well as their RES Directive with regards to greater implementation of renewables in the heating, electricity production, and transport sectors.

The Law on Energy includes a dedicated chapter on renewable energy sources (RES). It proposes a 10-year action plan aimed at further developing the electric power system. This plan focuses on introducing smart grids and energy storage systems to ensure reliable operation as the share of RES increases. The law also offers financial incentives for renewable energy producers, in line with Directive 2009/28/EC. These incentives include feed-in premiums to support "preferred producers" and encourage greater market integration of renewables. The law stipulates that the electricity distribution system operator must prioritize access and distribution for RES-generated electricity. This must be done in an objective, transparent, and non-discriminatory manner, considering the operational limits of the power system. Additionally, the law states that no license is required for producing electricity from RES for personal use. Surplus energy can be supplied to the distribution network under conditions set by secondary rules and regulations. To protect the environment, RES electricity generation plants are considered public interest projects.

The use of RES in electricity generation is also addressed in the Law on Energy Efficiency, adopted in 2022. This law aims to regulate energy use and draft policies to increase efficiency in production, transmission, distribution, and supply. It also seeks to support higher shares of renewables in the energy mix. The Law on Energy Efficiency introduces the concept of an "energy aggregate." This refers to a service provider that combines load curves from multiple consumers to sell or auction energy on organized markets. The goal is to reduce peak loads, balance energy from renewable sources, and enhance supply security. However, the law places more emphasis on using RES for heating rather than electricity generation. A key provision focuses on building design and major renovations. It requires a mandatory energy analysis by a building inspector to assess the potential for decentralized RES systems, combined energy production systems, heat pump systems, or centralized heating and cooling systems supplied by RES.

While RES application is not immediately attributed to any remaining legislative acts, the existing Law on Concessions and Public-private Partnerships, as well as the Law on Environment and the Law on the Protection of Nature, have indirectly facilitated the accelerated implementation of RES in electricity production. Similarly, the Law on Waste Management and the Law on Battery Waste Management, in line with circular economy agendas to prolong a product's life and recycling could potentially stimulate the creation of battery energy storage systems (BESS) by repurposing old electric vehicle batteries [7].

Proposed regulation

In recent years, North Macedonia has made consistent efforts to harmonize its energy legislation with that of the EU. The guidelines outlined in the energy sector development strategies, alongside the passage of the Law on Energy, have led to the drafting of numerous primary and secondary regulations. However, the process of passing and implementing these laws has been slow and with varying degrees of success. The previous application of the renewable energy provisions within the Law on Energy revealed gaps that need to be addressed to better align with new trends and emerging needs in both the global and domestic energy sectors. In many neighbouring countries, renewable energy is governed by dedicated laws separate from general energy policy. Recognizing this, North Macedonia has moved toward adopting a distinct Law on Renewable Energy Sources [8].

This new law seeks to fill the gaps left by the Law on Energy, focusing on encouraging greater consumer adoption of renewable energy, promoting the production of RES to meet local demand, and reducing long-term energy import dependency. It aims to decrease reliance on fossil fuels, protect the environment, and help mitigate climate change. As of late 2023, the Draft Law on RES proposes a series of support measures to help achieve the objectives of the 2040 Energy Development Strategy and the National Energy and Climate Plans. These focus on increasing the share of RES in gross final energy consumption. The draft law also calls for the development of the electric power system, incorporating smart grids, smart metering systems, and electricity storage solutions to ensure reliable system operation as the share of RES grows. Furthermore, it advocates for the integration of RES into the electricity

market, while avoiding market distortions and considering the costs of system integration and network stability. Additionally, the draft law emphasizes the need for urban planning documents to align with the construction of RES production facilities, ensuring proper approval processes for building or reconstructing such facilities.

Moreover, this newly drafted law details the conditions of becoming a preferred electricity producer and the responsibilities towards the country's electricity production and distribution system ensured by the application of higher technical standards of the installed systems and the licensing of both the production plant and the installers. All RES electricity producers will have to meet the technical-technological conditions, and the connection requirements set out in the Network Rules for Electricity Distribution [9, 10] and must be recorded within the country's registry by their production capacity.

Households and small consumers could be self-sustained by building their own photovoltaic system or small wind farm with 4 kW of installed capacity for households, and 20 kW of installed capacity for small consumers. According to the Draft Law on RES [8], the produced electricity surplus from these units would be handed over to the electricity distribution network at a price calculated as:

$$C = \text{PCE} \cdot 0.9, \quad \text{if} \quad E_i \geq E_p$$

or

$$\text{C} = \text{PCE} \cdot 0.9 \cdot E_i / E_p, \quad \text{if} \quad E_i < E_p$$

where:

E_i = the total electricity delivered by the supplier and taken by the consumer-producer within a calculation period and expressed in kWh,

E_p = the total electrical energy delivered to the electrical distribution network from the consumer-producer within a calculation period and expressed in kWh,

PCE = average price of electricity that the consumer-producer pays to the supplier for the purchased electricity, without compensation for using the network (net fee) and other fees and taxes, within a calculation period and expressed in MKD/kWh.

Finally, the issue of energy storage is briefly addressed. The draft law allows a preferred electricity producer to establish an energy storage facility, which can be used to store the electricity generated by their own power plant – specifically, the plant that receives financial support (such as a premium) for its energy production, which is then supplied to the distribution network. At the same time, the law prohibits the preferred producer from using the storage facility to store electricity drawn from the network.

In summary, despite being an important piece of legislature, in this draft stage, some points of the law seem too vague, while others are deliberately left loosely defined. However, the proposed Law on RES is currently open to suggestions and public debate over its contents [11] and will likely see some future additions made by representatives from the expert community, academia and both the private and public sectors.

Of the remaining proposed legislation, North Macedonia ratified the Paris Agreement as a non-Annex I Party to UNFCCC, with the next most important strategic measures being the adoption of a Long-Term Climate Action Strategy and a Law on Climate Action. The country is in the process of adopting both in order to establish a strong and sustainable framework for coordinating climate action through the development of a national strategic and legal framework harmonized with the EU and supported by the financing mechanism of the EU Instrument for Pre-Accession Assistance (IPA II). Drafting of the Climate Action Law (including the transposition of Regulation (EU) No. 525/2013 on monitoring mechanisms) has begun, and the first draft was prepared in April 2020.

Work on the Long-Term Climate Action Strategy began in March 2019 and was finalized with its publication in May 2021. The strategy aims to significantly reduce greenhouse gas emissions and enhance the resilience of society, the economy, and ecosystems to the impacts of climate change. It focuses on establishing a highly efficient energy system that is predominantly powered by renewable energy sources (RES). The goals of the strategy are embedded in the Law on Climate Action. This includes proposing measures to promote the production of renewable or CO_2-free energy, together with measures to improve energy conservation and efficiency across all sectors of the economy. The strategy also emphasizes the need to foster investments in climate-friendly projects, support research, and encourage best practices in key areas, such as renewable energy production, energy distribution and management, energy storage, smart grid technologies, and data centers for utilizing renewable energy.

3. ANALYSIS OF THE 2018–2023 TIMEFRAME: RES IN ELECTRICITY PRODUCTION

The electricity production capability of North Macedonia, historically, has relied on coal-fired thermal power plants and hydro power plants as the main electricity generation capacities. The main electricity production entity in the country is a state-owned company – Elektrani na Makedonija (ELEM), which accounts for ~70% of the total installed capacity, as the owner of two large coal-fired thermal power plants, Bitola and Oslomej. The total installed electricity production capacity of the country is 2.06 GW with ~48% belonging to thermal power plants, ~34% to both large and small hydro power plants, ~15% to combined natural gas fired plants, and only ~3% to other RES [12].

In recent years electricity generation from coal in North Macedonia has been decreasing steadily and has amounted to ~60% in 2017. On the other hand, overall, RES generation capacity has been increasing (from 2010 until 2018) amounting to 37% (including hydro power), which has led to the increase of RES generation up to almost 25% in the overall generation in 2017 and 2018 [12]. It should also be noted, that in 2018, RES accounted for 18.1% of the gross energy consumption in the country, which is almost identical to the quantities reported by EU-28 countries for the same time period. At the end of 2017, with regards to RES there were 170 eligible producers with 128 MW installed capacity that have been using financial incentives in the form of feed-in premium tariffs with 67.5 MW hydro, 16.8 MW solar PV, 36.8 MW wind and 7 MW of biogas, respectively. The overall paid incentives to eligible producers of electricity have been rising steeply and added up to 35.7 mil EUR in 2017. Back then, the government revealed its plans to continue with the feed-in tariff mechanism, to introduce market-based premiums and provide the legal backdrop against which these changes can be performed in the form of the revised Law on Energy.

North Macedonia has a theoretical ~7.3 GW potential for exploiting RES for electricity production, especially solar and wind RES [13]. The highest share of this potential comes from wind of up to 4.9 GW, followed by solar PV up to 1.4 GW, and hydro up to 0.67 GW. The largest cost-competitive solar PV potential is on a utility scale, while large-scale hydro potential is mainly located on the Vardar river and to a lesser extent on the Black Drim river. Due to the major revisions and additions to the Law on Energy in 2018, in the field of RES, the ERC announced that during 2022 it issued 267 new RES power plant licenses with a total installed capacity of 152.2 MW [14]. With that, the total installed capacity (Figure 2) for electricity production in the country increased by 7%. Most investments were made in PV power plants – 106.5 MW, followed by 36 MW in wind power plants, 7.2 MW in small hydropower plants and, 2.5 MW in biogas thermal power plants [14]. With the introduction of a Program for the promotion on the use of RES in 2022 [15] that details and eases the application conditions for feed-in premiums for large RES plants and subsidies for households and small consumers, this investment trend was expected to continue in 2023, with another 250–300 MW, however factual reports if this was the case are still not published.

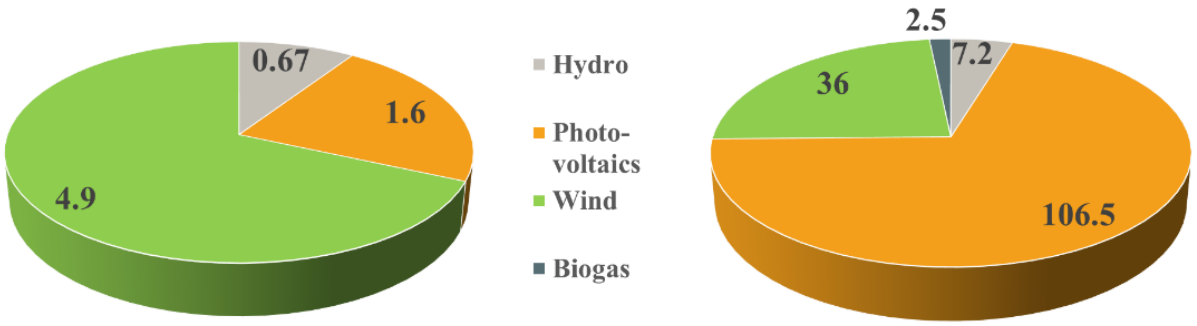

Fig. 2. Theoretical energy potential and installed capacity in 2022

Until recently, North Macedonia used the cheapest electricity in the region, which is why most industrial facilities as well as its citizens were comfortable on the issue of energy. But, following the energy crisis brought by Covid 19, significantly exacerbated by the war in Ukraine, with energy prices increasing by 400–500% [16], it became obvious paying the new tariffs will likely take a

major financial toll. In 2021, the prices of all energy sources reached a historical peak, with electricity prices reaching 450 EUR per MW/h, in contrast to pre-crisis prices of 55–65 EUR per MW/h [16]. From today's perspective, energy prices are not likely to drop to their pre-crisis rates, and investment into RES has been seen as a potential energy sector stabilization measure, with investments in PV power plants being the only faster option through which industrial facilities, companies and even homes can reach a lower electricity bill.

It is clear that renewable energy sources, and particularly PV electricity production systems, have the potential to lower electricity costs, especially for businesses. Their hurried introduction in North Macedonia, however, coupled with their intermittent nature have led to infrastructural and transmission challenges. This was identified in 2022 by the ERC, as new PV capacities strained the stability and even threatened to overload the distribution network. A potential solution currently considered by the ERC is the introduction of battery energy storage systems capable of balancing electricity production with the actual needs and the peaks and lows of electricity demand. Official studies by the ERC are reportedly ongoing, but experience has shown that the BESS should be able to store 10–20% of the installed capacity of the PV power plant. A legislative obligation to install BESS along with larger PV plants is also considered although this will increase the price of the investment by 20–30%, which might have to be alleviated through BESS subsidies to reduce the difference [16].

4. DISCUSSION

According to the 2040 Energy Development Strategy [6] RES share in the gross final energy consumption increases over all three proposed development scenarios as part of the strategy, landing in the range of 35–45% in 2040. The utilization level of the renewables as an important factor for decarbonization of the energy sector, has been considered relevant even in the most unfavorable – the Reference scenario, where 33% RES share is projected after 2030, and by taking into account heat pumps, the RES share in gross final energy consumption would become even higher, reaching almost 40% in the more favorable Moderate transition scenario and 45% in the Green scenario. All three scenarios (Figure 3) envisage a steep growth of electricity generated from RES (~7 times more in 2040 vs. 2017) with hydro maintaining its largest share in electricity generation, but PV and wind being the fastest growing technologies.

According to the 2040 Energy Development Strategy [6], the share of Renewable Energy Sources (RES) in gross final energy consumption is projected to increase across all three proposed development scenarios, reaching between 35% and 45% by 2040. The role of renewables in decarbonizing the energy sector remains critical, even under the most challenging scenario – the Reference scenario – which forecasts a 33% RES share post-2030. When factoring in the use of heat pumps, the RES share would rise further, reaching nearly 40% under the Moderate transition scenario and 45% under the Green scenario. All three scenarios (Figure 3) predict a significant rise in electricity generated from RES, with a projected sevenfold increase by 2040 compared to 2017. Hydropower will continue to contribute the largest share of electricity generation, while PV and wind energy technologies are expected to grow the most rapidly.

However, North Macedonia still faces relatively high levels of electricity supply interruptions in its distribution network compared to regional averages. As such, there is considerable potential for improving the reliability of the country's power supply. To integrate more RES, the country will need to invest in further developing its distribution network and continuously enhance its overall reliability.

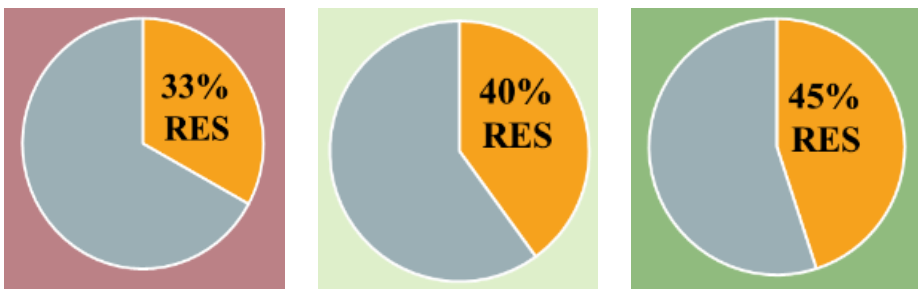

Fig. 3. RES share in gross final energy consumption over three proposed scenarios following 2030 [6]

Additionally, to integrate more variable RES necessitates to manage system flexibility. Besides the huge amount of solar PVs (up to 1,400 MW), the scenarios envisage up to 750 MW of wind, which are less predictable in terms of hourly generation. This will add to the complexity of daily operations for grid management, and some of the likely solutions include:

– Implementation of viable demand response options, including vehicle-to-grid, power-to-heat and battery storage. Although the average available capacity is similar in Reference and Green scenarios, the differences in spread between peak demand and maximum theoretical available capacity (–23% for Green scenario vs. –8% for Reference scenario) emphasizes the critical need for investments in flexibility in the Green scenario.

– Implementing a balancing mechanism as a short-term step (including system services for secondary and fast tertiary regulation). In this direction, cross-border balancing could enable a cost-effective solution, while in the mid and long-term, the steps include use of existing and construction of new power plants such as pumped-storage hydropower plants or gas fired power plants (including combined heat and power). Additional flexibility could be gained from biomass and biogas small-scale plants.

5. CONCLUSIONS

Efficient use of energy and renewables are the cornerstone of the EU's energy transition as set out in the EGD and the most immediate response to its energy dependency on Russian gas. Therefore, although zero carbon fuels are expected to have a much more significant role in the future primary energy consumption, RES should be the ones winning the growth race. North Macedonia, being an accession candidate to the EU has been dedicated to harmonizing its legislation with that of the EU's energy community while also trying to lessen the effects of the 2021 global energy crisis. These efforts have translated into major revisions of its Law on Energy and the subsequent creation of multiple national action plans (on energy efficiency, on energy and climate, and on the use of RES) which along with the financial incentives derived from them have led to significant penetration of renewables, and particularly PV systems have increased the electricity production capacity and the total gross consumption of electricity derived from RES in North Macedonia.

However, in spite of the detailed scenarios developed as part of the 2030 and 2040 Energy Development Strategies, North Macedonia is lacking an overall proactive approach in the legislative segment, since most regulations are being passed reactively or rather once a challenge for the energy sector is exposed. The current policies offer limited guidance on several key issues, including the reliable integration of new electricity generation infrastructure, the ongoing improvement of the grid through soft measures, and plans for new investments and upgrades to the distribution network. They also lack provisions for advanced concepts such as smart grids, energy storage systems, and vehicle-to-grid technologies. Drafting the new Law on RES is a step in the right direction, but even it, with all its strong suits, might be arriving a little too late. While this law offers potential solutions and incentives for new users it does little to protect the grid of potential overloads and balancing out the peaks and lows of electricity production and demand. To effectively implement the new energy sector policies, which introduce numerous obligations, it is essential to strengthen the capacity of North Macedonia's energy institutions. At present, institutional capacity is limited, and intergovernmental coordination is almost nonexistent. The establishment of the new Ministry of Energy, Mining, and Mineral Resouces, however, offers a glimmer of hope, as it presents itself as a vital step toward addressing these challenges.

In summary, North Macedonia's energy sector sentiments are in the right place looking to increase RES penetration in electricity production but lack the legislative framework that would allow this to happen without endangering future electricity production and grid integrity.

REFERENCES

[1] Manev. N., Nikolov, E. (2022): The European Green Deal and the EU's energy transition in the wake of the war in Ukraine. *International Scientific Journal Contemporary Macedonian Defence*. Vol. **22** (43).

[2] JustTransition (2021): North Macedonia pioneering energy transition in the Western Balkans. Available at: https://www.just-transition.info/north-macedonia-pioneering-energy-transition-in-the-western-balkans/

[3] Energy Regulatory Commission (2023a): January 2022 – October 2023 Report. New renewable energy production capacities. Available at: https://telma.com.mk/2023/11/11/rke-za-140-procenti-e-zgolemen-instaliraniot-kapacitet-za-proizvodstvo-na-struja-od-sonce/

[4] Ministry of Economy (2010): *Strategy for Energy Development of the Republic of Macedonia until 2030*.

[5] Deutsche Welle (2023): *Boom of Photovoltaics Installation* (orig. in Macedonian). Available at: https://www.dw.com/mk/bum-na-fotovoltaicite-vo-makedonija-se-bara-nacin-kako-da-se-skladira-strujata/a-64745449

[6] Ministry of Economy (2019): *Strategy for Energy Development of the Republic of North Macedonia up to 2040*.

[7] N. Manev, E. Jovanovikj, D. Dimitrovski (2022): The challenges and environmental justification of recycling Li-ion EV batteries. *Mechanical Engineering Scientific Journal*. **40** (2), pp. https://doi.org/10.55302/MESJ22402653085m

[8] ENER (2024): *Draft of the Proposed Law on Rrenewable Eenergy Sources.* National Electronic Registry of Regulations. Available at: https://ener.gov.mk/Default.aspx?Item=pub_regulation&subitem=view_reg_detail&itemid=81522

[9] RES Rulebook (2018): Rulebook on the use of Renewable Energy Sources. *Official Gazette of the Republic of North Macedonia* Number 96/2018

[10] ElektroDistribucija (2019): Network rules for electricity distribution. *OfficialGgazette of the Republic of North Macedonia*, No. 191 from 17.09.2019.

[11] ENER (2023): Open call for public input on the Draft Law on Renewable Energy Sources. National Electronic Registry of Regulations. Available at: https://ener.gov.mk/Default.aspx?item=top_news&subitem=view_pr_detail&itemid=5Sd71W+MdMG8vpoPsvKXog==

[12] GIZ (2022): *National Plan for Energy and Climate of the Republic of North Macedonia*.

[13] IRENA, Joanneum Research and University of Ljubljana (2017): *Cost-Competitive Renewable Power Generation: Potential across South East Europe*. International Renewable Energy Agency (IRENA), Abu Dhabi

[14] Energy Regulatory Commission (2023b): *New 150 MW from renewables, photovoltaic plants will now have to invest in batteries* (orig. in Macedonian). Report. Available at: https://www.slobodnaevropa.mk/a/32218888.html

[15] Ministry of Economy (2023): Program for the promotion of renewable energy sources and encouragement of energy efficiency in households for the year 2023. *Official Gazette of the Republic of North Macedonia Number 27 from 08.02.2023.*

[16] Deutsche Welle (2022): *Photovoltaic rush in North Macedonia. Economy Section News*. Available at: https://www.dw.com/mk/фотоволтаична-треска-во-северна-македонија/a-61757846

Mechanical Engineering – Scientific Journal, Vol. **42,** No. 2, pp. 127–132 (2024)
Number of article: 687 In print: ISSN 1857–5293
Received: November 19, 2024 On line: ISSN 1857–9191
Accepted: November 27, 2024 UDC: 621.31:502.131.1]:[004.4:004.52(497.7)
https://doi.org/10.55302/MESJ244221271s

Original scientific paper

ANALYSIS OF PRODUCTION CAPACITIES AND SUSTAINABILITY OF THE ENERGY SECTOR OF THE REPUBLIC OF NORTH MACEDONIA USING THE ENERGYPLAN SOFTWARE

Ivica Stojanovski, Igor Šešo

Faculty of Mechanical Engineering, "Ss. Cyril and Methodius" University in Skopje,
P.O.Box 464, MK-1001 Skopje, Republic of North Macedonia
i.stojanovski2571@student.mf.ukim.edu.mk

A b s t r a c t: The energy sector of the Republic of North Macedonia faces considerable challenges in achieving sustainable transition and reducing greenhouse gas emissions. Using the EnergyPLAN software, various scenarios were analyzed to evaluate the potential for a complete phase-out of coal and oil-fired thermal power plants, replaced by renewable sources and new natural gas cogeneration plants. The results indicate that increasing the share of renewables significantly enhances energy security and contributes to CO_2 emissions reduction, aligning with set climate targets. These findings highlight the need for a strategic approach to modernizing the energy sector, which would foster long-term sustainability, reduce dependence on energy imports, and enable greater energy independence for North Macedonia.

Key words: CO_2 emissions; EnergyPLAN; energy sector; renewable energy sources; sustainable development

АНАЛИЗА НА ПРОИЗВОДСТВЕНИТЕ КАПАЦИТЕТИ И ОДРЖЛИВОСТА НА ЕНЕРГЕТСКИОТ СЕКТОР НА РЕПУБЛИКА СЕВЕРНА МАКЕДОНИЈА СО ПРИМЕНА НА СОФТВЕРОТ ENERGYPLAN

А п с т р а к т: Енергетскиот сектор на Република Северна Македонија се соочува со значителни предизвици во насока на одржлива транзиција и намалување на стаклениčките гасови. Користејќи го софтверот EnergyPLAN, анализирани се различни сценарија за целосно исклучување на термоцентралите на јаглен и мазут со нивна замена со обновливи извори и нови когенеративни постројки на природен гас. Резултатите покажуваат дека зголемувањето на уделот на обновливите извори значително ја подобрува енергетската сигурност и води до намалување на емисиите на CO_2 за поставените климатски цели. Овие наоди нагласуваат потреба од стратегиски пристап кон модернизацијата на енергетскиот сектор, кој ќе ја поттикне долгорочната одржливост и ќе ја намали зависноста од увоз на енергија, овозможувајќи поголема енергетска независност за Македонија.

Клучни зборови: емисии на CO_2; EnergyPLAN; обновливи извори на енергија; одржлив развој; енергетски сектор

1. INTRODUCTION

The energy sector in North Macedonia faces significant challenges in its transition towards renewable energy sources, aiming to reduce greenhouse gas emissions and enhance energy independence [1]. Within the global context of sustainable development efforts, transforming national energy systems is essential, especially in countries highly dependent on fossil fuels [2]. North Macedonia strives to reduce emissions through a strategy focused on expanding the share of renewables, posing both technical and economic challenges for the country [3].

Previous studies on energy transition in North Macedonia focus on analyzing various scenarios and methods for integrating renewables using different simulation models.

Čosić, Krajačić, and Duić [4] analyze the potential for a 100% renewable energy system in North Macedonia by 2050, utilizing the EnergyPLAN model to simulate scenarios of 50% and 100% renewable sources. The results show that such a transition would require substantial investments in infrastructure and energy storage technologies yet would significantly reduce carbon emissions and increase energy independence.

A study published by the Macedonian Academy of Sciences and Arts [5] highlights how degraded and unused agricultural land could be repurposed for solar and wind installations, allowing for a significant increase in renewable energy production without altering natural resources. By fully utilizing these areas, North Macedonia could achieve high energy independence, reducing import dependency and enhancing system stability.

The paper "Assessment of Solar and Wind Energy Resources in Serbia" [6] evaluates the potential for solar and wind energy in Serbia by analyzing meteorological data and identifying optimal regions for renewable sources. The complementarity of these resources offers stability potential for energy systems relevant to similar systems such as North Macedonia's.

Lazova and Šešo [7] analyze North Macedonia's energy capacity, emphasizing the importance of developing infrastructure for renewable sources and introducing cogeneration plants. Their study evaluates scenarios for increasing the share of renewables, assessing impacts on system stability and the potential to reduce import dependency. The research suggests that proper planning and development of renewable energy infrastructure could significantly contribute to the country's energy independence and long-term system stability.

In their study, Mijakovski, Lutovska, and Mojsovski [8] examine the impact of the European energy crisis on North Macedonia, exploring measures to strengthen energy security through the integration of renewables. The findings indicate that expanding solar and wind capacities could substantially reduce import dependence and contribute to the stability of the energy sector.

This research aims to analyze the possibilities for the gradual phase-out of coal- and oil-fired power plants in North Macedonia by replacing them with renewable sources and new natural gas cogeneration plants. Using the EnergyPLAN software, detailed simulations of renewable integration scenarios are conducted to assess impacts on energy security, economic viability, and emissions reduction. Transitioning to renewable sources not only reduces imports but also contributes to economic stability by efficiently utilizing domestic and natural resources.

2. METHODOLOGY

The research employs a quantitative analysis method using EnergyPLAN software, designed to evaluate national energy systems and optimize energy resource distribution. EnergyPLAN facilitates the integration of renewable sources and assesses impacts on energy security, stability, and CO_2 emissions, providing iterative adjustments toward efficient, optimal solutions. This methodology is particularly suitable for modeling energy transitions in countries with systems similar to North Macedonia's.

Primary data sources include annual reports and databases from the Energy Regulatory Commission [9–13], AD ESM [14], and AD EVN [15], covering capacity, production, and energy imports-exports. The collected data span installed capacities (renewable and non-renewable), energy and fuel import-export figures (e.g., coal, natural gas, oil), fuel prices, electricity production, and consumption, as well as seasonal and daily demand variations. Additionally, information on consumption patterns across sectors enables an in-depth analysis of demand dynamics and resource allocation.

Data collection methods consist of reviewing reports from relevant institutions, accessing national and international databases, and analyzing official statistics, ensuring comprehensive and reliable data for simulations.

The analysis spans the years 2019 to 2023, capturing the impact of significant events on the energy sector, such as the COVID-19 pandemic and the Russia-Ukraine conflict, both of which have affected energy demand and supply. The pandemic led to reduced industrial and transport demand, accompanied by a rise in household energy use [16]. The conflict, on the other hand, has created global resource shortages and sharp price increases, underscoring the need for diversification and a transition to renewable sources [17].

Based on this analysis, two alternative scenarios are defined. Both involve constructing the Čebren pumped storage hydropower plant to balance the

electricity supply during high demand or low renewable generation. The scenarios differ regarding thermal power plant roles: in the first, one unit of the REK Bitola thermal plant remains operational as the sole active coal and oil-fired capacity; in the second, all thermal plants are retired, with coal fully replaced by renewables and new gas-based cogeneration.

Each scenario is examined from two perspectives: one prioritizes continuous operation to meet total energy demand, while the other focuses on economic viability, operating only when most cost-effective. The economic assessment considers the following costs: Čebren pumped storage – €1 billion, coal – €4/GJ, natural gas – €19/GJ, biomass – €9/GJ, €230 million for the new gas cogeneration plant, €790 million for new wind turbines, and €741 million for photovoltaic panels. A detailed descripttion of the scenarios is provided in Table 1.

T a b l e 1

Installed capacities of energy sources in N. Macedonia: actual capacities and two alternative scenarios

2023						
CHP	TPP	Dammed Hydro	HPP River Hydro	Pumped Back	Wind	PV
287.41	1034	557.4	162.4	0	72.8	310
Scenario 1:						
CHP	TPP	Dammed Hydro	HPP River Hydro	Pumped Back	Wind	PV
287.41	233	1015	162.4	458	600	1000
Scenario 2:						
CHP	TPP	Dammed Hydro	HPP River Hydro	Pumped Back	Wind	PV
487.41	0	1015	162.4	458	600	1000

3. RESULTS AND DISCUSSION

The analysis compares real data on North Macedonia's energy status, provided by the Energy Regulatory Commission, with theoretically possible scenarios simulated in EnergyPLAN. This comparison provides a detailed understanding of current opportunities for reducing imports by increasing domestic electricity production, as well as the potential for lowering CO_2 emissions. Through the additional two proposed alternative scenarios, the key role of renewable sources in the transition toward energy independence is also identified, contributing to the sector's long-term stability and sustainability.

The production of thermal energy from cogeneration plants and heating stations in Macedonia exhibits notable fluctuations throughout the analyzed period. These variations are attributed to several factors, including the growing demand for thermal energy, the condition of energy facilities, and the influence of policies aimed at promoting energy efficiency and the use of renewable sources. Simulations reveal that cogeneration plants possess significant potential to increase real production levels, with 2021 marking the highest recorded output compared to other years (Figure 1).

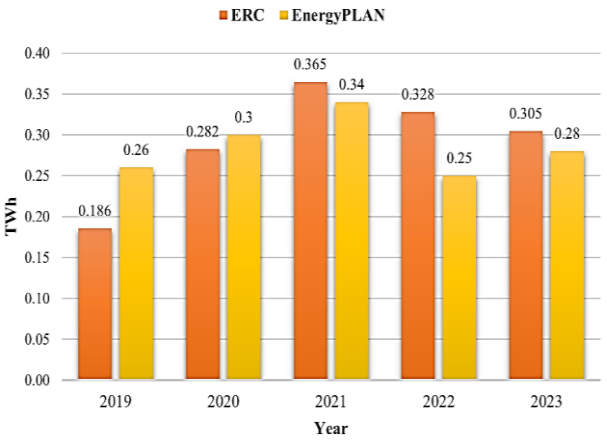

Fig. 1. Heat production from cogeneration plants during the analyzed period

This trend is crucial to the country's long-term energy strategy, as increased production from cogeneration sources may contribute to achieving energy independence and enhancing system stability. Additionally, heating stations, as traditional sources of thermal energy, continue to play a substantial role, although their contribution varies depending on market conditions and regulatory policies (Figure 2).

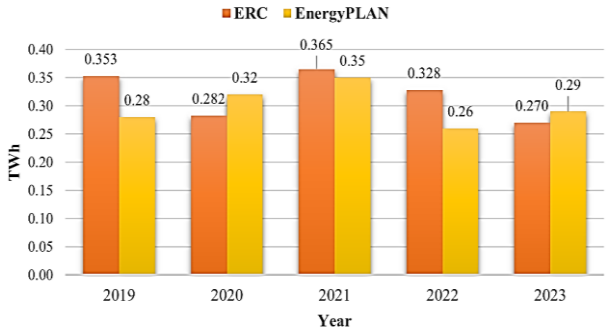

Fig. 2. Heat production from heating plants during the analyzed period

Electricity production from renewable sources and hydropower plants in Macedonia showed substantial growth over the analyzed period, particularly notable in 2023. This upward trend reflects ongoing investments and policy shifts favoring renewable technologies. Figure 3 illustrates this progress, highlighting increased energy generation from hydropower, wind, and solar sources. The 2023 peak production, the highest compared to previous years, underscores the effectiveness of strategies aimed at diversifying the energy mix. These results suggest Macedonia is gradually achieving its environmental goals, energy independence, and sustainable development, reducing reliance on fossil fuels and energy imports.

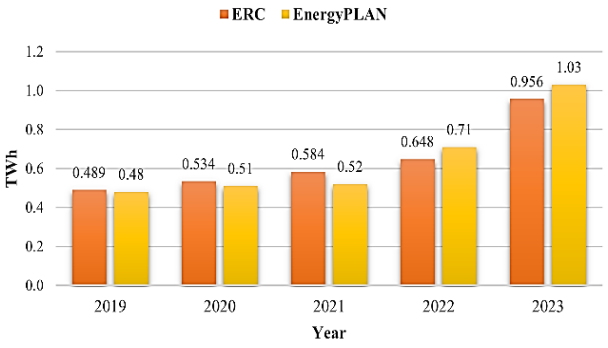

a) Electricity production from PV and wind

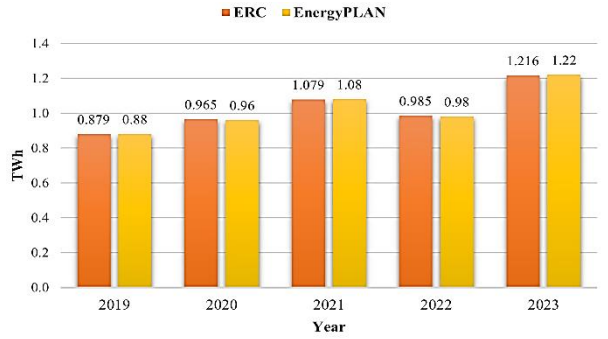

b) Electricity production from hydropower plants

Fig. 3. Electricity production from renewable sources during the analyzed period

According to data provided by the Energy Regulatory Commission, electricity production from thermal power plants and cogeneration facilities in North Macedonia has not demonstrated a clear trend of decline from 2019 to 2023. However, simulations conducted using the EnergyPLAN software indicate a potential decrease in production due to the gradual reduction in fossil fuel use and the shift toward more sustainable energy sources (Figure 4).

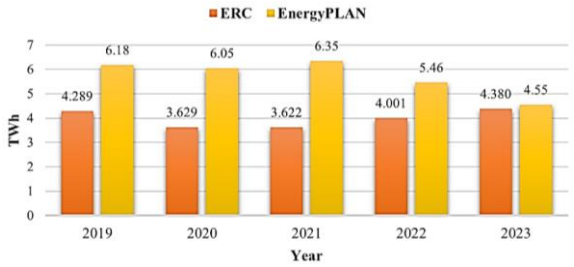

Fig. 4. Total electricity production from thermal power plants and cogeneration plants

These projections align with global and local decarbonization efforts in the energy sector, resulting in significant reductions in CO_2 emissions (Figure 5). This positive impact represents a critical step toward achieving the country's climate goals, supporting the global fight against climate change, and positioning

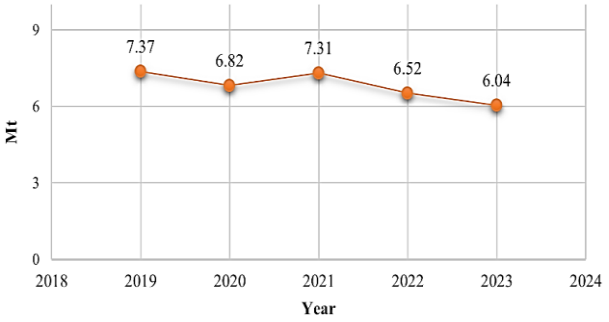

Fig. 5. CO_2 emissions from the energy sector in Macedonia during the analyzed period

North Macedonia is an active participant in global sustainability initiatives. Despite these projections, simulations suggest that thermal power plants and cogeneration facilities will continue to play an essential role in ensuring energy stability, particularly during periods of increased electricity demand or limited capacity from renewable sources.

Electricity imports, as depicted in Figure 6, have shown a steady decline, reaching their lowest point in 2023. Data indicate that electricity imports

dropped by 89.9% in 2023 compared to 2019, decreasing from 1.826 TWh in 2019 to just 0.185 TWh in 2023. This trend is particularly significant as it reflects North Macedonia's growing energy independence, achieved through increased domestic production and enhanced energy efficiency.

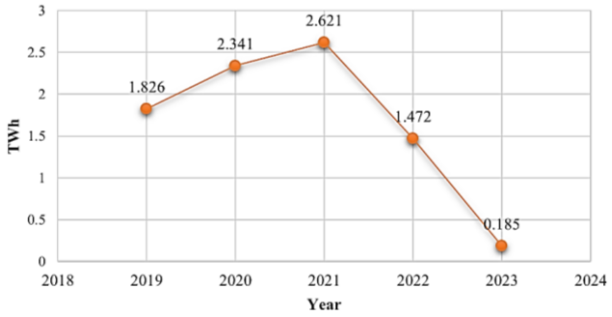

Fig. 6. Graphical representation of the trend in the reduction of electricity imports

The comparative graphs between the actual electricity generation from cogeneration plants and thermal power stations and the theoretically possible and necessary output, as shown in the software simulations, further highlight the system's reliance on electricity imports as a function of thermal power production. These graphs reveal that in years where the gap between actual production from cogeneration and thermal plants and the projected levels in the simulations is the greatest, a heightened need for electricity imports arises. This suggests that although cogeneration plants and thermal power stations have adequate capacity, various factors have prevented them from producing sufficient energy to fully meet the system's demands.

The two alternative scenarios for Macedonia's energy future reveal a strong potential for achieving full energy independence by increasing the use of renewable sources and optimizing existing capacities. Each scenario includes the installation of 600 MW of wind and 1000 MW of photovoltaic capacity, part of which is already underway. The first scenario involves the operation of a single unit from the REK Bitola plant (233 MW), providing a stable supply without imports and generating 0.66 TWh for export. The second scenario proposes the replacement of all coal capacities with a 200 MW gas cogeneration plant, allowing for 0.34 TWh in exports (Figure 7). Additionally, both scenarios anticipate the construction of the Čebren hydropower plant (458 MW), adding to supply and export potential.

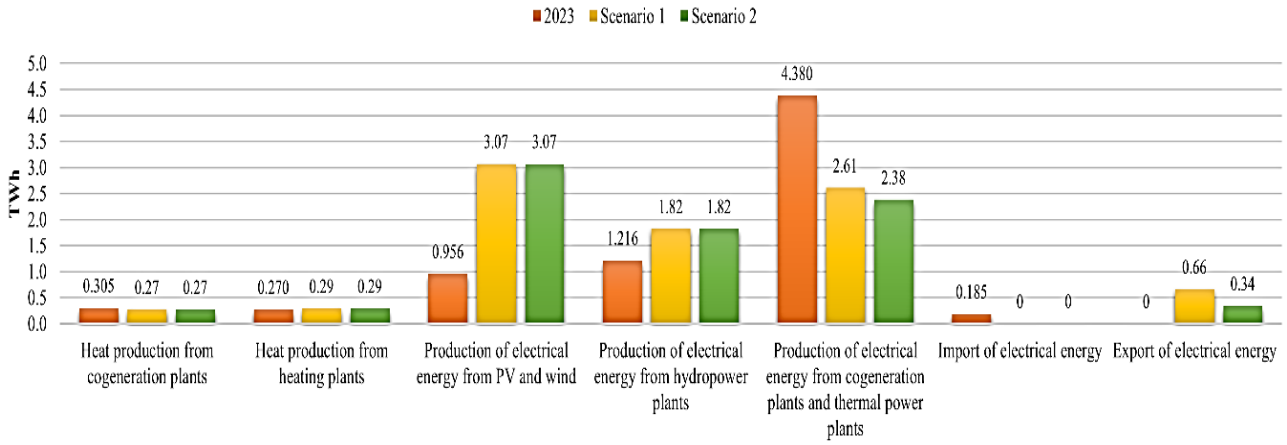

Fig. 7. Comparison of production capacities in the energy sector in Macedonia (2023 and Scenarios 1 and 2)

In the first scenario, CO_2 emissions would be reduced by 29%, while in the second, emissions would drop by 30.3% compared to 2023 levels (Figure 8), highlighting environmental and economic benefits, particularly concerning potential carbon taxes. These results indicate that Macedonia could make a significant contribution to the global fight against climate change while strengthening its energy stability and reducing costs associated with energy imports.

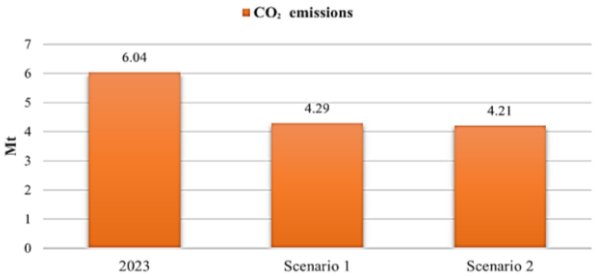

Fig. 8. Comparison of CO_2 emissions after the implementation of the two alternative scenarios

When analyzing the proposed scenarios from an investment perspective, where production capacities are activated only during the most economically viable periods, the results reveal significant challenges. The limited capacity of North Macedonia's existing distribution grid cannot adequately absorb and transmit energy from new installations, particularly renewable sources such as wind and solar. This infrastructure shortfall calls for substantial investment to upgrade and expand the transmission network.

The simulations also indicate that economically driven production increases the need for electricity imports, creating a greater dependency on external sources. To overcome these challenges, investments in the expansion and modernization of the electricity distribution network should be considered, enabling better integration of renewable sources. Such investments would entail increased costs for constructing new transmission lines, and transformer stations and improving systems for managing energy flows.

4. CONCLUSION

Based on analyses conducted for North Macedonia's energy sector from 2019 to 2023, this study reveals significant opportunities for advancing energy independence and reducing greenhouse gas emissions by increasing the use of renewable energy sources. These measures are crucial for achieving the country's climate goals and align with global trends toward decarbonization and sustainability of energy systems. The simulations indicate that North Macedonia has the potential to establish a stable electricity supply and enhance energy security through the achievement of energy independence.

The integration of new capacities, such as the Čebren pumped-storage hydropower plant, wind farms, and solar panels, plays a central role in this transition, yet presents a significant technological and economic challenge requiring substantial investment and support from the government and private sector. The findings also suggest that the addition of new cogeneration facilities could enhance energy stability and security while simultaneously reducing CO_2 emissions, which is essential for meeting national climate targets.

This research confirms the need to intensify efforts to modernize the energy sector and stimulate investments in renewable energy sources. Such measures will not only provide energy independence but will also contribute to the country's economic and environmental sustainability. Additionally, this approach will position North Macedonia as an exemplar of successful sustainable energy transition and increase its resilience to global and regional energy crises.

REFERENCES

[1] The World Bank Group. (2024): *North Macedonia – Country Climate and Development Report*. https://documents1.worldbank.org/curated/en/099092624072036221/pdf/P17920510eb24a0561a98b1a8b00a307db2.pdf

[2] International Energy Agency (IEA). (2021): *World Energy Outlook*. https://www.iea.org/reports/world-energy-outlook-2021

[3] CEE Legal Matters (2021): *Issue CEELM 8.8*, p. 90. https://ceelegalmatters.com/Magazines/ISSUE_CEELM_8.8_free.pdf

[4] Ćosić, B., Krajačić, G., Duić, N. (2012): A 100% renewable energy system in the year 2050: The case of Macedonia. *Energy*, **48** (1), 80–87. https://doi.org/10.1016/j.energy.2012.06.078

[5] Research Center for Energy and Sustainable Development of the Macedonian Academy of Sciences and Arts (MANU) (2023): *Accelerating a Renewable Future: Using Brownfields and Barren Lands for Wind and Solar Energy Siting in North Macedonia*. The Nature Conservancy.

[6] Gburčik, V., Mastilović, S., Vučinić, Ž. (2013): Assessment of solar and wind energy resources in Serbia. *Journal of Renewable and Sustainable Energy*, **5** (4), 041822. https://doi.org/10.1063/1.4819504

[7] Lazova, E., Shesho, I. (2023): Assessment of the Macedonian power system potential toward green energy transition. *Annals of Faculty Engineering Hunedoara – International Journal of Engineering*, Tome XXI, Fascicule 2, pp. 27–34.

[8] Mijakovski, V., Lutovska, M., Mojsovski, F. (2022): *Energy transition in North Macedonia in the wake of the European Energy Crisis.* SimTerm2022. https://eprints.uklo.edu.mk/id/eprint/8504/1/Mijakovski,%20Lutovska,%20Mojsovski-SIMTERM%202022.pdf

[9–13] Regulatory Commission for Energy of North Macedonia (2019–2023): *Annual Reports*. https://www.erc.org.mk/page.aspx?id=342

[14] ESM – *Power Plants of North Macedonia*. Website of ESM.

[15] EVN Macedonia. *Energy Procurement*.

[16] Jiang, P., Fan, Y. V., Klemeš, J. J. (2021): Impacts of COVID-19 on energy demand and consumption: Challenges, lessons and emerging opportunities. *Applied Energy*, **285**, 116441. https://doi.org/10.1016/j.apenergy.2021.116441

[17] Chen, Y., Jiang, J., Wang, L., Wang, R. (2023): Impact assessment of energy sanctions in geo-conflict: Russian–Ukrainian war. *Energy Reports*, **9**, 3082–3095. https://doi.org/10.1016/j.egyr.2023.01.124

Mechanical Engineering – Scientific Journal, Vol. **42,** No. 2, pp. 133–136 (2024)
CODEN: MINSC5 In print: ISSN 1857–5293
On line: ISSN 1857–9191

INSTRUCTIONS FOR AUTHORS

The *Mechanical Engineering – Scientific Journal* is published twice yearly. The journal publishes **original scientific papers, short communications, reviews** and **professional papers** from all fields of mechanical engineering.

The journal also publishes (continuously or occasionally) the bibliographies of the members of the Faculty, book reviews, reports on meetings, informations of future meetings, important events and data, and various rubrics which contribute to the development of the corresponding scientific field.

Original scientific papers should contain hitherto unpublished results of completed original scientific research. The number of pages (including tables and figures) should not exceed 15 (28 000 characters).

Short communications should also contain completed but briefly presented results of original scientific research. The number of pages should not exceed 5 (10 000 characters) including tables and figures.

Reviews are submitted at the invitation of the Editorial Board. They should be surveys of the investigations and knowledge of several authors in a given research area. The competency of the authors should be assured by their own published results.

Professional papers report on useful practical results that are not original but help the results of the original scientific research to be adopted into scientific and production use. The number of pages (including tables and figures) should not exceed 10 (18 000 characters).

Acceptance for publication in the Journal obliges the authors not to publish the same results elsewhere.

SUBMISSION

The article and annexes should be written on A4 paper with margins of 2.5 cm on each side with a standard font Times New Roman 11 points and should be named with the surname of the first author and then if more and numbered. It is strongly recommended that on MS Word 2003 or MS Word 2007 and on PDF files of the manuscript be sent by e-mail:

mesj@mf.edu.mk.

A letter must accompany all submissions, clearly indicating the following: title, author(s), corresponding author's name, addres and e-mail addres(es), suggested category of the manuscript and a suggestion of five referees (their names, e-mail and affiliation).

Articles received by the Editorial Board are sent to two referees (one in the case of professional papers). The suggestions of the referees and Editorial Board are sent to the author(s) for further action. The corrected text should be returned to the Editorial Board as soon as possible but in not more than 30 days.

PREPARATION OF MANUSCRIPT

The papers should be written in the shortest possible way and without unnecessary repetition.

The original scientific papers, short communications and reviews should be written in English, while the professional papers may also be submitted in Macedonian.

Only SI (Système Internationale d'Unites) quantities and units are to be used.

Double subscripts and superscripts should be avoided whenever possible. Thus it is better to write $\nu_3(PO_4)$ than $\nu_{3_{PO_4}}$ or exp(–E/RT) than $e^{-E/RT}$. Strokes (/) should not be used instead of parentheses.

When a large number of compounds have been analyzed, the results should be given in tabular form.

Manuscript should containt: title, author(s) full-name(s), surname(s), address(es) and e-mail of the corresponding author, short abstract, key words, introduction, experimental or theoretical background, results and discussion, acknowledgment (if desired) and references.

The **title** should correspond to the contents of the manuscript. It should be brief and informative and include the majority of the key words.

Each paper should contain an **abstract** that should not exceed 150 words, and **3–5 key words**. The abstract should include the purpose of the research, the most important results and conclusions.

The **title**, **abstract** and **key words** should be translated in Macedonian language. The ones written by foreign authors will be translated by the Editorial Board.

In the **introduction** only the most important previous results related to the problem in hand should be briefly reviewed and the aim and importance of the research should be stated.

The **experimental** section should be written as a separate section and should contain a description of the **materials used and methods** employed – in form which makes the results reproducible, but without detailed description of already known methods.

Manuscripts that are related to **theoretical studies**, instead of experimental material, should contain a sub-heading and the **theoretical background** where the necessary details for verifying the results obtained should be stated.

The **results and discussion** should be given in the same section. The discussion should contain an analysis of the results and the conclusions that can be drawn.

Figures (photographs, diagrams and sketches) and **mathematical formulae** should be inserted in the correct place in the manuscript, being horizontally reduced to 8 or 16 cm. The size of the symbols for the physical quantities and units as well as the size of the numbers and letters used in the reduced figures should be comparable with the size of the letters in the main text of the paper. Diagrams and structural formulae should be drawn in such a way (e.g. black Indian ink on white or tracing paper) as to permit high quality reproduction. The use of photographs should be avoided. The tables and the figures should be numbered in Arabic numerals (e.g., Table 1, Figure 1). Tables and figures should be self-contained, i.e. should have captions making them legible without resort to the main text. The presentation of the same results in the form of tables and figures (diagrams) is not permitted. The use of equation editor (MS Word, Microsoft Equation, Math Type 6.0 Equation) for typesetting the equations is recommended. Strokes (/) should not be used instead of parentheses.

Figures and tables must be centred in the column. Large figures and tables may span across both columns (Figure 1).

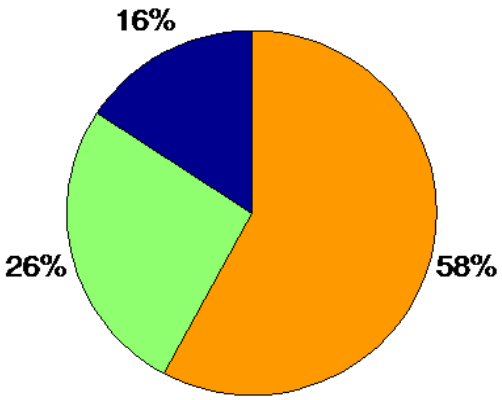

Fig. 1. Example of a graph and a single-line caption (colour)

Graphics may be full colour. Please use only colours which contrast well both on screen and on a black-and-white hardcopy because the Journal is published in black-and-white, as shown in Figure 2. The colour version is only for the electronic version of the Journal.

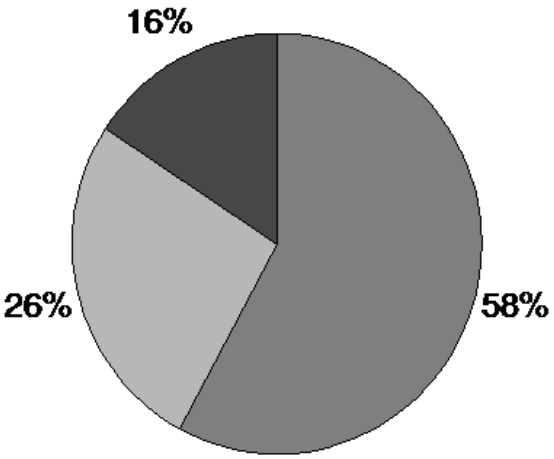

Fig. 2. Example of a graph and a single-line caption (bleck and vhite)

Please check all figures in your paper both on screen and on a black-and-white hardcopy. When you check your paper on a black-and-white hardcopy, please ensure that:

– the colours used in each figure contrast well (Figure 3),

– the image used in each figure is clear,

– all text labels in each figure are legible.

Please check all figures in your paper both on screen and on a black-and-white hardcopy. When you check your paper on a black-and-white hardcopy, please ensure that the image used in each figure is clear and all text labels in each figure are legible.

Fig. 3. Example of an image as it will appear at the electronic version of the Journal and a multi-line caption

Footnotes are also not permitted.

The **reference** should be given in a separate section in the order in which they appear in the text. The surname of one or two authors may be given in the text, whereas in the case of more than two authors they should be quoted as, for example:

Examples of reference items of different categories shown in the References section include:

- example of a book in [1]
- example of a book in a series in [2]
- example of a journal article in [3]
- example of a conference paper in [4]
- example of a patent in [5]
- example of a website in [6]
- example of a web page in [7]
- example of a databook as a manual in [8]
- example of a datasheet in [9]
- example of a master/Ph.D. thesis in [10]
- example of a technical report in [11]
- example of a standard in [12]

All reference items must be in 9 pt font. Please use Regular and Italic styles to distinguish different fields as shown in the References section. Number the reference items consecutively in square brackets (e.g. [1]).

When referring to a reference item, please simply use the reference number, as in [2]. Do not use "Ref. [3]" or "Reference [3]" except at the beginning of a sentence, e.g. "Reference [3] shows …". Multiple references are each numbered with separate brackets (e.g. [2], [3], [4–6]).

The **category** of the paper is proposed by the author(s), but the Editorial Board reserves for itself the right, on the basis of the referees' opinion, to make the final choice.

Proofs are sent to the author(s) to correct printers' errors. Except for this, alterations to the text are not permitted. The proofs should be returned to the Editorial Board in 2 days.

The author(s) will receive, free of charge, 1 reprints of every paper published in the Journal.

REFERENCES

[1] Surname, N(ame).; Surname, N(ame). (Year): *Name of the Book*, Publisher.

[2] Surname, N(ame).; Surname, N(ame). (Year): *Name of the Book*, Name of the Series. Publisher, **vol.** XXX.

[3] Surname, N(ame).; Surname N(ame). (Year): Title of the article, *Name of the Journal*, **vol. XX,** No. XX, pp. XXX–XXX.

[4] Surname, N(ame).; Surname N(ame). (Year): Title of the article, *Proceedings of the Name of the Conference*, vol. **XX,** pp. XXX–XXX.

[5] Surname, N(ame).; Surname, N(ame).: *Name of the Patent*, Institution that issued the patent and Number of the patent (Date dd. mm. yyyy).

[6] N.N. (Year): *The XXX web site*, web address.

[7] Surname, N. (Year): *XXX homepage on XXX*, web address.

[8] N.N. (Year): *Title of the Manual*, Name of the Organization.

[9] N.N.: *XXX data sheet*, Name of the Organization.

[10] Surname, N. (Year): *Title of the Thesis*, Master/Ph.D. thesis (in Language), Institution.

[11] Surname, N(ame).: Surname, N(ame). (Year): *Title of the Report*, Organization that issued the report, number of the report.

[12] Institution that issued the standard (Year): *Name of the Standard* & Number of the standard.